Osteogenic Differentiation of Rat Bone Marrow Stromal Cells Encapsulated in Poly(Pro-Hyp-Gly) Hydrogels

(Poly(Pro-Hyp-Gly)ハイドロゲルに包埋したラット骨髄間質細胞の骨分化)

Farah Nurlidar

2017

Graduate School of Materials Science

Nara Institute of Science and Technology

CONTENTS

GENERAL INTRODUCTION

1.   Tissue Regeneration

The demands for organ transplantation to recover damaged tissue are increasing. However, organ transplantation is limited by donor shortage, immune rejection, and disease transfer [1-4]. Tissue engineering aims to regenerate damaged tissue by implanting three-dimensional (3D) scaffolds that contain stem cells or differentiated cells into the tissue [1-4]. Schematic illustration of using stem cells for tissue regeneration is shown in **Figure 1.** Stem cells play an important role in tissue regeneration because of their capability to develop into more mature or specialized cells [1]. For example, bone marrow stromal cells are progenitors of skeletal tissue components and have the ability to differentiate into cells of the connective tissue lineage, such as osteoblasts, chondrocytes, and adipocytes [5].

Culturing stem cells in 3D scaffolds has gained interest in tissue regeneration because of their advantages over two-dimensional (2D) cell culture in providing more natural microenvironments for cell growth and differentiation [6,7]. In addition, more cell-cell and cell-scaffold interactions can be provided by the 3D scaffolds [6]. Cells grown on 2D culture

may not behave cells grown in *in-vivo* microenvironments [6,7]. For example, chondrocytes lose their phenotype and functions when cultured on tissue culture plates. They regain their phenotype and functions when embedded in 3D scaffolds of agarose gel [7].

The 3D scaffolds for tissue regeneration have to support cell viability and differentiation. This goal can be achieved by reproducing cell microenvironments, such as extracellular matrices (ECMs) [1-4]. ECMs are complex networks of proteins and polysaccharides that are secreted by cells and provide structural, adhesive, and biochemical signaling supports [8].

An arginine-glycine-aspartic acid (RGD) is an amino acid sequence that appears in many ECM molecules, such as fibronectin, vitronectin, von Willebrand factor, laminin, collagen, and protocadherins [9-11]. RGD serves as a ligand for cell adhesion receptors, integrin [12,13]. To create 3D scaffolds that can reproduce the features of ECMs, RGD-containing peptides have been chemically conjugated into various polymers, such as alginate and polyethylene glycol (PEG) [13,14]. Encapsulation of mesenchymal stem cells in a 3D alginate scaffold containing an RGD-derived peptide resulted in the promotion of cell attachment, spreading, and proliferation [14].

Another effort to create ECM-like scaffolds can be achieved by introducing growth factors into the 3D scaffolds. Growth factors can stimulate cellular functions, such as cell proliferation and differentiation [15]. Various families of growth factors, such as

transforming growth factor-beta (TGF-β) superfamily and fibroblast growth factor family, have been identified to play a crucial role in cell proliferation, differentiation, and apoptosis [15]. Bone morphogenetic protein-2 (BMP-2) is a member of TGF-β superfamily. Tanihara *et al.* reported that BMP-2 residues 73-92 (KIPKASSVPTELSAISTLYL-NH$_2$, bone forming protein (BFP)) conjugated to alginate gel particles can accelerate the repair of rat tibia bone defects [16]. BFP-conjugated alginate gel particles co-implanted with rat bone marrow stromal cells (rBMSCs) were shown to induce differentiation of the cells into osteoblasts, and activate the osteoblasts to promote repair of bone defects [16]. Another report showed that incorporation of an RGD peptide and a BFP onto poly(lactide-co-ethylene oxide fumarate) hydrogel can synergistically enhance osteogenic differentiation of seeded BMSCs [17].

2.   Hydrogels as 3D Scaffolds for Tissue Regeneration

For tissue regeneration, cells are often encapsulated into 3D scaffolds before implantation into the damaged tissue. Cells differentiate into specialized cells and produce a new tissue utilizing 3D matrices as temporary scaffolds [1]. Cells can be encapsulated into 3D scaffolds before or after scaffold fabrication. After 3D scaffold fabrication, cells can be encapsulated into the scaffolds by static, injection, centrifugation or vacuum methods

[18,19]. However, it is difficult to achieve homogeneous cell distribution with these methods. Simultaneous cell encapsulation with scaffold fabrication offers homogeneous cell distribution which enables homogeneous tissue reconstruction [20,21].

Hydrogels, 3D hydrated polymer networks, are attractive materials that can encapsulate cells simultaneously and/or prior to their formation [20,21]. In simultaneous cell encapsulation, polymer solution and cells are mixed, and crosslinking reaction is conducted to encapsulate cells within the hydrogels. To design a cytocompatible hydrogel for cell encapsulation, the polymers and the process for hydrogel formation should show low cytotoxicity. In addition, the polymers are preferable to be soluble in an aqueous solution with physiological pH and osmolarity to prevent any cell damages [20,21].

Recently, various chemical and physical crosslinking strategies have been used to fabricate hydrogels for cell encapsulation [4,21-38]. The properties of hydrogels, such as degree of crosslinking, polymer network density, mechanical stiffness, and swelling ratio, can be controlled both by choosing the type of crosslinking, chemical or physical crosslinking, and by controlling the crosslinking conditions, such as concentrations of polymers and crosslinkers, and gelation time [22-25]. The hydrogel properties have been shown to have significant effects on the cell viability, proliferation, and differentiation [22-25]. Hydrogel composite of oligo-PEG fumarate and gelatin microparticles has been developed as a carrier for cartilage tissue engineering [24]. Enhanced in chondrogenic

differentiation of rabbit marrow mesenchymal stem cells was observed in hydrogel composites with higher swelling ratio [24]. Another study by Tan *et al.* showed that osteogenic differentiation of encapsulated mouse C2C12 myoblast cells in transglutaminase cross-linked gelatin gel was affected by hydrogel stiffness [25]. Therefore, development of hydrogels that can support cellular functions is important for designing 3D scaffolds for tissue regeneration.

2.1. *Physically-crosslinked hydrogels*

Physical crosslinking strategies utilize non-covalent bondings, such as ionic, hydrophobic, and hydrogen bondings, to form reversible hydrogels [21,26-29]. The use of physical crosslinking offers the possibility to encapsulate cells prior to hydrogel formation without the presence of any chemical-crosslinking reagents [21,26-29]. Physical crosslinking can be disrupted by changing external environments, such as pH, temperature, and ionic strength [21,26-29].

A solution containing modified chitosan, *N*-palmitoyl chitosan (NPCS), forms hydrogel when injected into a physiological solution at 37 °C [26]. Hydrogel formation is attributed to hydrophobic interaction between hydrophobic side chains (palmitoyl group) of chitosan. However, low pH of the NPCS solution (pH = 6.5) may damage cells [26].

Hydrogen bonding was used for fabricating poly(vinyl alcohol) hydrogel by freeze-thawing techniques. The hydrogel has been used for encapsulating vascular smooth muscle cells in the presence of ε-poly-L-Lysine as a cryoprotectant [27]. The encapsulated cells showed a decrease in viability after thawing process, presumably because of the formation of intracellular and intercellular ice crystal during freezing process [27].

MAX8, a 20-peptide residues containing seven lysine residues and one glutamic acid residue, forms hydrogel in response to salt concentration change because of self-assembly of the peptide from a random-coil into a β-sheet structure [28]. The encapsulated mesenchymal stem cells were distributed homogenously within the hydrogel. Live-dead staining of the encapsulated cells 3 h after incubation showed that the cells in the hydrogel remain viable. However, some dead cells were observed in the hydrogel [28]. Another study showed that viability of chondrocytes encapsulated in the MAX8 hydrogel significantly decreased after 24 h [29]. It is presumably because of electrostatic interaction between MAX8 and the encapsulated cells [29]. Compounds with higher cationic charge densities may induce inflammatory response of the encapsulated cells and may cause cell necrosis [30].

2.2. *Chemically-crosslinked hydrogels*

Chemically-crosslinked hydrogels are irreversible hydrogels and show a high stability because of covalent bond formations between the polymer chains. Various chemical crosslinking techniques, such as Michael-addition, Diels-Alder reaction, Schiff-base formation, diisocyanate-crosslinking, and photocrosslinking have been used for encapsulating cells into hydrogels [21,31-36].

Michael-addition involves a reaction between a nucleophile, such as polymers containing thiol group, and an electrophile, such as α,β-unsaturated carbonyl compounds [31]. Four-arm PEG was modified with acrylate, diacrylate, vinyl sulfone or maleimide. The modified PEG was reacted with dithiol-containing peptides to form hydrogels. The hydrogels were successfully used for myoblast encapsulation [31]. However, the hydrogels were fabricated under basic conditions, which might decrease the viability of the encapsulated cells.

Polymers modified with maleimide group were also used for cell encapsulation via Diels-Alder crosslinking [32]. The hydrogels are formed by a reaction between maleimide groups of PEG-dimaleimide and furan group of hyaluronic acid-furan (HA-furan). However, it requires long gelation time (more than 1 h) for completing the gelation process. Cytotoxicity assay of PEG-dimaleimide and HA-furan hydrogel formed with different gelation time revealed that long gelation time is toxic to the encapsulated murine chondrocytic cell line [32]. In addition, maleimide groups are highly reactive and can react

with amino groups of proteins of the encapsulated cells.

Schiff-base formation was used to encapsulate bovine chondrocytes into chitosan/HA hydrogels [33]. This system utilizes a reaction between amino group of *N*-succinyl chitosan and aldehyde group of modified-HA. Confocal laser scanning microscopy showed that 93% of cells in the hydrogel survived 24 h after encapsulation [33]. However, aldehyde group of modified-HA can also react with amino groups of proteins, which limits the use of Schiff-base hydrogels for cell encapsulation [21]. Another study showed that BMSCs seeded into a Schiff-base hydrogel of aldehyde-alginate/*N*-succinyl chitosan had a low cell viability [34].

A diisocyanate-crosslinker, 1,6-hexamethylene diisocyanate, has been used for fabricating polyurethane scaffolds containing poly(ε-caprolactone) (PCL), PEG, and glycerol for cell encapsulation [35]. Polyurethane scaffolds were fabricated in organic solvents. After scaffold formation, the cells were encapsulated into the PCL/PEG/glycerol hydrogel by immersing the scaffold in medium containing cells [35]. This process may lead to inhomogeneous distribution of the encapsulated cells. Furthermore, the remains of organic solvents in the scaffolds may decrease cell viability.

Photocrosslinking techniques utilize radical formation under ultraviolet (UV)/visible light irradiation of photoinitiators to initiate crosslinking reactions. UV-photocrosslinking was successfully used to fabricate methacrylated alginate-acrylated RGD hydrogel in the

presence of 0.05% w/v 2-hydroxy-1-[4-(2-hydroxylethoxy) phenyl]-2-methyl-1-propanone (Irgacure 2959) [14]. Encapsulated human mesenchymal stem cells (hMSCs) in the hydrogel showed a high cell viability even after 28 days of culture, demonstrating good biocompatibility of the photocrosslinked hydrogels for long term cell encapsulation [14]. However, UV light has potential to damage cellular DNA [36].

Visible light photocrosslinking was successfully used for encapsulating hMSCs within PEG diacrylate (PEGDA) hydrogel by irradiating PEGDA solution with visible light in the presence of eosin Y, triethanolamine, and 1-vinyl-2 pyrrolidinone (NVP) [37]. The hydrogel system supported chondrogenic differentiation of the hMSCs throughout 6 weeks of incubation in chondrogenic medium. However, the cells encapsulated with high concentration of eosin Y/triethanolamine (0.1 mM eosin Y and 0.75% triethanolamine) hydrogel showed a low cell viability and low expression of collagen matrices [37]. It may be caused by the toxicity of radicals formed during the photocrosslinking reaction.

Considering the limitations of physical and chemical crosslinking techniques for cell encapsulation as described above, the use of proper crosslinking techniques and polymers is important to maintain cell viability during crosslinking process and following cultivation periods.

3.   Collagen-like Polypeptide

Hydrogels can be synthesized from various natural and synthetic polymers. Among natural polymers, animal-derived collagens are the most useful biomaterials because of their biocompatibility and biodegradability. They have been widely used for tissue regeneration and drug delivery systems [38-40]. Rat MSCs cultured in a collagen scaffold showed an increase in osteocalcin and alkaline phosphatase expression, indicating that the collagen hydrogel supports osteogenic differentiation of the encapsulated cells [40]. However, animal-derived collagens have a possibility to transfer pathogenic substances, such as prion, to patients [41]. In addition, they have low thermal stability [42]. Synthetic polymers, such as PEG derivatives, are commonly used as substituting materials for fabricating 3D scaffolds for tissue regeneration [43]. However, these polymers are not biodegradable, which limit their application for tissue regeneration [43,44].

Poly(Pro-Hyp-Gly) is a synthetic polymer containing Pro-Hyp-Gly sequences which is commonly found in the triple-helical domain of collagen [45]. The poly(Pro-Hyp-Gly) sponge has been shown to degrade at the same rate as Terudermis® (Olympus Terumo Biomaterials, Tokyo, Japan), a heat-crosslinked bovine atelocollagen, when embedded subcutaneously into the dorsal area of a rat [46]. Furthermore, epithelialization of a full-thickness wound on a rabbit's ear pad was significantly promoted in the presence of the

poly(Pro-Hyp-Gly) sponge in comparison with Terudermis® [46].

Hydroxy group of Hyp residues of poly(Pro-Hyp-Gly) can be tailored with various functional groups by specific modification to enhance its functionality as a scaffold for tissue regeneration. Shibasaki *et al.* showed that poly(Pro-Hyp-Gly) conjugated with cell adhesion peptides, Gly-Arg-Gly-Asp-Ser and Pro-His-Ser-Arg-Asn, enhances an NIH3T3 cell adhesion and migration, and rabbit corneal epithelial cell stratification [47]. Therefore, poly(Pro-Hyp-Gly) is an attractive candidate to reproduce physical and biochemical properties of natural collagens. An ideal 3D scaffold for tissue regeneration can be developed by further modification of the poly(Pro-Hyp-Gly).

4.   **Purpose of This Work**

As described in section 2, various crosslinking techniques and polymers have been used for fabricating hydrogels for cell encapsulation. However, there were problems of potential toxicity of initiators and crosslinking process. A collagen-like polypeptide, poly(Pro-Hyp-Gly), is a good candidate as a material for synthesizing hydrogels for tissue regeneration because of its similar physical properties, biocompatibility, and biodegradability to those of animal-derived collagens. In this study, to develop cytocompatible hydrogels that can encapsulate cells, maintain their viability, and support

their differentiation, the author fabricated poly(Pro-Hyp-Gly) hydrogels by both physical and chemical crosslinking. Based on processes to fabricate poly(Pro-Hyp-Gly) hydrogels for stem cell encapsulation, this thesis consists of the following two chapters.

Chapter 1 describes encapsulation of rBMSCs into a physically-crosslinked poly(Pro-Hyp-Gly) hydrogel. The hydrogel was fabricated by polyionic interaction of a polyanion, succinylated poly(Pro-Hyp-Gly), and a polycation, arginylated poly(Pro-Hyp-Gly), at physiological pH (pH = 7.4) allowing simultaneous encapsulation of the rBMSCs.

Chapter 2 describes stem cell encapsulation into chemically-crosslinked poly(Pro-Hyp-Gly) hydrogels. The hydrogels were fabricated by visible light photocrosslinking of methacrylated poly(Pro-Hyp-Gly) in the presence of eosin Y, triethanolamine, and NVP. In this chapter, the influences of hydrogel properties on cell viability and osteogenic differentiation of the encapsulated rBMSCs were investigated.

The results of this study indicate that physically-crosslinked and chemically-crosslinked poly(Pro-Hyp-Gly) hydrogels support cell viability and differentiation, suggesting that the poly(Pro-Hyp-Gly) hydrogels are promising 3D scaffolds for tissue regeneration.

References

1. Dvir T, Timko BP, Kohane DS, Langer R. Nanotechnological strategies for engineering complex tissues. Nat Nanotechnol 2011;6:13–22.

2. Chen G, Ushida T, Tateishi T. Scaffold design for tissue engineering. Macromol Biosci 2002;2:67–77.

3. O'Brien FJ. Biomaterials and scaffolds for tissue engineering. Mater Today 2011; 14:88–95.

4. Lee KY, Mooney DJ. Hydrogels for tissue engineering. Chem Rev 2001;101:1869–1879.

5. Bianco P, Riminucci M, Gronthos S, Robey PG. Bone marrow stromal stem cells: Nature, biology, and potential applications. Stem cells 2001;19:180–192.

6. Edmondson R, Broglie JJ, Adcock AF, Yang L. Three-dimensional cell culture systems and their applications in drug discovery and cell-based biosensors. Assay Drug Dev Technol 2014;12:207–218.

7. Benya PD, Shaffer JD. Dedifferentiated chondhrocytes reexpress the differentiated collagen phenotype when cultured in agarose gels. Cell 1982;30:215–224.

8. Griffith LG, Swartz MA. Capturing complex 3D tissue physiology in vitro. Nat Rev Mol Cell Biol 2006;7:211–224.

9. Simmons D, Makgoba MW, Seed B. ICAM, an adhesion ligand of LFA-1, is homologous to the neural cell adhesion molecule NCAM. Nature 1988;331:624−627.

10. Yagi T. Clustered protocadherin family. Dev Growth Differ 2008;50:S131−S140.

11. Schaffner P, Dard MM. Structure and function of RGD peptides involved in bone biology. Cell Mol Life Sci 2003;60:119−132.

12. Barczyk M, Carracedo S, Gullberg D. Integrins. Cell Tissue Res 2010;339: 269−280.

13. Ruoslahti E. RGD and other recognition sequences for integrins. Annu Rev Cell Dev Biol 1996;12:697−715.

14. Jeon O, Alsberg E. Photofunctionalization of alginate hydrogels to promote adhesion and proliferation of human mesenchymal stem cells. Tissue Eng Part A 2013;19: 1424−1432.

15. Danišovič Ľ, Varga I, Polák Š. Growth factors and chondrogenic differentiation of mesenchymal stem cells. Tissue Cell 2012;44:69−73.

16. Saito A, Suzuki Y, Ogata S, Ohtsuki C, Tanihara M. Accelerated bone repair with the use of a synthetic BMP-2-derived peptide and bone-marrow stromal cells. J Biomed Mater Res A 2005;72A:77−82.

17. He X, Ma J, Jabbari E. Effect of grafting RGD and BMP-2 protein derived peptides to a hydrogel substrate on osteogenic differentiation of marrow stromal cells. Langmuir 2008;24:12508−12516.

18. Villalona GA, Udelsman B, Duncan DR, McGillicuddy E, Sawh-Martinez RF, Hibino N, Painter C, Mirensky T, Erickson B, Shinoka T, Breuer CK. Cell-seeding techniques in vascular tissue engineering. Tissue Eng Part B Rev 2010;16:341−350.

19. Zhang ZZ, Jiang D, Wang SJ, Qi YS, Zhang JY, Yu JK. Potential of centrifugal seeding method in improving cells distribution and proliferation on demineralized cancellous bone scaffolds for tissue-engineered meniscus. ACS Appl Mater Interfaces 2015;22:15294−15302.

20. Nicodemus GD, Bryant SJ. Cell encapsulation in biodegradable hydrogels for tissue engineering applications. Tissue Eng Part B Rev 2008;14:149−165.

21. Yang JA, Yeom J, Hwang BW, Hoffman AS, Hahn SK. *In situ*-forming injectable hydrogels for regenerative medicine. Prog Polym Sci 2014;39:1973−1986.

22. Bian L, Hou C, Tous E, Rai R, Mauck RL, Burdick JA, The influence of hyaluronic acid hydrogel crosslinking density and macromolecular diffusity on human MSC chondrogenesis and hypertrophy. Biomaterials 2013;34:413−421.

23. Temenoff JS, Park H, Jabbari E, Conway DE, Sheffield TL, Ambrose CG, Mikos AG. Thermally cross-linked oligo(poly(ethylene glycol) fumarate) hydrogels support osteogenic differentiation of encapsulated marrow stromal cells in vitro. Biomacromolecules 2004;5:5−10.

24. Park H, Guo X, Temenoff JS, Tabata Y, Caplan AI, Kasper FK, Mikos AG. Effect of

swelling ratio of injectable hydrogel composites on chondrogenic differentiation of encapsulated rabbit marrow mesenchymal stem cells in vitro. Biomacromolecules 2009;10:541−546.

25. Tan S, Fang JY, Yang Z, Nimni ME, Han B. The synergetic effect of hydrogel stiffness and growth factor on osteogenic differentiation. Biomaterials 2014;35:5294−5306.

26. Chiu YL, Chen SC, Su CJ, Hsiao CW, Chen YM, Chen HL, Sung HW. pH-triggered injectable hydrogels prepared from aqueous *N*-palmitoyl chitosan: *in vitro* characteristics and *in vivo* biocompatibility. Biomaterials 2009;30:4877−4888.

27. Vrana NE, Matsumura K, Hyon SH, Geever LM, Kennedy JE, Lyons JG, Higginbotham CL, Cahill PA, McGuinness GB. Cell encapsulation and cryostorage in PVA-gelatin cryogels: incorporation of carboxylated ε-poly-L-Lysine as cryoprotectant. J Tissue Eng Regen Med 2012;6:280−290.

28. Haines-Butterick L, Rajagopal K, Branco M, Salick D, Rughani R, Pilarz M, Lamn MS, Pochan DJ, Schneider JP. Controlling hydrogelation kinetics by peptide design for three-dimensional encapsulation and injectable delivery of cells. Proc Natl Acad Sci U S A 2007;104:7791−7796.

29. Sinthuvanich C, Haines-Butterick LA, Nagy KJ, Schneider JP. Iterative design of peptide-based hydrogels and the effect of network electrostatics on primary chondrocyte behavior. Biomaterials 2012;33:7478−7488.

30. Bhatia SR, Khattak SF, Roberts SC. Polyelectrolytes for cell encapsulation. Curr Opin Colloid Interface Sci 2005;10:45–51.

31. Phelps EA, Enemchukwu NO, Fiore VF, Sy JC, Murthy N, Sulchek TA, Barker TH, García AJ. Maleimide cross-linked bioactive PEG hydrogel exhibits improved reaction kinetics and cross-linking for cell encapsulation and in situ delivery. Adv Mater 2102;24:64–70.

32. Yu F, Cao X, Li Y, Zeng L, Zhu J, Wang G, Chen X. Diels-Alder crosslinked HA/PEG hydrogels with high elasticity and fatigue resistance for cell encapsulation and articular cartilage tissue repair. Polym Chem 2014;5:5116–5123.

33. Tan H, Chu CR, Payne KA, Marra KG. Injectable *in situ* forming biodegradable chitosan-hyaluronic acid based hydrogels for cartilage tissue engineering. Biomaterials 2009;30:2499–2506.

34. Liu X, Peng W, Wang Y, Zhu M, Sun T, Peng Q, Zeng Y, Feng B, Lu X, Weng J, Wang J. Synthesis of an RGD-grafted oxidized sodium alginate-*N*-succinyl chitosan hydrogel and *in vitro* study of endothelial and osteogenic differentiation. J Mater Chem B 2013;1:4484–4492.

35. Li Z, Li J. Control of hyperbranched structure of polycaprolactone/poly(ethylene glycol) polyurethane block copolymers by glycerol and their hydrogels for potential cell delivery. J Phys Chem B 2013;117:14763–14774.

36. Fairbank BD, Schwartz MP, Bowman CN, Anseth KS. Photoinitiated polymerization of PEG-diacrylate with lithium phenyl-2,4,6-trimethylbenzoylphosphinate: polymerization rate and cytocompatibility. Biomaterials 2009;30:6702–6707.

37. Bahney CS, Lujan TJ, Hsu CW, Bottlang M, West JL, Johnstone B. Visible light photoinitiation of mesenchymal stem cell-laden bioresponsive hydrogels. Eur Cells Mater 2011;22:43–55.

38. Cunha CB, Klumpers DD, Li WA, Koshy ST, Weaver JC, Chaudhuri O, Granja PL, Mooney DJ. Influence of the stiffness of three-dimensional alginate/collagen-I interpenetrating networks on fibroblast biology. Biomaterials 2014;35:8927–8936.

39. Singh A, Elisseeff J. Biomaterials for stem cell differentiation. J Mater Chem 2010;20:8832–8847.

40. Donzelli E, Salvadè E, Mimo P, Viganò M, Morrone M, Papagna R, Carini F, Zaopo A, Miloso M, Baldoni M, Tredici G. Mesenchymal stem cells cultured on a collagen scaffold: *In vitro* osteogenic differentiation. Arch Oral Biol 2007;52:64–73.

41. Nemoto T, Horiuchi M, Ishiguro N, Shinagawa M. Detection methods of possible prion contaminants in collagen and gelatin. Arch Virol 1999;144:177–184.

42. Leikina E, Mertts MV, Kuznetsova N, Leikin S. Type I collagen is thermally unstable at body temperature. Proc Natl Acad Sci U S A 2002;99:1314–1318.

43. Ohya Y, Takahashi A, Nagahama K. Biodegradable polymeric assemblies for

biomedical materials. Adv Polym Sci 2012;247:65–114.

44. Kim J, Dadsetan M, Ameenuddin S, Windebank AJ, Yaszemski MJ, Lu L. *In vivo* biodegradation and biocompatibility of PEG/sebacic acid-based hydrogels using a cage implant system. J Biomed Mater Res A 2010;95A:191–197.

45. Kishimoto T, Morihara Y, Osanai M, Ogata S, Kamitakahara M, Ohtsuki C, Tanihara M. Synthesis of poly(Pro-Hyp-Gly)$_n$ by direct polycondensation of (Pro-Hyp-Gly)$_n$, where n = 1, 5, and 10, and stability of the triple-helical structure. Biopolymers 2005;79:163–172.

46. Tanihara M, Kajiwara K, Ida K, Suzuki Y, Kamitakahara M, Ogata S. The biodegradability of poly(Pro-Hyp-Gly) synthetic polypeptide and the promotion of a dermal wound epithelialization using a poly(Pro-Hyp-Gly) sponge. J Biomed Mater Res A 2008;85:133–139.

47. Shibasaki Y, Hirohara S, Terada K, Ando T, Tanihara M. Collagen-like polypeptide poly(Pro-Hyp-Gly) conjugated with Gly-Arg-Gly-Asp-Ser and Pro-His-Ser-Arg-Asn peptides enhances cell adhesion, migration, and stratification. Biopolymers Pept Sci 2011;96:302–315.
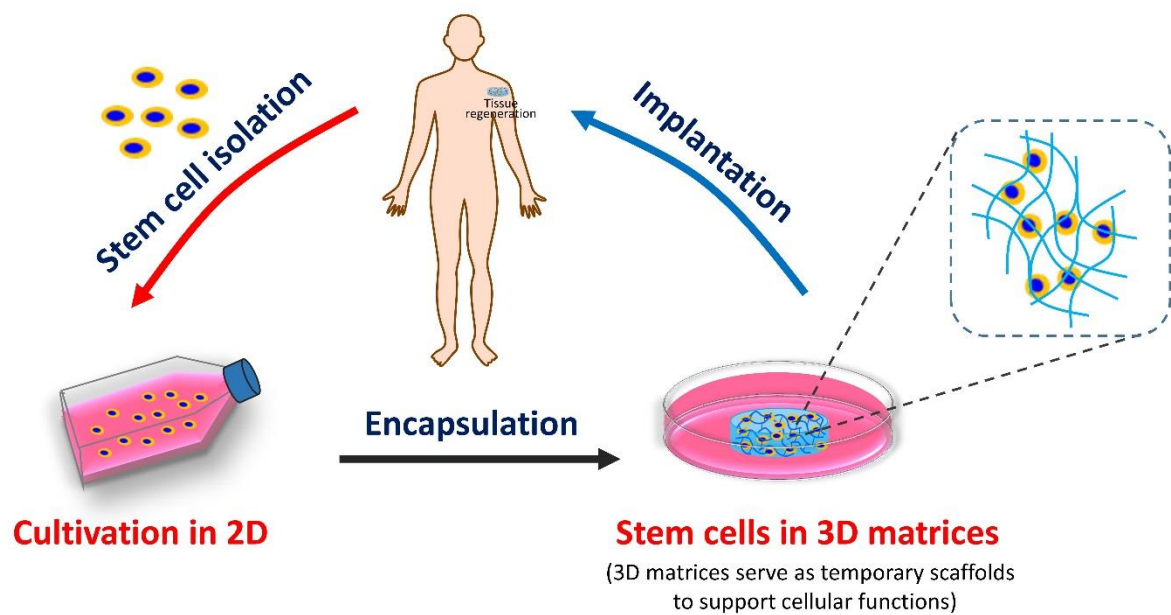
Figure 1 Schematic diagram of using stem cells for tissue regeneration. 3D matrices serve as temporary scaffolds to support cellular functions, such as cell proliferation and differentiation [1].

CHAPTER 1

Encapsulation of Rat Bone Marrow Stromal Cells in Polyion Complex Gel of Succinylated Poly(Pro-Hyp-Gly) and Arginylated Poly(Pro-Hyp-Gly)

1-1.   Introduction

Physically-crosslinked hydrogels offer a great promise for encapsulating cells because they can be fabricated in the absence of any chemical crosslinking reagents, which are potentially toxic to the cells [1,2]. The hydrogels form by non-covalent bondings, such as hydrophobic, ionic, and hydrogen bondings [1,2]. Among non-covalent bondings, ionic bonding has been extensively investigated to crosslink polysaccharides, such as alginate and chitosan [1]. Ionic bonding hydrogel is formed by electrostatic interactions between polyions and multivalent ions of the opposite charge or between polyanions and polycations [3,4].

Ionic interactions between carboxy group of alginate and calcium ion (Ca^{2+}) leads to hydrogel formation. The hydrogels have been used to encapsulate a range of cells, including

hMSCs, calf adrenal chromaffin cells, and neuronal stem cells [3-6]. However, the number of Ca^{2+}-alginate bonds in the hydrogels decrease with time because of Ca^{2+} release. The Ca^{2+} released from the hydrogels may disturb the osmolarity of the medium and cause cell damage. Banerjee *et al.* reported that Ca^{2+} released from the hydrogels upregulates the expression of inflammatory cytokines and chemokines when the hydrogels were injected subcutaneously into mice [7].

Hydrogels formed by ionic bonding of polyanions and polycations offers a better stability. Kusumastuti *et al.* fabricated polyion complex (PIC) gel of poly(Pro-Hyp-Gly) and chitosan by mixing a polyanion, succinylated poly(Pro-Hyp-Gly) (Suc-poly(Pro-Hyp-Gly)), and a polycation, chitosan. The PIC gel was successfully used to encapsulate rBMSCs simultaneously during its formation [8]. The rBMSCs in the PIC gel proliferated during 7 days of culture period. However, the number of viable cells decreased drastically at day 1 because of low pH of the chitosan solution [8]. In this study, the initial decrease in the cell number will be prevented by mixing polyanions and polycations that can form negative and positive charges at physiological pH (pH = 7.4), respectively. Encapsulating stem cells into a PIC gel at physiological pH can maintain the viability of the encapsulated cells.

To synthesize a polyanion and a polycation, poly(Pro-Hyp-Gly) was modified with succinyl group and arginine methyl ester, respectively, to obtain Suc-poly(Pro-Hyp-Gly) and Arg-poly(Pro-Hyp-Gly). At physiological pH, the carboxy group of Suc-poly(Pro-Hyp-Gly)

(pK_a = 5.2) and the guanidinium group of Arg-poly(Pro-Hyp-Gly) (pK_a = 12.4) form

negative and positive charges, respectively. They can interact to form multiple ionic

bondings and result in the formation of PIC gel. To investigate the capability of the PIC gel

to support cell viability and differentiation, rBMSCs were simultaneously encapsulated into

the PIC gel during its formation. Viability and osteogenic differentiation of the encapsulated

rBMSCs were then assessed.

1-2.   Materials and Methods

1-2-1. Materials

Pro-Hyp-Gly, 1-hydroxybenzotriazole (HOBt), *N*-hydroxysuccinimide (HOSu), and 1-ethyl-3-(3-dimethyl-aminopropyl)-carbodiimide   hydrochloride   (EDC·HCl)   were purchased from the Peptide Institute (Osaka, Japan). *N,N*-Diisopropylethylamine (DIPEA) was purchased from Applied Biosystems (Carlsbad, CA, USA). L-Arginine methyl ester dihydrochloride, L-ascorbic acid 2-phosphate sesquimagnesium salt hydrate, and β-glycerophosphate disodium salt hydrate were purchased from Sigma-Aldrich (St Louis, MO, USA). Succinic anhydride was purchased from Wako Pure Chemical Industries Ltd. (Osaka, Japan) and recrystallized from 2-propanol prior to use. Other reagents were purchased from Wako Pure Chemical Industries Ltd. Amino acids used in this study are all in L-form.

1-2-2. Synthesis   of   poly(Pro-Hyp-Gly),   Suc-poly(Pro-Hyp-Gly),   and Arg-poly(Pro-Hyp-Gly)

Poly(Pro-Hyp-Gly) was synthesized according to the previous report [9]. Briefly, Pro-Hyp-Gly (0.7 mmol) and HOBt (0.14 mmol) were dissolved in 4 mL phosphate buffer

(PB, 10 mM, pH 7.4) and mixed with EDC·HCl (3.5 mmol). The mixture was stirred at 400

rpm for 2 h at 0 °C and then for 46 h at 20 °C. The reaction was terminated by addition of 8

mL of Dulbecco's phosphate buffered saline (PBS, pH = 7.4). After homogenization using a

Waring blender (Waring Products Division, New Hartford, CT, USA), the mixture was

stirred for 24 h at room temperature and then dialyzed against Milli-Q water (Merck-

Millipore, Billerica, MA, USA) for 8 days at 4 °C using a dialysis membrane (molecular

weight cut-off (MWCO) = 14000 Da, UC20-32-100, EIDIA Co., Ltd., Tokyo, Japan) to

remove any residual reagents.

To synthesize Suc-poly(Pro-Hyp-Gly), poly(Pro-Hyp-Gly) was mixed with 50-fold

molar excess of both succinic anhydride and DIPEA to the hydroxy group of Hyp residues

of poly(Pro-Hyp-Gly) on ice for 2 h and then for 24 h at room temperature [8]. The obtained

Suc-poly(Pro-Hyp-Gly) was dialyzed against 1 M NaCl for 2 days and then with Milli-Q

water for 5 days.

To synthesize Arg-poly(Pro-Hyp-Gly), Suc-poly(Pro-Hyp-Gly) was mixed with

20-fold molar excess of both HOSu and EDC·HCl to the carboxy group of

Suc-poly(Pro-Hyp-Gly) and stirred on ice. After 15 min, 20-fold molar excess of arginine

methyl ester and DIPEA were added to the mixture and stirred for 2 h. The mixture was then

stirred overnight at room temperature. The obtained Arg-poly(Pro-Hyp-Gly) was dialyzed

against 1 M NaCl for 2 days and with Milli-Q water for 5 days.

Schematic illustration of the synthesis of Suc-poly(Pro-Hyp-Gly) and Arg-poly(Pro-Hyp-Gly) is shown in **Scheme 1-1.**

1-2-3. Characterization of poly(Pro-Hyp-Gly), Suc-poly(Pro-Hyp-Gly), and Arg-poly(Pro-Hyp-Gly)

Poly(Pro-Hyp-Gly), Suc-poly(Pro-Hyp-Gly), and Arg-poly(Pro-Hyp-Gly) were analyzed using gel permeation chromatography (GPC), circular dichroism (CD), fourier transform infrared (FTIR), and ^{1}H nuclear magnetic resonance (^{1}H NMR).

GPC analysis was carried out with an ÄKTA purifier system on a Superdex 200 HR 10/300 GL column (GE Healthcare Biosciences, Piscataway, NJ, USA). The elution buffer was PBS and flow rate was 0.5 mL/min at room temperature with the detection wavelength of 215 nm. The molecular weight of the obtained polypeptides was calculated based on PEG standards (Waters, Milford, MA, USA).

CD spectra of the polypeptides at a concentration of 0.25 mg/mL in Milli-Q water were recorded from 270–190 nm in a quartz cell of 0.1 cm optical path length on a J-820 spectropolarimeter (Jasco, Tokyo, Japan) at room temperature.

FTIR spectra were recorded at 400 - 4000 cm^{-1} using a Spectrum One FTIR spectrometer (PerkinElmer, Wellesley, MA, USA) based on the KBr method with 16 scans

and a resolution of 1 cm^{-1}.

To calculate degree of succinylation (DS_{COO^-}) and degree of arginylation (DS_{Arg^+}), and to determine pK_a of Suc-poly(Pro-Hyp-Gly), potentiometric titration was conducted using a DL 58 Titrator (Mettler-Toledo, Schwerzenbach, Switzerland). A solution containing 1 mL of Suc-poly(Pro-Hyp-Gly) or Arg-poly(Pro-Hyp-Gly), 5 mL of 0.02 M HCl, and 24 mL of Milli-Q water was titrated with 0.02 M NaOH. Volume of NaOH needed for titrating Suc-poly(Pro-Hyp-Gly) or Arg-poly(Pro-Hyp-Gly) was determined by subtracting blank titration curve from the sample titration curve. DS_{COO^-} was then calculated by **Equation 1-1** and DS_{Arg^+} was calculated by **Equation 1-2** and **1-3**.

$$\frac{DS_{COO_1^-}}{267.3\left(1 - DS_{COO_1^-}\right) + 389.3\,DS_{COO_1^-}} = \frac{\Delta V \times \text{Molarity of NaOH}}{\text{Weight of Suc-(Pro-Hyp-Gly)}} \qquad (1-1)$$

$$\frac{DS_{COO_2^-}}{267.3\left(1 - DS_{COO_1^-}\right) + 389.3\,DS_{COO_2^-} + 573.8\left(DS_{COO_1^-} - DS_{COO_2^-}\right)} = \frac{\Delta V \times \text{Molarity of NaOH}}{\text{Weight of Arg-(Pro-Hyp-Gly)}} \qquad (1-2)$$

$$DS_{Arg^+} = DS_{COO_1^-} - DS_{COO_2^-} \qquad (1-3)$$

(267.3, 389.3, and 573.8 are average tripeptide unit molecular weight of Pro-Hyp-Gly, Suc-(Pro-Hyp-Gly), Arg-(Pro-Hyp-Gly), respectively)

^{1}H NMR spectra of the poly(Pro-Hyp-Gly), Suc-poly(Pro-Hyp-Gly), and Arg-poly(Pro-Hyp-Gly) were recorded on a JNM-ECX 500 spectrometer (JEOL, Tokyo, Japan). The concentration of the poly(Pro-Hyp-Gly), Suc-poly(Pro-Hyp-Gly), and Arg-poly(Pro-Hyp-Gly) were 4 mg/mL in deuterium oxide (D$_2$O; Cambridge Isotope Laboratories Inc., Andover, MA, USA) with tetramethylsilane (TMS; Cambridge Isotope Laboratories Inc.) as an internal reference. DS$_{COO^-}$ and DS$_{Arg^+}$ was calculated based on **Equation 1-4** and **1-5**, respectively.

$$DS_{COO^-} = \frac{\text{Peak area of Hyp-C}_\gamma H \text{ of Suc-(Pro-Hyp-Gly) (f}''\text{)}}{\text{Sum of peak areas of Hyp-C}_\gamma H \text{ of Pro-Hyp-Gly (f) and Suc-(Pro-Hyp-Gly)(f}''\text{)}} \times 100\% \qquad (1-4)$$

$$DS_{Arg^+} = \frac{\text{Peak area of Arg-C}_\alpha H \text{ (}l\text{)}}{\text{Sum of peak areas of Hyp-C}_\gamma H \text{ of Pro-Hyp-Gly (f) and Suc-(Pro-Hyp-Gly)(f}''\text{)}} \times 100\% \qquad (1-5)$$

1-2-4. PIC gel formation

Suc-poly(Pro-Hyp-Gly) (DS$_{COO^-}$ = 0.55) and Arg-poly(Pro-Hyp-Gly) (DS$_{Arg^+}$ = 0.58) solutions as precursors for PIC gel formation were concentrated by evaporation. Each concentrated precursor was dissolved in PBS by adding 10% of 10× concentrated PBS. The concentration of Suc-poly(Pro-Hyp-Gly) and Arg-poly(Pro-Hyp-Gly) in PBS were 16.7 and 22.7 mg/mL, respectively. PIC gels were fabricated by dropping Suc-poly(Pro-Hyp-Gly) and

Arg-poly(Pro-Hyp-Gly) solutions on microscope glass coverslips at molar ratio of carboxy

to guanidinium groups of 1:2, 1:1, and 2:1. The microscope glass coverslips containing

precursors were then placed in Petri dishes and incubated at 37 °C for 1 h. The obtained PIC

gels were washed with PBS to remove unreacted polypeptides and weighed to obtain the

weight of the hydrogels. The hydrogels were then washed with Milli-Q water and freeze-

dried to obtain dried gels. The gelation and swelling ratio of the PIC gels were calculated

using the following equations:

$$\text{Gelation (\%)} = \frac{\text{Weight of the PIC gel}}{\text{Total weight of precursor solutions}} \times 100\% \qquad (\mathbf{1-6})$$

$$\text{Swelling ratio} = \frac{\text{Weight of wet gel} - \text{weight of dried gel}}{\text{Weight of dried gel}} \qquad (\mathbf{1-7})$$

1-2-5. Encapsulation of rBMSCs into the PIC gel of poly(Pro-Hyp-Gly)

Bone marrow cells were obtained from the femora of a six-week-old female Wistar

rat, as described previously [10]. The rBMSCs obtained were suspended in α-minimum

essential medium (α-MEM; Gibco Invitrogen Corp. Grand Island, NY, USA) containing

20% fetal calf serum (FCS; HyClone, Logan UT, USA) and cultured in a 80 cm^2 tissue

culture flask (153732; Nalge Nunc International, Roskilde, Denmark) at 37 °C under 5%

CO_2. After three days, the attached cells were washed with PBS and treated with an aliquot

of 0.02% ethylenediamine tetraacetic acid and 0.25% trypsin. After centrifugation at 1,200

rpm for 5 min, the cells were suspended in 20% FCS/α-MEM. The rBMSC suspension was

then prepared at a density of 5 $\times$ 10^6 cells/mL.

Suc-poly(Pro-Hyp-Gly) (DS_{COO^-} = 0.58) and Arg-poly(Pro-Hyp-Gly) (DS_{Arg^+} =

0.52) solutions as precursors for PIC gel formation were concentrated by evaporation. Then,

each concentrated precursor was dissolved in PBS by adding 10% of 10× concentrated PBS.

The final concentration of Suc-poly(Pro-Hyp-Gly) and Arg-poly(Pro-Hyp-Gly) solution in

PBS were 18.1 and 21.6 mg/mL, respectively. The Suc-poly(Pro-Hyp-Gly) and

Arg-poly(Pro-Hyp-Gly) solutions in PBS were sterilized using Millex-HP filters (Merck

Millipore) with 0.45 µm of pore size. One hundred microliters of filter-sterilized

Arg-poly(Pro-Hyp-Gly) (2.1 µmol) in PBS was dropped on a 24-well tissue culture plate

(Nalge Nunc International). Ninety microliters of filter-sterilized Suc-poly(Pro-Hyp-Gly)

(2.1 µmol) in PBS was mixed with rBMSCs (5 × 10^4 cells) and then was dropped on the top

of a droplet of Arg-poly(Pro-Hyp-Gly). The mixture was incubated at 37 °C under 5% CO_2.

After one hour, 1 mL of 20% FCS/α-MEM was added into the well containing PIC gel.

The same number of rBMSCs without a PIC gel was cultured on another well of a

24-well tissue culture plate as a 2D control. The viable cells at days 1, 3, and 7 were

quantified using water soluble tetrazolium salt (WST-8; Dojindo Molecular Technologies

Inc. Kumamoto, Japan) according to the manufacturer's instructions. The optical density

(OD) at 450 nm was measured using a SpectraFluor Plus microplate reader (Tecan,

Männedorf, Switzerland).

The morphology of the rBMSCs in the PIC gel and on 2D control was observed using

a phase contrast microscope (Axiovert 100M, Carl Zeiss, Oberkochen, Germany) and

captured using an AxioCamHRc camera fixed to the microscope.

1-2-6. Osteogenic differentiation of rBMSCs in the PIC gel of poly(Pro-Hyp-Gly)

PIC gel of poly(Pro-Hyp-Gly) containing rBMSCs was fabricated as described in

Section *1-2-5* and incubated in 20% FCS/α-MEM at 37 °C under 5% CO_2. After 24 h, the

medium was changed to an osteogenic medium, which was 20% FCS/α-MEM supplemented

with 10 nM dexamethasone, 100 µM L-ascorbic acid-2-phosphate, and 10 mM β-

glycerophosphate, and incubated at 37 ºC under 5% CO_2 for 28 days. Every three or four

days, half of the medium was replaced with fresh osteogenic medium. Bone nodule

formation in the PIC gel and 2D control was observed using a phase contrast microscope

(Axiovert 100M).

1-2-7. Statistical analysis

All statistical evaluations were performed using the one-way analysis of variance routine of KaleidaGraph 4.5 (Synergy Software, Reading, PA, USA) followed by Tukey's honest significant difference test. A value of $p < 0.05$ was accepted as statistically significant. All data were presented as mean $\pm$ standard deviation, with $n = 3$.

1-3.   Results and Discussion

1-3-1. Synthesis and characterization of poly(Pro-Hyp-Gly), Suc-poly(Pro-Hyp-Gly), and

Arg-poly(Pro-Hyp-Gly)

GPC   profiles   of   poly(Pro-Hyp-Gly),   Suc-poly(Pro-Hyp-Gly),   and

Arg-poly(Pro-Hyp-Gly) are shown in **Figures 1-1(A), (B),** and **(C),** respectively**.** The GPC

profiles of the polypeptides showed a peak molecular weight more than 120 kDa based on

PEG standards, suggesting the high molecular weight of the obtained polypeptides.

CD   spectra   of   poly(Pro-Hyp-Gly),   Suc-poly(Pro-Hyp-Gly),   and

Arg-poly(Pro-Hyp-Gly) showed the appearance of a weak positive Cotton effect near 225

nm and a strong negative Cotton effect near 197 nm that are correlated to $n \to \pi^*$ and $\pi \to$

π^* transitions, respectively, of the amide bond in the polypeptide backbone (**Figure 1-2(A)**).

These results suggest that the polypeptides contain a collagen-like triple-helical structure

[11-14]. The ratio of positive to negative cotton peaks (R_{pn}) can be used to estimate

triple-helical content in the polypeptides [13,14]. A higher R_{pn} value indicates a higher triple-

helical content [13,14]. A (Pro-Hyp-Gly)$_{10}$ and calfskin collagen have an R_{pn} value about

0.12 [13-15]. Calculation of the R_{pn} of the poly(Pro-Hyp-Gly), Suc-poly(Pro-Hyp-Gly), and

Arg-poly(Pro-Hyp-Gly) showed that incorporation of succinyl group and arginine methyl

ester into the poly(Pro-Hyp-Gly) significantly increased the triple-helical content of the

poly(Pro-Hyp-Gly) ($p < 0.05$) (**Figure 1-2(B)**). These results may be caused by the

possibility of the succinyl group and arginine methyl ester participated in the formation of

water-mediated hydrogen bonding that can stabilize the triple-helical structure of the

polypeptides. Crystal structure analysis of triple-helical structure of a collagen-like peptide,

(Pro-Hyp-Gly)$_3$-Ile-Thr-Gly-Ala-Arg-Gly-Leu-Ala-Gly-Pro-Hyp-Gly-(Pro-Hyp-Gly)$_3$,

showed that arginine side chain in the peptide is able to make intrachain and interchain

connections to carbonyl backbone of the peptide through direct and/or water-mediated

hydrogen bonding [16]. Another result showed that glutamic acid and lysine side chains in

the triple-helical structure of a collagen-like peptide, (Pro-Hyp-Gly)$_4$-Glu-Lys-Gly-(Pro-

Hyp-Gly)$_5$, form direct and/or water-mediated intrachain and interchain hydrogen bonding

with carbonyl in the peptide backbone [17].

In addition, the inductive effect from electron withdrawing groups of the succinyl

group and arginine methyl ester may also stabilize the triple-helical structure of the

polypeptides [18].

Figure 1-3 shows the FTIR spectra of the poly(Pro-Hyp-Gly),

Suc-poly(Pro-Hyp-Gly), and Arg-poly(Pro-Hyp-Gly). Peaks at 1648 and 1552 cm^{-1}

observed in the spectra of the polypeptides were assigned as amide I and amide II of

poly(Pro-Hyp-Gly) backbone, respectively. A peak at 1735 cm^{-1} appeared in the spectrum of

Suc-poly(Pro-Hyp-Gly) was assigned to the carbonyl stretching of ester group of Suc-poly(Pro-Hyp-Gly) (**Figure 1-3(B)**), suggesting that succinyl group was successfully conjugated into Hyp residues of the poly(Pro-Hyp-Gly) through an ester bond. The FTIR spectrum of Arg-poly(Pro-Hyp-Gly) was similar to that of Suc-Poly(Pro-Hyp-Gly) (**Figure 1-3(C)**). The peak at 1735 cm^{-1} showed in the spectrum of Arg-Poly(Pro-Hyp-Gly) was assigned to the carbonyl stretching of ester groups of Suc-poly(Pro-Hyp-Gly) and arginine methyl ester.

The DS_{COO^-} of Suc-poly(Pro-Hyp-Gly) was verified by potentiometric titration using 0.02 M NaOH as a titrant (**Figure 1-4(A)**). Potentiometric titration revealed that DS_{COO^-} of Suc-poly(Pro-Hyp-Gly) was 58% of the hydroxy group of Hyp residues of Suc-poly(Pro-Hyp-Gly), with a pK_a of approximately 5.2 (**Figure 1-4(B)**).

DS_{Arg^+} was determined indirectly by measuring the remaining carboxy group that was not conjugated by arginine methyl ester. Based on the potentiometric titration curve of Arg-poly(Pro-Hyp-Gly) (**Figure 1-5**), DS_{Arg^+} was 52% of the hydroxy group of Hyp residues of poly(Pro-Hyp-Gly), indicating that about 90% of succinyl group has been conjugated by arginine methyl ester through an amide bond formation. However, this method can not be used to determine pK_a of the guanidinium group of Arg-poly(Pro-Hyp-Gly) because of its high pK_a value. The pK_a of guanidinium group was then estimated by titrating solution containing 0.5 mmol of arginine methyl ester and 1 mmol of 1 M HCl with 1 M NaOH. The

pK_a of the guanidinium group of the arginine methyl ester was estimated to be 12.4 (**Scheme 1-2** and **Figure 1-6**).

^{1}H NMR measurement was further used to characterize the poly(Pro-Hyp-Gly), Suc-poly(Pro-Hyp-Gly), and Arg-poly(Pro-Hyp-Gly). ^{1}H NMR spectrum of the poly(Pro-Hyp-Gly) showed peaks at 3.2 and 3.6 ppm, and 3.8 and 3.9 ppm that were assigned to Pro-C$_\delta$*H* and Hyp-C$_\delta$*H*, respectively, in the triple-helical structure of poly(Pro-Hyp-Gly) (**Figure 1-7(A)**) [19]. The result suggests that the poly(Pro-Hyp-Gly) contains a collagen-like triple-helical structure supporting the CD result described before.

^{1}H NMR spectrum of Suc-poly(Pro-Hyp-Gly) showed signals at 2.6 and 2.7 ppm which were assigned to four methylene protons of a succinyl group of Suc-poly(Pro-Hyp-Gly) (**Figure 1-7(B)**). Signals at 4.1 and 5.5 ppm are assigned to the proton of Hyp-C$_\delta$*H* and Hyp-C$_\gamma$*H*, respectively, that were shifted downfield because of electron-withdrawing effect of oxygen of the ester group of Suc-poly(Pro-Hyp-Gly). The electron-withdrawing group in the Hyp residue of poly(Pro-Hyp-Gly) will decrease the electron density around the Hyp-C$_\gamma$*H* and resulted in increase in the chemical shift [20]. The DS$_{COO^-}$ of Suc-poly(Pro-Hyp-Gly) was estimated by comparing peak area of Hyp-C$_\gamma$*H* of Suc-(Pro-Hyp-Gly) (5.5 ppm) with the peak area of Hyp-C$_\gamma$*H* of Pro-Hyp-Gly (4.6 ppm). From the ^{1}H NMR spectrum of Suc-poly(Pro-Hyp-Gly), the DS$_{COO^-}$ was estimated to be 55%.

The ^{1}H NMR spectrum of Arg-poly(Pro-Hyp-Gly) showed peaks at 1.7, 1.9, 3.3, 3.8,

and 4.5 ppm that were assigned to Arg-C$_\gamma$*H*, Arg-C$_\beta$*H*, Arg-C$_\delta$*H*, methyl proton, and

Arg-C$_\alpha$*H* of arginine methyl ester, respectively (**Figure 1-8**). The peak of Arg-C$_\alpha$*H* was

shifted downfield because of an amide bond formation between amino terminal of arginine

methyl ester and succinyl group in the Suc-poly(Pro-Hyp-Gly). Based on the ^{1}H NMR

spectrum, about 100% of succinyl group of Suc-poly(Pro-Hyp-Gly) has been conjugated by

arginine methyl ester.

1-3-2.   PIC gels of poly(Pro-Hyp-Gly)

PIC gels of poly(Pro-Hyp-Gly) were fabricated by simply mixing the polyanion,

Suc-poly(Pro-Hyp-Gly), and the polycation, Arg-poly(Pro-Hyp-Gly). To accomplish stable

PIC gel formation, high molecular weight and high charge densities of the polypeptides are

required [21]. However, polypeptides with higher DS_{COO^-} and DS_{Arg^+} may enhance their

water solubility and decrease gel formation. It has been reported that increased negative

surface charge of protein correlates strongly with increased protein solubity [22]. Therefore,

the polypeptides with about 50% of DS_{COO^-} and DS_{Arg^+} are thought to be appropriate for the

PIC gel formation.

The Suc-poly(Pro-Hyp-Gly) and Arg-poly(Pro-Hyp-Gly) were dissolved in PBS to

reproduce the pH and the osmotic pressure of cells' physiological microenvironment. At

physiological pH, the carboxy group of Suc-poly(Pro-Hyp-Gly) (pK_a = 5.2) and the

guanidinium group of Arg-poly(Pro-Hyp-Gly) (pK_a = 12.4) form carboxylate anion and

guanidinium cation, respectively, enabling ionic interaction between the polyions. To

reproduce a physiological cell microenvironment, the PIC gel formation was conducted at

physiological temperature, 37 °C. At this temperature, the polypeptide chain motion and

flexibility is higher than that at room temperature because of a weakening interaction

between the polypeptides chains in the triple-helical structure [12]. An increase in

polypeptide chain flexibility increases the possibility of the polypeptides to interact with

each other to form PIC gel. A schematic drawing of PIC gel formation is shown in **Scheme

1-3**. The PIC gel formation is initiated by macroscopic phase separation that is driven by

diffusion process of the polyanion and the polycation, and leads to the co-existence of dilute

and rich phases (**Figure 1-9**) [23-25]. The dilute phase contains counter ions and unreacted

polypeptides, while the rich phase contains PIC gel [23-25].

The degree of crosslinking of the obtained PIC gels was estimated by measuring

gelation and swelling ratio of the PIC gels in PBS. A gelation shows the fractions of

Suc-poly(Pro-Hyp-Gly) and Arg-poly(Pro-Hyp-Gly) that are included in the PIC gel

compared with the initial amount of them before PIC gel formation. A higher gelation

represents a higher amount of the polypeptides in the PIC gel. The results showed that

gelations of the PIC gels at molar ratio of carboxy to guanidinium groups of 1:2, 1:1, and

2:1 were 7.7 ± 1.6%, 19.9 ± 5.4%, and 9.2 ± 2.2%, respectively, and were significantly affected by the molar ratio ($p < 0.05$) (**Figure 1-10(A)**). The optimum gelation ratio was obtained at 1:1 molar ratio of carboxy to guanidinium groups suggesting that PIC gel formation is mainly caused by ionic interaction between the carboxy and guanidinium groups. These results are in agreement with the previous study by Kusumastuti *et al.*, who found that the formation of PIC gel of Suc-poly(Pro-Hyp-Gly) and chitosan was optimum at an equimolar concentration of carboxy group of Suc-poly(Pro-Hyp-Gly) and amino group of chitosan [8].

The swelling ratio represents the amount of PBS that can be absorbed by the PIC gel. The results showed that the PIC gels exhibited a high swelling ratio up to 22.8 ± 8.4 (**Figure 1-10(B)**). Hydrogels with high swelling ratio are preferable because they can facilitate diffusion of nutrients, waste, and oxygen during cell encapsulation [26,27].

1-3-3. Encapsulation of rBMSCs into the PIC gel of poly(Pro-Hyp-Gly)

To investigate cytocompatibility of the PIC gel of poly(Pro-Hyp-Gly) as a 3D scaffold that can support cell viability and proliferation, rBMSCs were simultaneously encapsulated into the PIC gel at an equimolar concentration of carboxy group of Suc-poly(Pro-Hyp-Gly) to guanidinium group of Arg-poly(Pro-Hyp-Gly). The rBMSCs

were first mixed with the polyanion, Suc-poly(Pro-Hyp-Gly), to minimize possible

inflammatory effects from the polycation, Arg-poly(Pro-Hyp-Gly) (**Scheme 1-4**). It has been

widely reported that polycations tend to induce an inflammatory response of the

encapsulated cells, which may cause cell necrosis [28,29]. The viability assay using WST-8

demonstrated that rBMSCs in the PIC gel were alive and proliferated (**Figure 1-11**),

indicating that the PIC gel is cytocompatible for simultaneous rBMSC encapsulation.

Phase contrast microscope observation of the rBMSCs in PIC gel showed that the

rBMSCs were homogeneously distributed in the hydrogel and formed a round shape

morphology (**Figure 1-12(A)**). Similar morphology was observed when breast

adenocarcinoma cells were encapsulated in alginate hydrogels [30]. Cells in the hydrogels

exhibit similar morphology with cells in *in vivo* microenvironment. In contrast, the rBMSCs

on 2D control exhibited a fibroblast-like morphology, and formed a confluent monolayer

(**Figures 1-12(B), (D), (F), and (H)**).

After three days of incubation, the rBMSCs in the PIC gel maintained their round

shape morphology (**Figure 1-12(C)**). Interestingly, some of the cells started to form

multicellular aggregates and the number of cell aggregates increased with incubation time

(**Figures 1-12(E) and (G)**). These results suggest that the PIC gel can facilitate cell

migration and the formation of cell aggregates. A similar result was obtained by Mie *et al*.,

who found that human lung adenocarcinoma epithelial A549 cells encapsulated in a self-

assemble peptide hydrogel formed multicellular aggregates during 7 days of incubation [31].

In cell aggregates, cell-cell and cell-ECM interactions are similar to cell interactions in *in vivo* cell microenvironment [32]. These results revealed that the rBMSCs within the PIC gel can adopt an *in vivo*-like cell morphology, suggesting that the PIC gel can reproduce the 3D cell microenvironment. While cell behavior on 2D culture does not represent *in vivo* cell behavior because the cells grown on a flat surface have usually more stretched morphology compared to that cells in the hydrogel [33].

1-3-4. Osteogenic differentiation of rBMSCs in the PIC gel of poly(Pro-Hyp-Gly)

To observe the ability of the PIC gel to support rBMSC differentiation into osteogenic lineages, the rBMSCs in the PIC gel were incubated in osteogenic medium for 28 days. Osteogenic differentiation of the rBMSCs was confirmed by the presence of bone nodule. Bone nodule contains calcium as a late marker for the osteogenic differentiation. The phase contrast microscope images of the rBMSCs in the PIC gel showed the formation of bone nodule (**Figure 1-13**), indicating the differentiation of the rBMSCs into osteogenic lineage.

1-4.   Conclusion

This chapter showed fabrication of physically-crosslinked poly(Pro-Hyp-Gly) hydrogel for rBMSC encapsulation. The hydrogel was fabricated by simply mixing polyanion and polycation derivatives of poly(Pro-Hyp-Gly) at physiological pH to form PIC gel. The polyanion, Suc-poly(Pro-Hyp-Gly), and the polycation, Arg-poly(Pro-Hyp-Gly), were synthesized by modifying hydroxy group of Hyp-residues of poly(Pro-Hyp-Gly) with succinyl group and arginine methyl ester, respectively. The obtained polypeptides contain a collagen-like triple-helical structure as revealed by CD and ^{1}H NMR analyses. PIC gel formation reached an optimum when an equimolar concentration of the carboxy group of Suc-poly(Pro-Hyp-Gly) and the guanidinium group of Arg-poly(Pro-Hyp-Gly) were mixed. This result suggests that the PIC gel formation is mainly caused by ionic interactions between the polyions of poly(Pro-Hyp-Gly). Simultaneous encapsulation of rBMSCs into the PIC gel was conducted at 1:1 molar ratio of carboxy to guanidinium groups of Suc-poly(Pro-Hyp-Gly) and Arg-poly(Pro-Hyp-Gly). Cell viability assay by WST-8 showed that the encapsulated rBMSCs were viable and proliferated in the PIC gel, suggesting the cytocompatibility of the PIC gel. To observe the morphology of the rBMSCs in the hydrogel, phase contrast microscope observation was conducted. As a 2D control, rBMSCs were cultured on a tissue culture dish. The results showed that the rBMSCs were homogeneously

distributed in the hydrogel as single cells and have a round shape morphology. After three

days, the rBMSCs formed multicellular aggregates. In contrast, the rBMSCs on 2D control

formed fibroblast-like morphology. The behavior of the rBMSCs in the PIC gel is more

reflective their behavior in *in vivo* microenvironment. Further incubation in osteogenic

medium showed the formation of bone nodules in the PIC gel, indicating the differentiation

of the encapsulated rBMSCs into osteogenic lineage. In conclusion, the PIC gel shows

promise as a 3D scaffold for tissue regeneration.

References

1. Yang JA, Yeom J, Hwang BW, Hoffman AS, Hahn SK. *In situ*-forming injectable hydrogels for regenerative medicine. Prog Polym Sci 2014;39:1973−1986.

2. Kharkar PM, Kiick KL, Kloxin AM. Designing degradable hydrogels for orthogonal control of cell microenvironments. Chem Soc Rev 2013;42:7335−7372.

3. Shoicet MS, Li RH, White ML, Winn SR. Stability of hydrogels used in cell encapsulation: An in vitro comparison of alginate and agarose. Biotechnol Bioeng 1996;50:374−381.

4. Nicodemus GD, Bryant SJ. Cell encapsulation in biodegradable hydrogels for tissue engineering applications. Tissue Eng Part B Rev 2008;14:149−165.

5. GD, Bryant SJ. Cell encapsulation in biodegradable hydrogels for tissue engineering applications. Tissue Eng Part B Rev 2008;14:149−165.

6. Banerjee A, Arha M, Choudhary S, Ashton RS, Bhatia SR, Schaffer DV, Kane RS. The influence of hydrogel modulus on the proliferation and differentiation of encapsulated neural stem cells. Biomaterials 2009;30:4695−4699.

7. Chan G, Mooney DJ. Ca^{2+} released from calcium alginate gels can promote inflammatory responses *in vitro* and *in vivo*. Acta Biomater 2013;9:9281−9291.

8. Kusumastuti Y, Shibasaki Y, Hirohara S, Kobayashi M, Terada K, Ando T, Tanihara M.

Encapsulation of rat bone marrow stromal cells using a poly-ion complex gel of chitosan and succinylated poly(Pro–Hyp–Gly). J Tissue Eng Regen Med 2017;11:869–876.

9. Kishimoto T, Morihara Y, Osanai M, Ogata S, Kamitakahara M, Ohtsuki C, Tanihara M. Synthesis of poly(Pro-Hyp-Gly)$_n$ by direct polycondensation of (Pro-Hyp-Gly)$_n$, where n = 1, 5, and 10, and stability of the triple-helical structure. Biopolymers 2005;79:163–172.

10. Saito A, Suzuki Y, Ogata S, Ohtsuki C, Tanihara M. Accelerated bone repair with the use of a synthetic BMP-2-derived peptide and bone-marrow stromal cells. J Biomed Mater Res A 2005;72A:77–82.

11. Shibasaki Y, Hirohara S, Terada K, Ando T, Tanihara M. Collagen-like polypeptide poly(Pro-Hyp-Gly) conjugated with Gly-Arg-Gly-Asp-Ser and Pro-His-Ser-Arg-Asn peptides enhances cell adhesion, migration, and stratification. Biopolymers Pep Sci 2011;96:302–315.

12. Tiffany ML, Krimm S. Effect of temperature on the circular dichroism spectra of polypeptides in the extended state. Biopolymers 1972;11:2309–2316.

13. Toniolo C, Formaggio F, Woody RW. Electronic circular dichroism of peptides. In: Berova N, Polavarapu PL, Nakanishi K, Woody RW, editors. Comprehensive chiroptical spectroscopy, Volume 2: Applications in stereochemical analysis of

synthetic compounds, natural products, and biomolecules. USA: John Wiley and Sons;2012. p.499–544.

14. Jenness DD, Sprecher C, Johnson WC Jr. Circular dichroism of collagen, gelatin, and poly(proline) II in the vacuum ultraviolet. Biopolymers 1976;15:513–521.

15. Akaike T, Kasai S, Nishizawa S, Kobayashi A, Miyata T. Hybrid biomaterials incorporated with living cells in modified collagens. In: Tsuruta T, Nakajima A, editors. Multiphase biomedical materials. The Netherlands: VSP;1989.p.73–87.

16. Kramer RZ, Bella J, Brodsky B, Berman HM. The crystal and molecular structure of a collagen-like peptide with a biologically relevant sequence. J Mol Biol 2001;311:131–147.

17. Kramer RZ, Venugopal MG, Bella J, Mayville P, Brodsky B, Berman HM. Staggered molecular packing in crystals of a collagen-like peptide with a single charged pair. J Mol Biol 2000;301:1191–1205.

18. Holmgren SK, Bretscher LE, Taylor KM, Raines RT. A hyperstable collagen mimic. Chem Biol 1999;6:63–70.

19. Li MH, Fan P, Brodsky B, Baum J. Two-dimensional NMR assignments and conformation of (Pro-Hyp-Gly)$_{10}$ and a designed collagen triple-helical peptide. Biochemistry 1993;32:7377–7387.

20. Silverstein RM, Webster FX, Kimle DJ. Spectrometric identification of organic

compounds. USA: John Wiley and Sons;2005.p.140−143.

21. Insua I, Wilkinson A, Fernandez-Trillo F. Polyion complex (PIC) particles: Preparation and biomedical applications. Eur Polym J 2016;81:198−215.

22. Kramer RM, Shende VR, Motl N, Pace CN, Scholtz. Toward a molecular understanding of protein solubility: increase negative surface charge correlates with increased solubility. Biophys J 2012;102:1907−1915.

23. Jha PK, Desai PS, Li J, Larson RG. pH and salt effects on the associative phase separation of oppositely charged polyelectrolytes. Polymers 2014;6:1414−1436.

24. Mende M, Petzold G, Buchhammer HM. Polyelectrolyte complex formation between poly(diallyldimethy-ammonium chloride) and copolymers of acrylamide and sodium-acrylate. Colloid Polym Sci 2002;280:342−351.

25. Staikos G, Bokias G, Bumbu GG. Water soluble polymer systems - phase behaviour and complex formation. In: Vasile C, Kulshreshtha AK, editors. Handbook of polymer blends and composites. UK: Rapra Technology Ltd.;2003. p.135−178.

26. Park H, Guo X, Temenoff JS, Tabata Y, Caplan AI, Kasper FK, Mikos AG. Effect of swelling ratio of injectable hydrogel composites on chondrogenic differentiation of encapsulated rabbit marrow mesenchymal stem cells in vitro. Biomacromolecules 2009;10:541−546.

27. Gasperini L, Mano JF, Reis RL. Natural polymers for the microencapsulation of cells.

J R Soc Interface 2014;11:20140817.

28. Strand BL, Ryan TL, Veld PI, Kulseng B, Rokstad AM, Skjåk-Braek G, Espevik T. Poly-L-Lysine induces fibrosis on alginate microcapsules via the induction of cytokines. Cell Transplant 2001;10:236–275.

29. Bhatia SR, Khattak SF, Roberts SC. Polyelectrolytes for cell encapsulation. Curr Opin Colloid Interface Sci 2005;10:45–51.

30. Cavo M, Fato M, Peñuela L, Beltrame F, Raiteri R, Scaglione S. Microenvironment complexity and matrix stiffness regulate breast cancer cell activity in a 3D in vitro model. Sci Rep 2016;6:35367.

31. Mie M, Oomuro M, Kobatake E. Hydrogel scaffolds composed of genetically synthesized self-assembling peptides for three-dimensional cell culture. Polym J 2013;45:504–508.

32. Edmondson R, Broglie JJ, Adcock AF, Yang L. Three-dimensional cell culture systems and their applications in drug discovery and cell-based biosensors. Assay Drug Dev Technol 2014;12:207–218.

33. Zhang J, Yang Z, Li C, Dou Y, Li Y, Thote T, Wang D, Ge Z. Cells behave distinctly within sponges and hydrogels due to differences of internal structure. Tissue Eng Part A 2013;19:2166–2175.
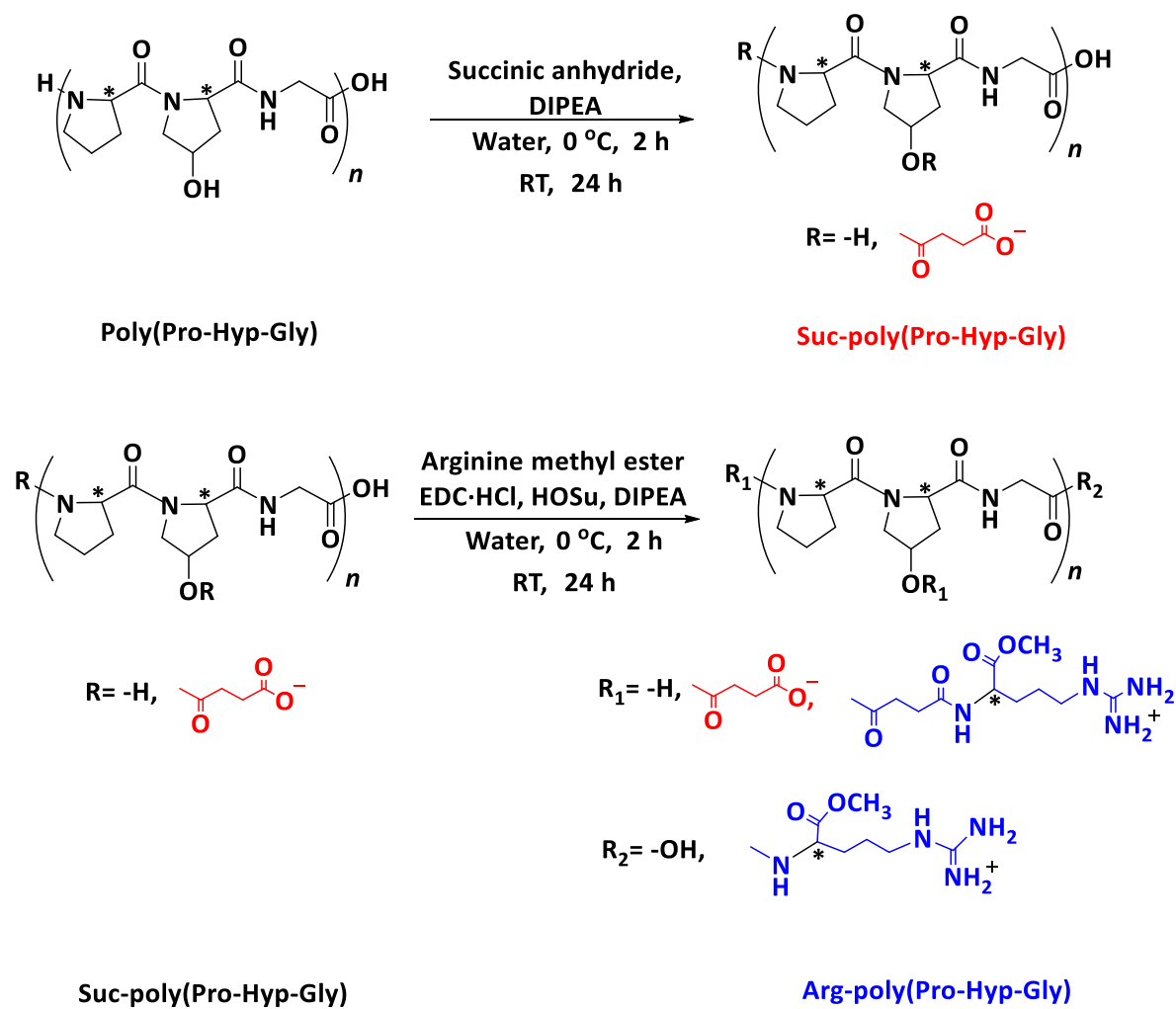
Scheme 1-1 Synthesis of Suc-poly(Pro-Hyp-Gly) and Arg-poly(Pro-Hyp-Gly). * indicate L-isomers.
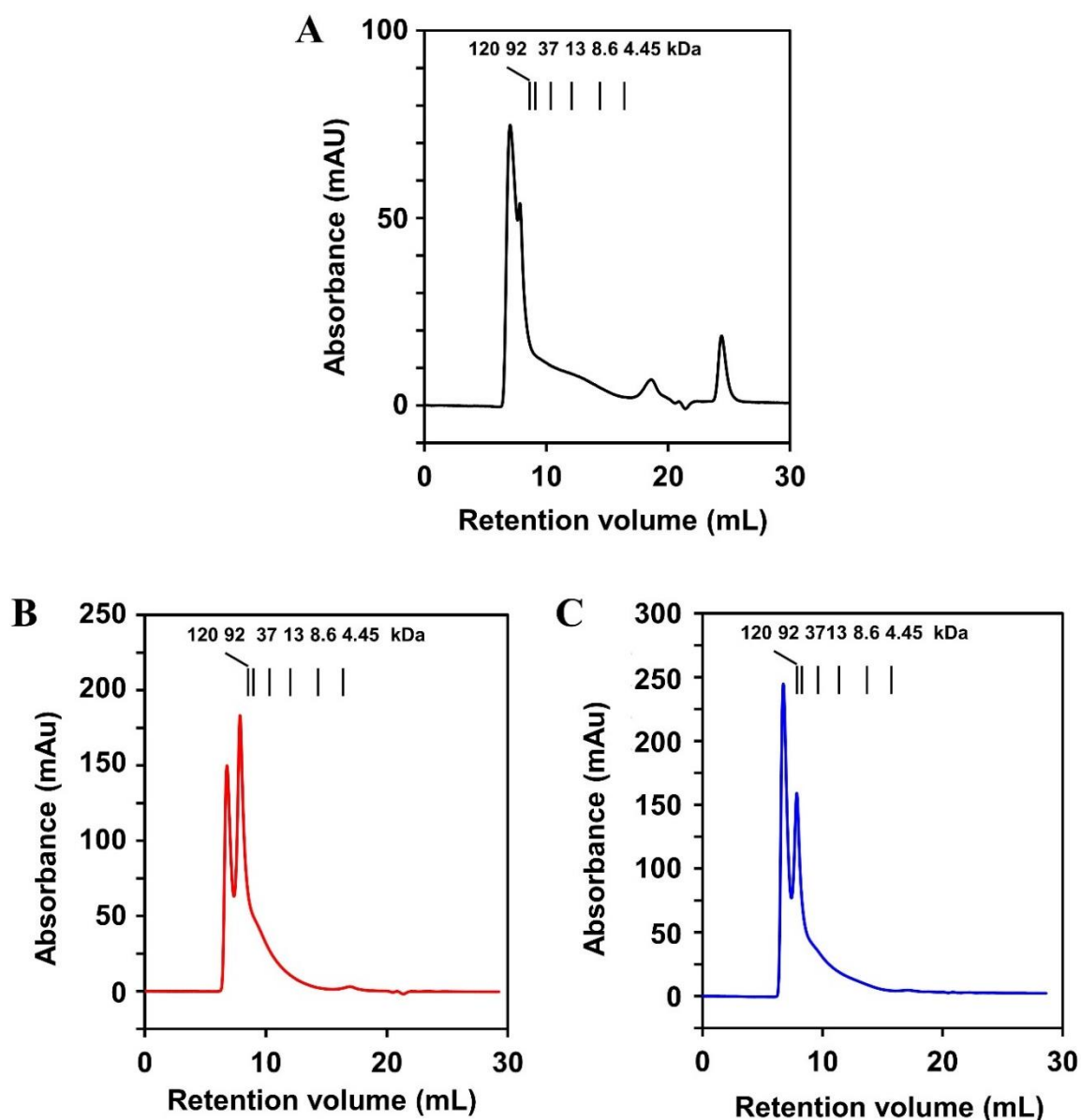
Figure 1-1 GPC profiles of poly(Pro-Hyp-Gly) (A), Suc-poly(Pro-Hyp-Gly) (B), and Arg-poly(Pro-Hyp-Gly) (C). The concentration of each sample was 0.5 mg/mL in PBS.
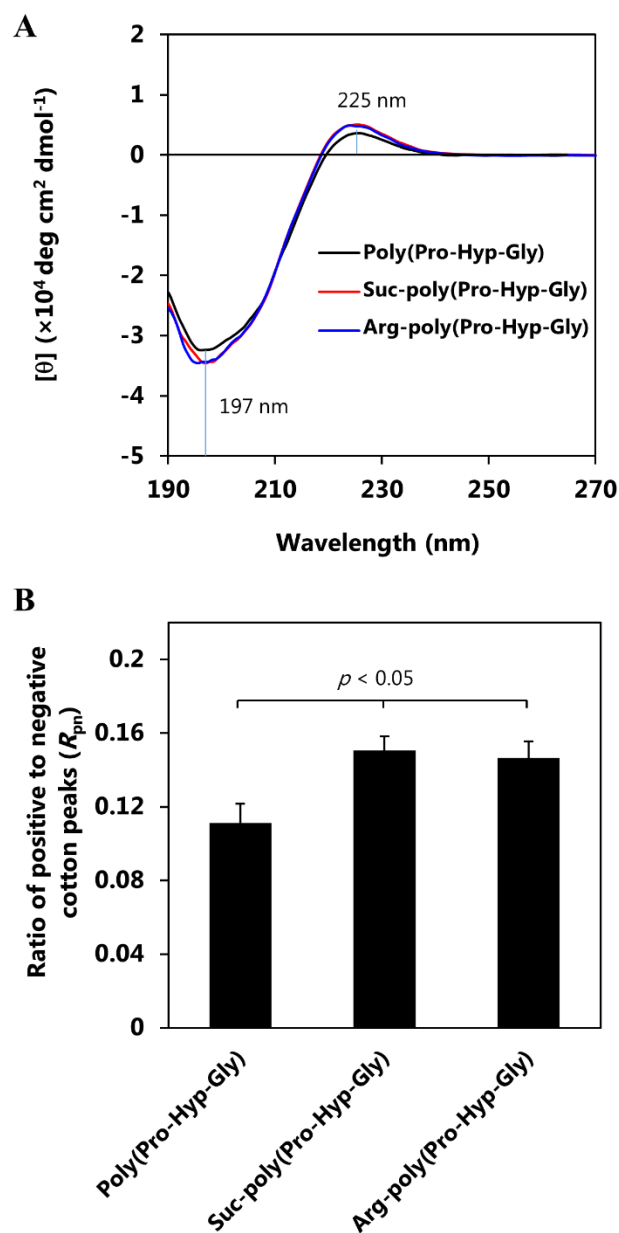
Figure 1-2 CD spectra (A) and R_{pn} value (B) of poly(Pro-Hyp-Gly), Suc-poly(Pro-Hyp-Gly), and Arg-poly(Pro-Hyp-Gly). The concentration of each sample was 0.25 mg/mL in Milli-Q water. Milli-Q water was used as a blank.
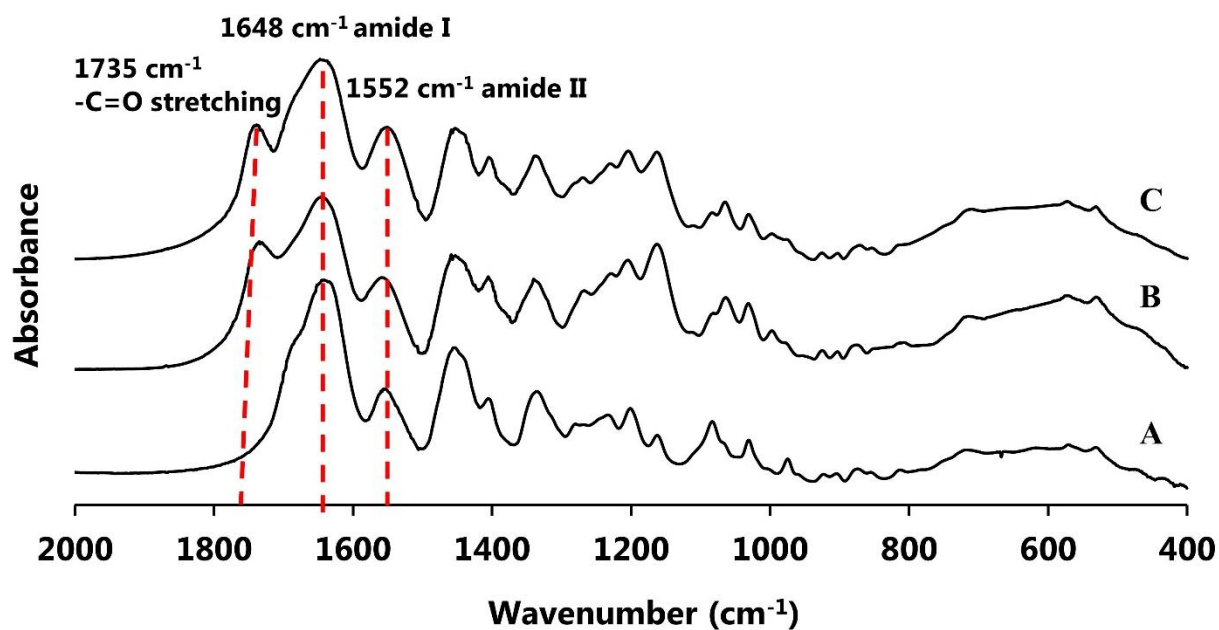
Figure 1-3 FTIR spectra of poly(Pro-Hyp-Gly) (A), Suc-poly(Pro-Hyp-Gly) (B), and Arg-poly(Pro-Hyp-Gly) (C). FTIR measurement was conducted using KBr method with resolution 1 cm^{-1} at room temperature.
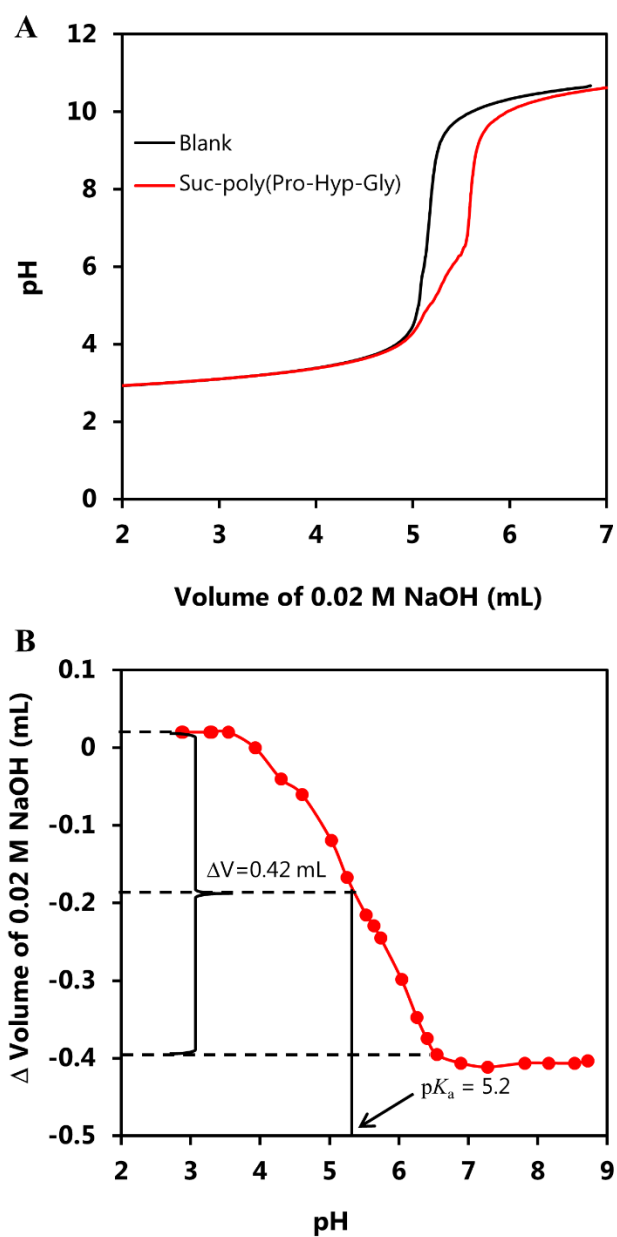
Figure 1-4 Potentiometric titration curves of a solution containing Suc-poly(Pro-Hyp-Gly) and 0.02 M HCl (A). Difference volume of titrant, 0.02 M NaOH, for blank and sample titrations (B).
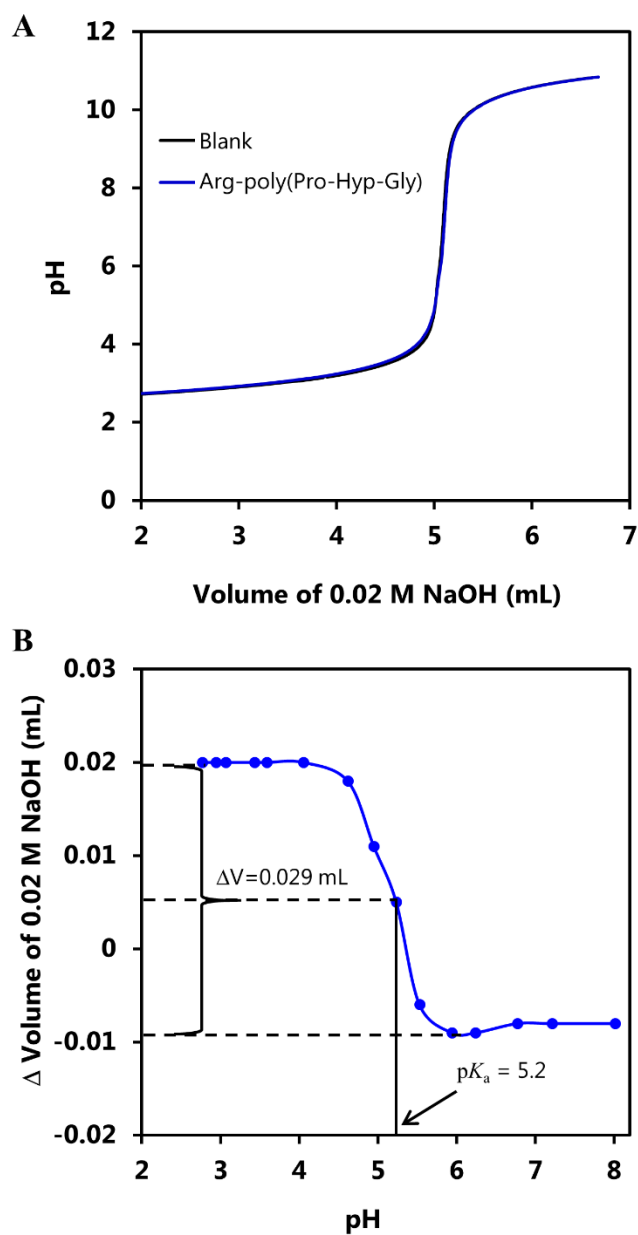
Figure 1-5 Potentiometric titration curves of a solution containing Arg-poly(Pro-Hyp-Gly) and 0.02 M HCl (A). Difference volume of titrant, 0.02 M NaOH, for blank and sample titrations (B).
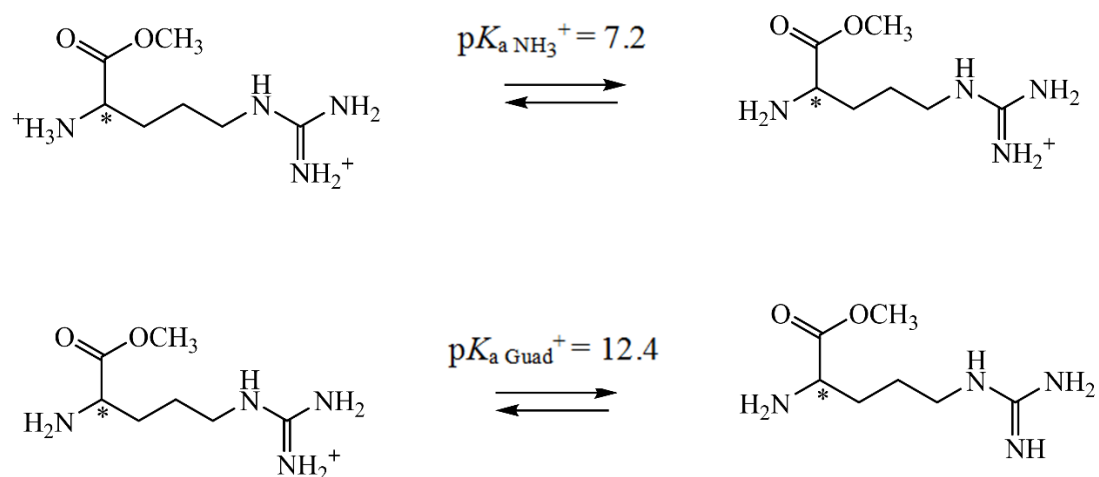
Scheme 1-2 Ionization of arginine methyl ester in water. $pK_{a\ NH_3}^+$ and $pK_{a\ Guad}^+$ are pK_a of amino and guanidinium groups of arginine methyl ester, respectively. * indicates L-isomer.
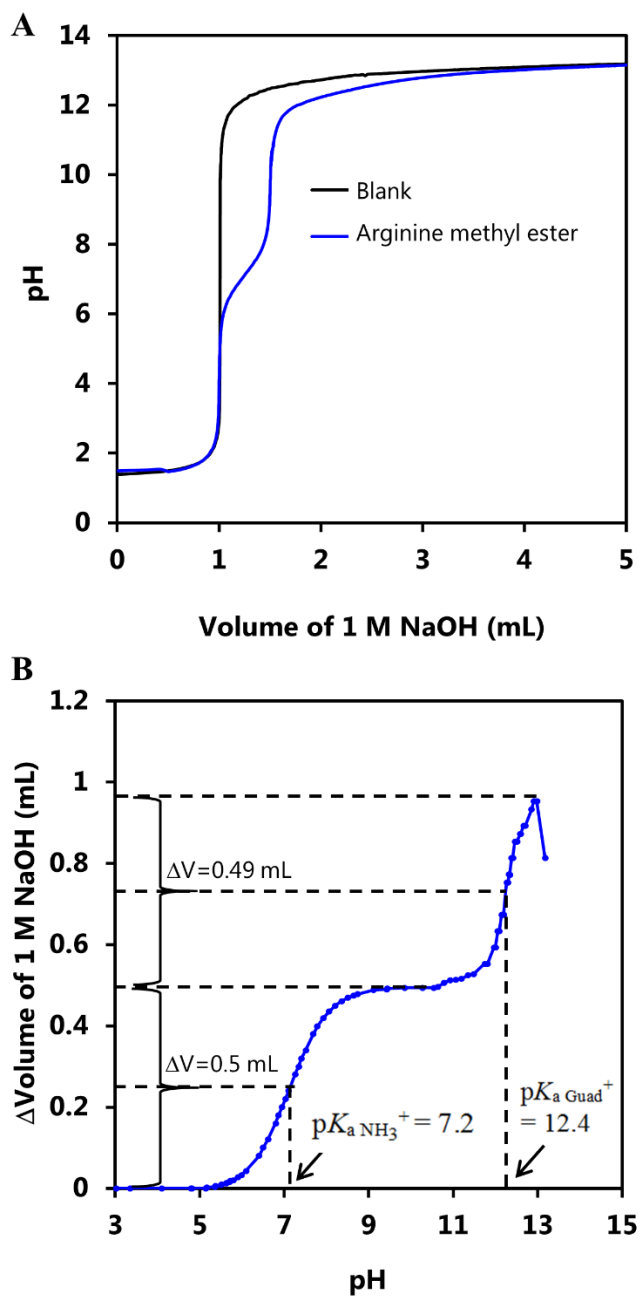
Figure 1-6 Potentiometric titration curves of a solution containing arginine methyl ester and 1 M HCl (A). Difference volume of titrant, 1 M NaOH, for blank and sample titrations (B).
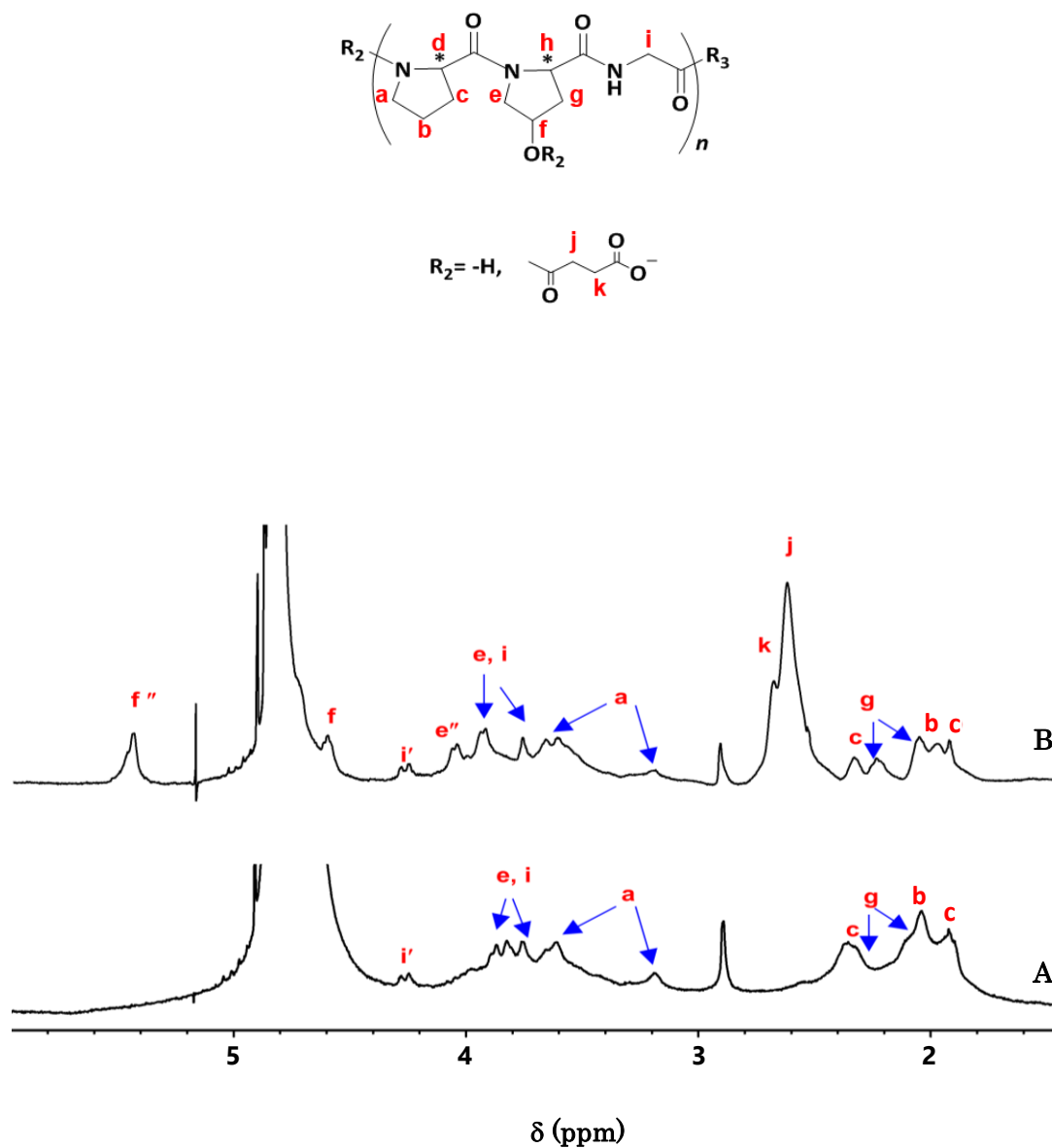
Figure 1-7 ^{1}H NMR spectra of poly(Pro-Hyp-Gly) (A) and Suc-poly(Pro-Hyp-Gly) (B). i′ is Gly-CαH in non-triple-helical structure of poly(Pro-Hyp-Gly). e″ and f ″ are Hyp-CδH and Hyp-CγH, respectively, which appeared because of withdrawing effect of succinyl group of Suc-poly(Pro-Hyp-Gly). The concentration of each sample was 4 mg/mL in D$_2$O with TMS as an internal standard. * indicate L-isomers.
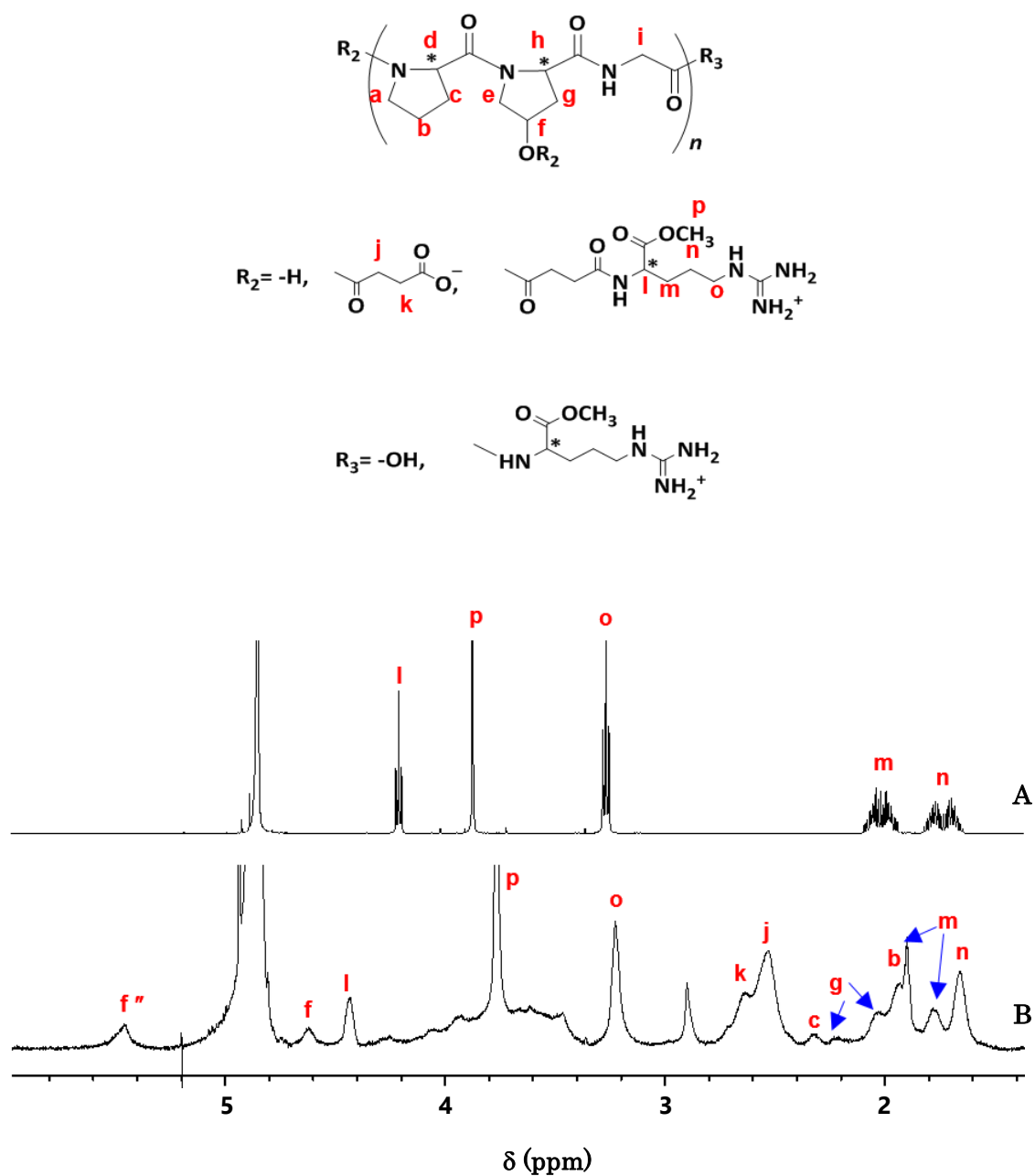
Figure 1-8 ^{1}H NMR spectra of arginine methyl ester (A) and Arg-poly(Pro-Hyp-Gly) (B). f″ is Hyp-CγH which appeared because of withdrawing effect of succinyl group of Suc-poly(Pro-Hyp-Gly). The concentration of each sample was 4 mg/mL in D$_2$O with TMS as an internal standard. * indicate L-isomers.
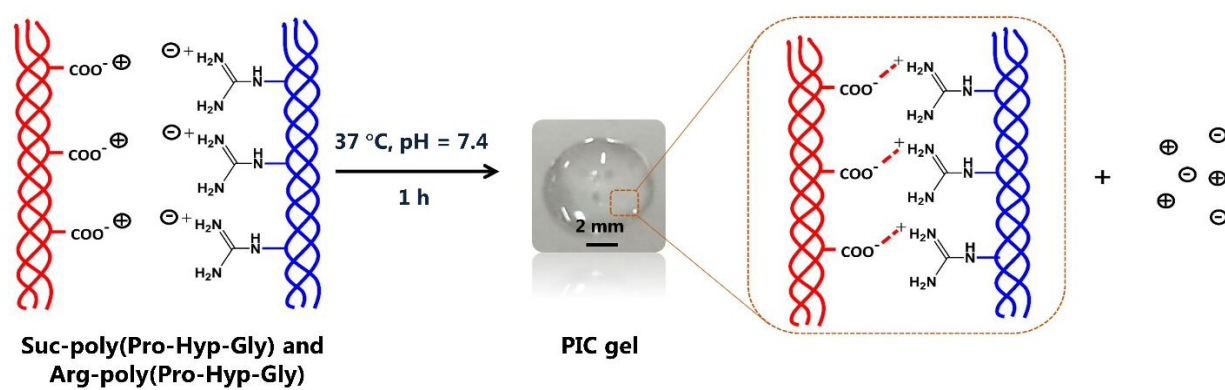
Scheme 1-3 Schematic diagram of PIC gel formation of Suc-poly(Pro-Hyp-Gly) and Arg-poly(Pro-Hyp-Gly). The scale bar represents 2 mm.
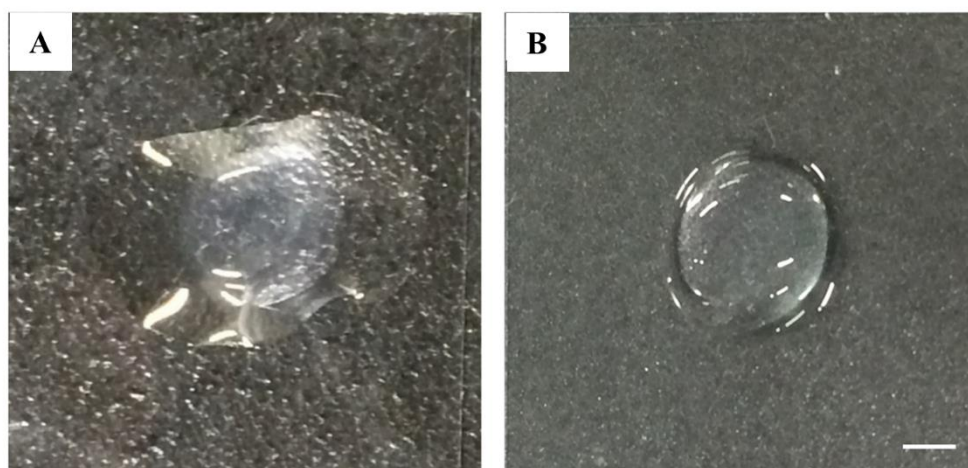
Figure 1-9 Phase separation during PIC gel formation (A) and PIC gel after washing (B).

Scale bar represents 2 mm.
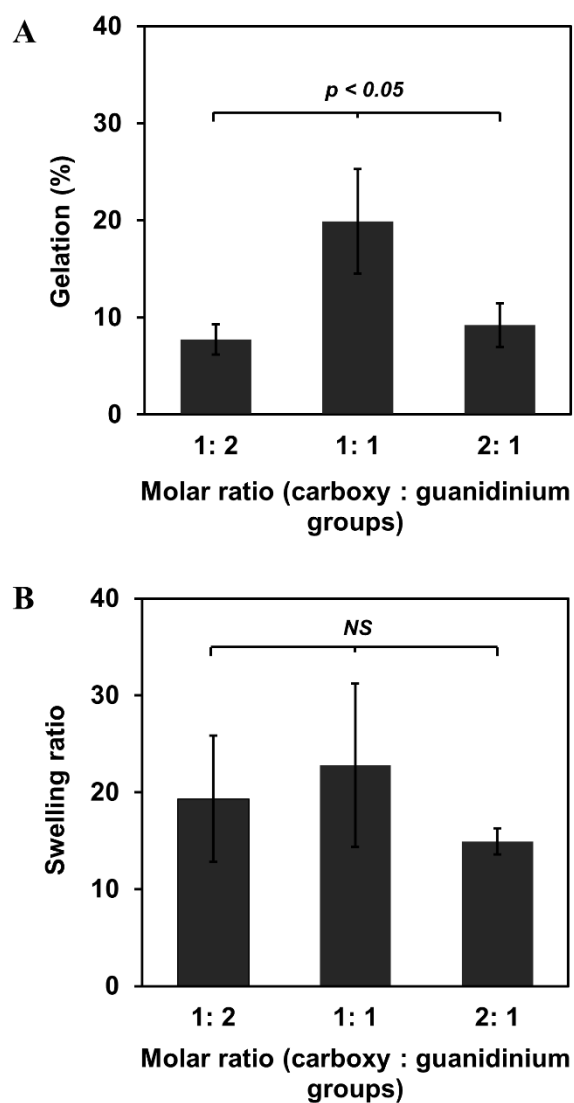
Figure 1-10 Gelation (A) and swelling ratio (B) of PIC gels of poly(Pro-Hyp-Gly) obtained at different molar ratios of carboxy to guanidinium groups. *NS* = Not significant.
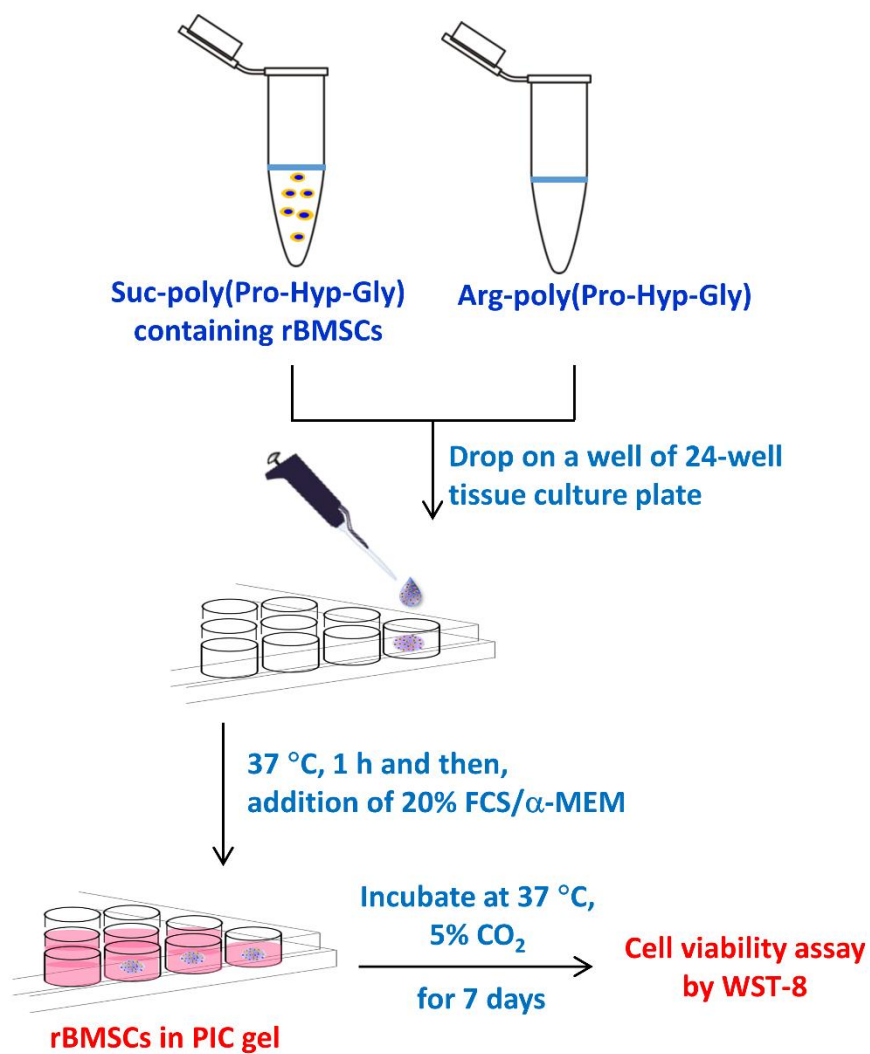
Scheme 1-4 Simultaneous encapsulation of rBMSCs into the PIC gel of poly(Pro-Hyp-Gly).
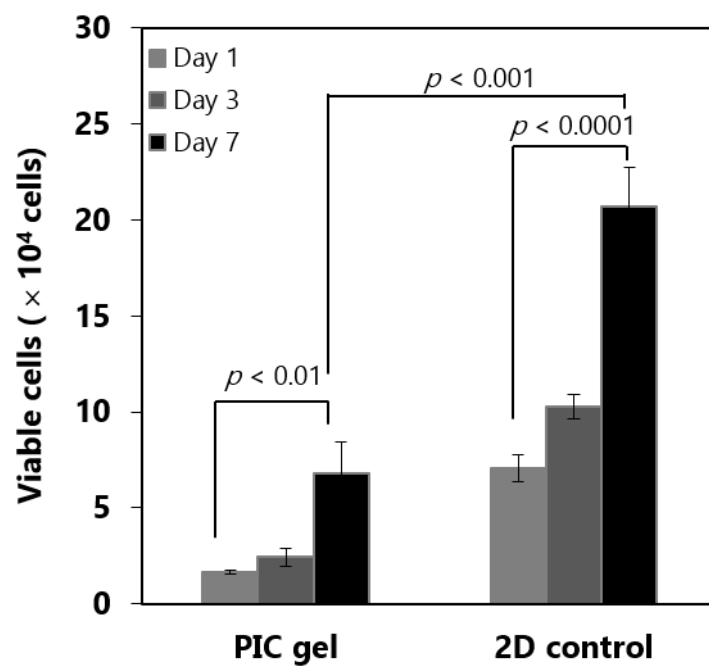
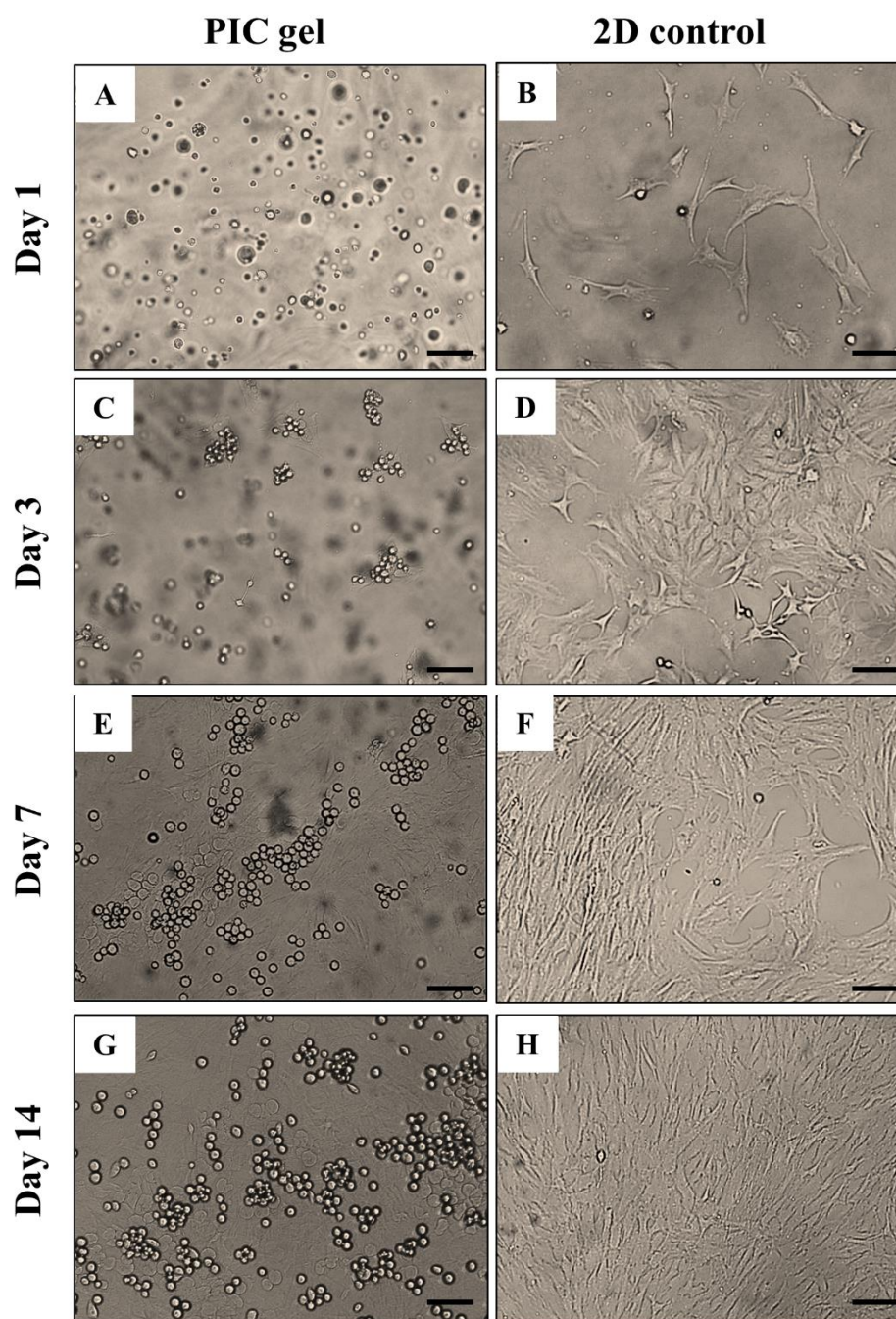**Figure 1-11** Cell viability of rBMSCs in the PIC gel of poly(Pro-Hyp-Gly) and a tissue culture plate as a 2D control.

PIC gel   **2D control**

Figure 1-12 Phase contrast microscope images of rBMSCs in the PIC gel of poly(Pro-Hyp-Gly) and on a tissue culture plate as a 2D control. Red arrows indicate cell aggregates. Bars represent 100 μm.
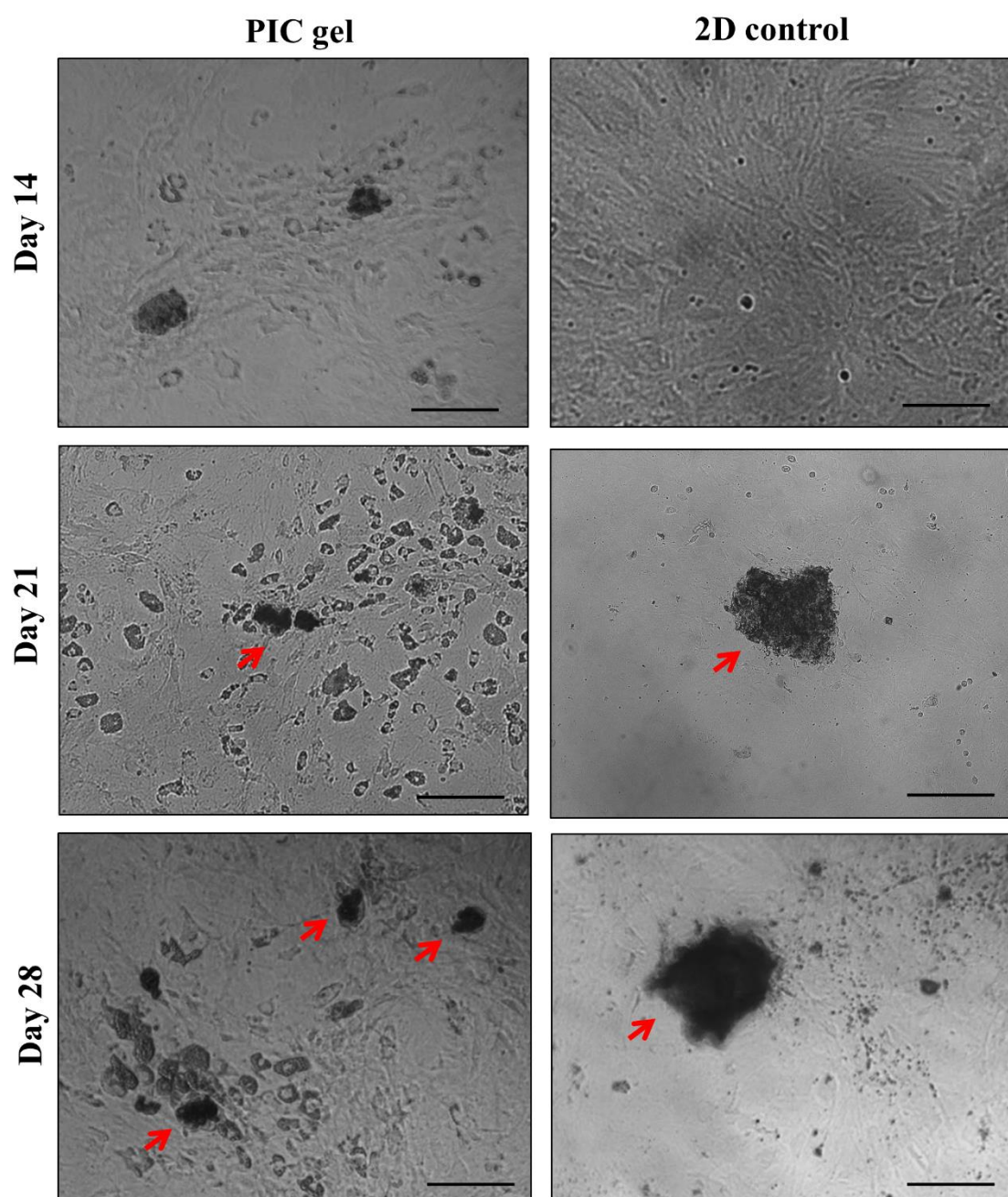
Figure 1-13 Bone nodule formation of rBMSCs in the PIC gel of poly(Pro-Hyp-Gly) and on a tissue culture dish as a 2D control. Red arrows indicate bone nodules. Bars represent 100 μm.

CHAPTER 2

Calcium Deposition in Photocrosslinked Poly(Pro-Hyp-Gly) Hydrogels Encapsulated Rat Bone Marrow Stromal Cells

2-1. Introduction

Photocrosslinking has attracted significant interests for the creation of hydrogels for tissue regeneration because of their rapid and mild reaction conditions, which allow simultaneous cell encapsulation at near body temperature and pH [1-3]. Various studies to encapsulate cells within photocrosslinked hydrogels have been conducted using UV and visible light irradiation [2,4-7].

Photocrosslinking needs photoinitiators that have absorption at UV or visible wavelength to produce radicals to initiate photocrosslinking reaction [1-7]. There are two types of photoinitiator, type I (cleavage type) and type II (proton transfer type) photoinitiators. Among the photoinitiators that have already investigated, a type I photoinitiator, Irgacure 2959, has been mainly used for photocrosslinking and it showed

cytocompatibility to encapsulate various cell lines at concentrations of 0.03–0.10% (w/v)

[2]. However, Irgacure 2959 has low water solubility and low molar absorptivity at 365 nm

(ε < 10 M^{-1} cm^{-1} at 365 nm), meaning it can only be activated using UV light which has a

potential to damage cellular DNA [2]. Visible light photocrosslinking is more feasible to

encapsulate cells because of its potential non-cytotoxicity [5].

Visible light photoencapsulation is commonly achieved by type II photoinitiator

system which typically consists of a dye as a photoinitiator and a tertiary amine as a

co-initiator [5]. Eosin Y is a type II photoinitiator that has been widely used as a

photoinitiator for visible light photocrosslinking because of its high water solubility,

cytocompatibility, and high molar absorptivity ($\varepsilon \sim 6.08 \times 10^4$ M^{-1} cm^{-1} at 539 nm) [7,8].

The photocrosslinking system containing eosin Y has been used to encapsulate various cells,

such as hMSCs [5] and murine fibroblasts [6] into the hydrogels. However, there are several

problems regarding to this system, such as cytotoxicity of the co-initiator at high

concentration and the generated radicals during the photocrosslinking reaction [5-7].

In this study, a cytocompatible hydrogel for cell survival and osteogenic

differentiation was developed by optimizing visible light photocrosslinking system

containing eosin Y as a photoinitiator and triethanolamine as a co-initiator. Acrylates and

methacrylates are the most common reactive group used for photocrosslinking reaction

because they react rapidly with radicals formed during light irradiation [9]. However,

molecules containing acrylates are more toxic than molecules containing methacrylates [10].

Therefore, poly(Pro-Hyp-Gly) modified with methacrylate group was used in this study. The

hydrogel formation was optimized by changing eosin Y and methacrylated

poly(Pro-Hyp-Gly) concentrations, and irradiation time. The influences of the hydrogel

properties, such as polymer network density and swelling ratio, on the rBMSC viability,

proliferation, and osteogenic differentiation were then evaluated.

2-2.   Materials and Methods

2-2-1. Materials

Pro-Hyp-Gly, HOBt, and EDC·HCl were purchased from the Peptide Institute. DIPEA and dimethylformamide (DMF) were purchased from Applied Biosystems. Methacrylic anhydride, eosin Y disodium salt, triethanolamine, NVP, dexamethasone, L-ascorbic acid 2-phosphate sesquimagnesium salt hydrate, and β-glycerophosphate disodium salt hydrate were purchased from Sigma-Aldrich. Other reagents were purchased from Wako Pure Chemical Industries Ltd. Amino acids used in this study are all in L-form.

2-2-2. Synthesis and characterization of poly(Pro-Hyp-Gly) and methacrylated poly(Pro-Hyp-Gly)

Poly(Pro-Hyp-Gly) was synthesized in accordance with previous reports, but with slight modifications [11,12]. Briefly, Pro-Hyp-Gly (0.70 mmol) and HOBt (0.14 mmol) were dissolved in PB and mixed with EDC·HCl (1.04 mmol). The mixture was stirred at 400 rpm for 75 min at 4 °C and the temperature was then raised to 20 °C. The reaction was terminated by the addition of PBS and dialyzed against Milli-Q water for five days at 4 °C using a

dialysis membrane (MWCO = 14000 Da, UC20-32-100, EIDIA Co., Ltd.) to remove any residual reagents.

Methacrylated poly(Pro-Hyp-Gly) was synthesized by reacting the hydroxy group of Hyp residues of poly(Pro-Hyp-Gly) with a 20-fold molar excess of both methacrylic anhydride and DIPEA. Briefly, methacrylic anhydride (2.4 mmol) solution in DMF and DIPEA (2.4 mmol) were added to a poly(Pro-Hyp-Gly) (0.12 mmol) solution in PB. The mixture was stirred on ice for 1 h and then, for 24 h at room temperature. After 24 h, the reaction was terminated by the addition of PBS. The methacrylated poly(Pro-Hyp-Gly) obtained was purified by dialysis against Milli-Q water for seven days at 4 °C.

The poly(Pro-Hyp-Gly) and methacrylated poly(Pro-Hyp-Gly) obtained were analyzed by GPC and CD. The GPC analysis of the polypeptides at a concentration of 0.5 mg/mL in PBS was carried out using an ÄKTA purifier system on a Superdex 200 HR 10/300 GL column (GE Healthcare Biosciences). The elution buffer was PBS and the flow rate was 0.5 mL/min at room temperature with the detection wavelength of 215 nm. The molecular weight of the obtained polypeptides was calculated based on PEG standards.

CD spectra of the polypeptides at a concentration of 0.25 mg/mL in Milli-Q water were recorded from 270–190 nm using a quartz cell with an optical path length of 0.1 cm on a J-820 spectropolarimeter (Jasco) at room temperature.

Conjugation of methacrylate group into the poly(Pro-Hyp-Gly) was confirmed by

FTIR and ^{1}H NMR spectroscopies. The FTIR spectra of the poly(Pro-Hyp-Gly) and

methacrylated poly(Pro-Hyp-Gly) were recorded at 400–4000 cm^{-1} using a Spectrum One

FTIR spectrometer (PerkinElmer) based on the KBr method. The ^{1}H NMR and ^{1}H

homonuclear correlation spectroscopy (COSY) spectra of the poly(Pro-Hyp-Gly) and

methacrylated poly(Pro-Hyp-Gly) were recorded on a JNM-ECX 500 spectrometer (JEOL).

The concentration of the polypeptides was 4 mg/mL in D_2O with TMS as an internal

reference. Based on the ^{1}H NMR spectrum, the degree of methacrylation (DS$_{Met}$) was

calculated by comparing peak areas of vinyl protons of methacrylate group with the sum of

the peak areas of Pro-C$_\delta H$, Hyp-C$_\delta H$, and Gly-C$_\alpha H$ of Pro-Hyp-Gly (**Equation 2-1**).

$$
DS_{Met} = \frac{\text{Number of protons of Pro-C}_\delta H, \ \text{Hyp-C}_\delta H, \text{and Gly-C}_\alpha H}{\text{Peak areas of Pro-C}_\delta H, \ \text{Hyp-C}_\delta H, \ \text{and Gly-C}_\alpha H} \times
$$

$$
\frac{\text{Peak areas of vinyl protons of methacrylated-(Pro-Hyp-Gly)}}{\text{Number of vinyl protons of methacrylated-(Pro-Hyp-Gly)}} \times 100\% \qquad (\mathbf{2-1})
$$

2-2-3. Fabrication of photocrosslinked poly(Pro-Hyp-Gly) hydrogels

Methacrylated poly(Pro-Hyp-Gly) was dissolved in PBS containing 10−30 μM eosin

Y, 10 mM triethanolamine, and 1 mM NVP. The final concentration of methacrylated

poly(Pro-Hyp-Gly) in the solution was 20−50 mg/mL. Photocrosslinked hydrogels were

prepared by dropping 30 μL of the solution on microscope glass coverslips covered by 3

mm-height of silicon rubber with circular holes punched out (diameter = 5 mm). The

solution was photocrosslinked under visible light using a KL 1500 LCD microscope

illuminator (Carl Zeiss) for 3 or 5 min. The hydrogels obtained were washed with PBS and

weighed. The hydrogels were then extensively washed with Milli-Q water and freeze-dried

to obtain dried gels. The dried gels were swollen in PBS at 37 ºC for 24 h. Gelation (%) and

swelling ratio were obtained as defined by following equations:

$$\text{Gelation (\%)} = \frac{\text{Weight of the obtained hydrogel}}{\text{Total weight of the precursor solutions}} \times 100\,\% \qquad (2-2)$$

$$\text{Swelling ratio} = \frac{\text{Weight of swollen gel} - \text{weight of dried gel}}{\text{Weight of dried gel}} \qquad (2-3)$$

2-2-4. Cytotoxicity of NVP, triethanolamine, and methacrylated poly(Pro-Hyp-Gly)

The rBMSC suspension was cultured at a density of 1,250 cells/well in a 96-well

tissue culture plate (167008; Nalge Nunc International) and incubated at 37 ºC under 5%

CO_2. After 24 h, NVP, triethanolamine or methacrylated poly(Pro-Hyp-Gly) solution in 20%

FCS/α-MEM was sterilized using Millex-HP filters with 0.22 μm of pore size. The

filter-sterilized solutions were then added to the wells containing rBMSCs and incubated for

further 24 h. The same number of rBMSCs without any addition of samples were cultured

in another well of 96-well plate as a control. Viable cells were quantified with WST-8 (Dojindo Molecular Technologies Inc.) according to the manufacturer's instruction. The optical density (OD) at 450 nm was measured using a SpectraFluor Plus microplate reader (Tecan). The relative cell viability was calculated, as defined by:

$$\text{Relative cell viability (\%)} = \frac{OD_{450} \text{ of sample} - OD_{450} \text{ medium}}{OD_{450} \text{ of control} - OD_{450} \text{ medium}} \times 100\% \qquad (2-4)$$

2-2-5. *Encapsulation of rBMSCs into the photocroslinked poly(Pro-Hyp-Gly) hydrogels*

Twenty microliters of a filter-sterilized solution containing 20–50 mg/mL methacrylated poly(Pro-Hyp-Gly), 20 μM eosin Y, 10 mM triethanolamine, and 5 mM NVP in 20% FCS/α-MEM was homogeneously mixed with rBMSCs (2.5×10^4 cells). The mixture was dropped onto a 35 mm bacteriological petri dish (35-1008; Falcon-Becton Dickinson, New Jersey, USA) and irradiated under visible light using a KL 1500 LCD microscope illuminator for 5 min. The obtained hydrogel was washed immediately with 2 mL of 20% FCS/α-MEM several times to remove free cells and to minimize cytotoxicity caused by the remaining photocrosslinking components. The hydrogel was then cultured in 2 mL of 20% FCS/α-MEM at 37 °C under 5% CO_2 atmosphere for seven days. Every two or three days, half of the medium was replaced with fresh medium. On the day of the viability

assay, hydrogels containing cells were transferred to a 24-well tissue culture plate. Viable cells in the hydrogels were then quantified using WST-8 assay. Viable cells in the hydrogel was stained using a Live-Dead staining kit (BioVision; 501-100, Milpitas, CA, USA) according to the manufacturer's instructions.

2-2-6. Osteogenic differentiation of rBMSCs in the photocroslinked poly(Pro-Hyp-Gly) hydrogels

Photocrosslinked hydrogels (20−50 mg/mL of methacrylated poly(Pro-Hyp-Gly)) containing rBMSCs were cultured in 2 mL of 20% FCS/α-MEM. After 24 h, the medium was changed to an osteogenic medium, which was 20% FCS/α-MEM supplemented with 10 nM dexamethasone, 100 µM L-ascorbic acid-2-phosphate, and 10 mM β-glycerophosphate, and incubated at 37 °C under 5% CO_2 atmosphere for 28 days. Every two or three days, half of the medium was replaced with fresh osteogenic medium.

At day 28, the cells in the hydrogels were fixed with 4% formaldehyde solution in PBS for 2 h at 4 °C, washed with PBS and treated twice with 20% sucrose in PBS for 4 h at 4 °C. The hydrogels were embedded into optimal cutting temperature compound (Sakura Finetek, Tokyo, Japan) and cut into 6 µm slices using a Leica CM1100 cryotome (Leica Microsystems, Wetzlar, Germany).

Calcium deposition on the slices was observed without gold coating using a scanning electron microscope (SEM; Model S-4800, Hitachi, Tokyo, Japan) at an acceleration of 15 kV. The calcium deposition was also observed with Alizarin Red S and von Kossa staining. For the staining, the slices were fixed on glass slides coated with Matsunami adhesive silane (Matsunami Glass, Tokyo, Japan), dried at room temperature, and washed three times with PBS.

Alizarin Red S staining was conducted by incubating the fixed slices in 2% Alizarin Red S solution (pH 4.1–4.3) for 30 min at room temperature. The excess stain was removed by washing four times with Milli-Q water [13]. The stained slices were dried at room temperature and observed with an optical microscope (Axioplan 2, Carl Zeiss).

Von Kossa staining was conducted by incubating the fixed slices in 1% silver nitrate solution for 45 min under UV light at room temperature. The excess stain was removed by washing four times with Milli-Q water. The slices were then treated with 3% sodium thiosulfate for 5 min, washed four times with Milli-Q water [13], dried at room temperature, and observed with the optical microscope. The positively stained area in the hydrogels was quantified using ImageJ software (National Institutes of Health, Bethesda, MD, USA).

2-2-7. Statistical analysis

All statistical evaluations were performed using the one-way analysis of variance routine of KaleidaGraph 4.5 (Synergy Software, Reading, PA, USA) followed by Tukey's honest significant difference test. A value of $p < 0.05$ was accepted as statistically significant. All data were presented as mean $\pm$ standard deviation, with $n = 3$.

2-3.　Results and Discussion

2-3-1. Synthesis and characterization of poly(Pro-Hyp-Gly) and methacrylated poly(Pro-Hyp-Gly)

Methacrylated poly(Pro-Hyp-Gly) as a precursor for photocrosslinked poly(Pro-Hyp-Gly) hydrogel formation was synthesized by modifying hydroxy group of Hyp residues of poly(Pro-Hyp-Gly) using methacrylic anhydride and DIPEA (**Scheme 2-1**). GPC profiles of poly(Pro-Hyp-Gly) and methacrylated poly(Pro-Hyp-Gly) showed a wide molecular weight distribution, with peak molecular weight of about 12 and 9 kDa, respectively, based on the standard curve using PEG (**Figure 2-1**). The GPC results revealed that conjugation of methacrylate group into the poly(Pro-Hyp-Gly) does not affect its molecular weight distribution.

CD spectra of the poly(Pro-Hyp-Gly) and methacrylated poly(Pro-Hyp-Gly) are shown in **Figure 2-2(A)**. CD spectra of the polypeptides showed a weak positive Cotton effect near 225 nm and a strong negative Cotton effect near 197 nm. The spectra are similar to that of bovine type I collagen suggesting that the polypeptides contain a collagen-like triple-helical structure [12,14]. The R_{pn} value was used to estimate triple-helical content in the polypeptides [14,15]. The R_{pn} value of poly(Pro-Hyp-Gly) and methacrylated

poly(Pro-Hyp-Gly) are 0.116 ± 0.002 and 0.144 ± 0.006, respectively ((**Figure 2-2(B)**)). The

R_{pn} value of the poly(Pro-Hyp-Gly) is similar to that $(Pro-Hyp-Gly)_{10}$ indicating that the

poly(Pro-Hyp-Gly) contains high triple-helical structure. The R_{pn} values of the

poly(Pro-Hyp-Gly) and methacrylated poly(Pro-Hyp-Gly) are significantly different ($p <$

0.01). These results may be caused by electron withdrawing effect of the methacrylate group

which may stabilize the triple-helical structure of the polypeptide through inductive effect.

The inductive effect constrains the pucker of the pyrrolidine ring and organizes the peptide

backbone into conformations that are favorable for triple-helix conformation [16].

The FTIR spectra of both polypeptides showed peaks at 1639 and 1552 cm^{-1}, which

are assigned as amide I and amide II of poly(Pro-Hyp-Gly) backbone, respectively (**Figures**

2-3(A) and (B)). A shoulder peak at 1717 cm^{-1} appeared in the spectrum of methacrylated

poly(Pro-Hyp-Gly) is attributed to the carbonyl stretching of ester group of the

methacrylated poly(Pro-Hyp-Gly) (**Figure 2-3(B)**). The peak shifted to a lower wavenumber

compared to that of carbonyl stretching of ester group, which is usually observed at 1735

cm[-1]. This shift is caused by conjugation of the double bond to the carbonyl group of

methacrylated poly(Pro-Hyp-Gly) (**Scheme 2-2**). The conjugation increases the single bond

character of the carbonyl group, which results in absorption at a lower wavenumber [17].

The ^{1}H NMR spectrum of poly(Pro-Hyp-Gly) showed peaks at 3.2 and 3.5 ppm, and

3.8 and 3.9 ppm that were assigned to Pro-C$_\delta H$ and Hyp-C$_\delta H$ in the triple-helical structure

of poly(Pro-Hyp-Gly), respectively (**Figure 2-4(A)**) [18]. This result is consistent with the

CD spectrum of the poly(Pro-Hyp-Gly), in which peaks correlated to a collagen-like

triple-helical structure were observed.

The introduction of methacrylate group into the poly(Pro-Hyp-Gly) was further

confirmed using ^{1}H NMR (**Figure 2-4(B)**) and COSY (**Figure 2-5**) spectroscopies. A signal

at 1.9 ppm was assigned to methyl proton, and signals at 5.8 and 6.2 ppm were assigned to

two vinyl protons of methacrylate group in the methacrylated poly(Pro-Hyp-Gly). Signals

at 4.1 and 5.5 ppm were assigned as Hyp-C$_\delta$*H* and Hyp-C$_\gamma$*H,* respectively, which appeared

because of the electron-withdrawing effect of oxygen of the ester group of the methacrylate

group. These results suggest that the methacrylate group was conjugated successfully into

the poly(Pro-Hyp-Gly) through an ester bond. The degree of methacrylation was calculated

to be 41% of hydroxy group of poly(Pro-Hyp-Gly).

2-3-2. *Photocrosslinked poly(Pro-Hyp-Gly) hydrogels*

Photocrosslinked poly(Pro-Hyp-Gly) hydrogels were fabricated by visible light

irradiation of methacrylated poly(Pro-Hyp-Gly) in the presence of eosin Y as a photoinitiator,

triethanolamine as a co-initiator, and NVP as a radical scavenger. During visible light

irradiation, eosin Y is excited and accepts an electron from triethanolamine which acts as an

electron donor [19,20]. Electron transfer from the co-initiator, triethanolamine, to eosin Y yields an excited-state charge-transfer complex (exciplex) [20,21]. This process is continued by a proton transfer from the amine to eosin Y to form a protonated eosin Y and an α-aminoalkyl radical of the triethanolamine [19] (**Scheme 2-3**). Finally, the α-aminoalkyl radical initiate photocrosslinking of methacrylated poly(Pro-Hyp-Gly) to form photocrosslinked poly(Pro-Hyp-Gly) hydrogel (**Scheme 2-4**). The radicals of eosin Y can not initiate the photocrosslinking because of its steric hindrance [19]. Macroscopic appearance of the photocrosslinked hydrogel is shown in **Scheme 2-5**.

In order to optimize the conditions of the photocrosslinking reaction, the influences of eosin Y and methacrylated poly(Pro-Hyp-Gly) concentrations, and the irradiation time on gelation and swelling ratio of the photocrosslinked hydrogels were investigated. A gelation represents the fraction of methacrylated poly(Pro-Hyp-Gly) that is involved in the 3D polymeric network of the photocrosslinked hydrogel compared to the initial amount of methacrylated poly(Pro-Hyp-Gly) before photocrosslinking. Results from gelation experiment of the hydrogels formed with different concentrations of eosin Y and 5 min irradiation showed that increasing concentration of eosin Y in the range of $10-30$ μM results in increasing gelation ratio ($p < 0.0001$) (**Figure 2-6(A)**). Hydrogels formed with 10 μM and 30 μM of eosin Y exhibited the lowest ($38.4 \pm 1.5\%$) and the highest ($82.5 \pm 8.2\%$) gelation, respectively.

From the swelling experiments, the hydrogels formed with 15−30 μM of eosin Y showed high swelling ratios in PBS (**Figure 2-6(B)**). There was no data for swelling ratio of hydrogel formed with 10 μM of eosin Y because the hydrogel was fragile and easily broken during incubation in PBS, indicating low degree of crosslinking of the obtained hydrogel. These results suggest that a higher concentration of eosin Y will result in a hydrogel with a higher degree of crosslinking because of a higher radical formation. However, for simultaneous cell encapsulation, high number of radicals can directly damage the cell. Therefore, 20 μM of eosin Y was chosen for further experiments.

To further optimize the photocrosslinking conditions, the influences of methacrylated poly(Pro-Hyp-Gly) concentration, and the irradiation time on the gelation and swelling ratio of photocrosslinked hydrogels were evaluated. The gelation of hydrogels formed with 5 min irradiation increased with an increase in the methacrylated poly(Pro-Hyp-Gly) concentration ($p < 0.0001$) (**Figure 2-7(A)**). Hydrogel formed with 20 mg/mL of methacrylated poly(Pro-Hyp-Gly) showed the lowest gelation ($44.6 \pm 2.9\%$), followed by the 30 mg/mL ($53.4 \pm 2.2\%$), 40 mg/mL ($65.8 \pm 5.8\%$), and 50 mg/mL ($69.0 \pm 2.0\%$)). The gelation of hydrogels formed with 3 min irradiation showed the same tendency with that of 5 min irradiation. There was no significant difference on the gelation between hydrogels formed with 3 and 5 min irradiation at the same concentrations of methacrylated poly(Pro-Hyp-Gly). However, with 20 mg/mL of methacrylated poly(Pro-Hyp-Gly) and 3

min irradiation, there was no hydrogel formation.

The swelling ratio of the hydrogels formed with 5 min irradiation tends to decrease with an increase in the methacrylated poly(Pro-Hyp-Gly) concentration ($p < 0.001$) (**Figure 2-7(B)**). It might be caused by an increase in polymer network density. Polymer network density will affect hydrogel mesh size (ξ) which represents the distance between two adjacent crosslinked polymer chains at swollen state [22]. The Flory-Rehner equation shows a relationship between volumetric swelling ratio and ξ as shown in **Equation 2-5** [22]. Lower swelling ratio indicates lower ξ and higher polymer network density.

$$\xi = Q^{1/3} \, (\overline{r_0^2})^{1/2} \qquad\qquad (2-5)$$

Q = volumetric swelling ratio

$(\overline{r_0^2})^{1/2}$ = root-mean-squared end-to-end distance of two crosslinked polymer chains

At 3 min irradiation, there was no significant difference in swelling ratio of hydrogels formed with different concentrations of methacrylated poly(Pro-Hyp-Gly). In addition, the swelling ratios of 3 min-irradiated hydrogels were significantly lower than those of 5 min-irradiated hydrogels at the same methacrylated poly(Pro-Hyp-Gly) concentrations. These results might be caused by fibril deformation in the 5 min-irradiated hydrogels. A

longer irradiation time will produce more radicals that would lead to the formation of hydrogels with a higher degree of crosslinking. A higher degree of crosslinking may cause fibril deformation because of molecular stretching [23].

Collectively, these data suggest that the hydrogel properties, such as polymer network density and swelling ratio, can be easily tuned by controlling the eosin Y and methacrylated poly(Pro-Hyp-Gly) concentrations, and the irradiation time.

2-3-3. *Cytotoxicity of NVP, triethanolamine, and methacrylated poly(Pro-Hyp-Gly)*

The possible toxicity of the polymers and crosslinkers to cell viability is an important factor to be considered particularly with respect to simultaneous cell encapsulation into hydrogels. In order to study the effects of the photocrosslinking components on cell viability, rBMSCs were incubated in medium containing either NVP, triethanolamine, or methacrylated poly(Pro-Hyp-Gly) for 24 h.

The results showed that NVP up to 5 mM does not influence rBMSC viability (**Figure 2-8(A)**). However, the viability of the rBMSCs was significantly affected by the concentrations of triethanolamine and methacrylated poly(Pro-Hyp-Gly) (**Figures 2-8(B) and (C)**). Cell viability in the presence of 1, 5, 10 and 50 mM of triethanolamine was 96.0 ± 2.4%, 99.1 ± 11.6%, 89.8 ± 7.4% and 31.2 ± 1.6%, respectively. Methacrylated

poly(Pro-Hyp-Gly) showed a slight cytotoxicity to the cells, about 43% of cells remained

alive in the medium containing 20 mg/mL of methacrylated poly(Pro-Hyp-Gly) and there

was no significant difference in cell viability between cells cultured in either 20 mg/mL or

30 mg/mL of methacrylated poly(Pro-Hyp-Gly). Based on these results together with data

from gelation and swelling ratio experiments, setting of 20 μM of eosin Y, 5 mM of NVP

and 10 mM of triethanolamine were then chosen for cell photoencapsulation experiments.

2-3-4. Viability and morphology of rBMSCs in the photocrosslinked poly(Pro-Hyp-Gly)

hydrogels

Recently, various studies indicated that properties of 3D scaffolds play an important

role in controlling cell viability and proliferation [24-26]. To investigate the influence of the

hydrogel properties on cell viability and proliferation, Live-Dead staining and WST-8 assay

of rBMSCs encapsulated in hydrogels formed with 20–50 mg/mL of methacrylated

poly(Pro-Hyp-Gly) at 5 min irradiation were performed (**Scheme 2-6**). Live-Dead staining

of the rBMSCs in the 20 mg/mL of methacrylated poly(Pro-Hyp-Gly) hydrogel revealed that

most of the cells in the hydrogel are alive (**Figure 2-9(A)**). Quantification of viable cells in

the hydrogels using WST-8 showed that the rBMSCs in the hydrogels survived during seven

days of culture period (**Figure 2-9(B)**). These results suggest that the photocrosslinked

poly(Pro-Hyp-Gly) hydrogels are cytocompatible for encapsulating rBMSCs.

The cells in the hydrogels formed with 30–50 mg/mL of methacrylated poly(Pro-Hyp-Gly) did not exhibit any significant difference in cell viability throughout seven days of incubation. However, the cells proliferated in the hydrogels formed with 20 mg/mL of methacrylated poly(Pro-Hyp-Gly) ($p < 0.05$). The ability of the 20 mg/mL methacrylated poly(Pro-Hyp-Gly) hydrogel to facilitate rBMSC proliferation might be caused by hydrogel's lower polymer network density and higher swelling ratio. Hydrogel with those properties can facilitate a better cell migration [27] and diffusion of nutrients, waste, and oxygen through the polymer network, which is important for cell viability and proliferation [28,29]. In addition, hydrogels with high polymer network density may act as physical barrier preventing cell proliferation [30].

To study the influence of hydrogel properties on cell morphology, phase contrast microscope observation was performed on the rBMSCs in the photocrosslinked poly(Pro-Hyp-Gly) hydrogels. At day 1, the microscope images show that the cells were distributed homogeneously in the hydrogels and had a round shape morphology (**Figure 2-10**). These results are in agreement with Maia *et al*., (2014), who observed that hMSCs in alginate hydrogels exhibited round shape morphology [31]. This morphology is similar to cell morphology in in vivo microenvironment [24]. After seven days of culturing, the cells in 30–50 mg/mL hydrogels showed no difference in cell morphology compared with day 1.

In contrast, some of the cells in the 20 mg/mL hydrogel showed an elongated and branched morphology after seven days of incubation. These results are in agreement with Engler *et al.* (2006), who observed that MSCs encapsulated in soft hydrogel exhibited an increasingly branched and filopodia-rich morphology, while the cells formed osteoblast-like morphology in rigid hydrogel [32]. Tan *et al.* (2014) also reported that pre-myoblast C2C12 cells in soft and rigid transglutaminase crosslinked gelatin hydrogel (TG-gel) exhibit branched and round morphology, respectively [33]. These results suggest that the rBMSCs in the hydrogels sense the differences in hydrogel properties, such as polymer network density and swelling ratio, resulting in changing their proliferation and morphology.

2-3-5. Calcium deposition in photocrosslinked poly(Pro-Hyp-Gly) hydrogels containing rBMSCs

The rBMSCs have multipotency and can differentiate into specific cell lineages, such as osteoblasts, chondrocytes, adipocytes, and fibroblasts [13]. In order to investigate the ability of the photocrosslinked poly(Pro-Hyp-Gly) hydrogels to support rBMSC differentiation, the osteogenic differentiation of the cells encapsulated in the 20−50 mg/mL methacrylated poly(Pro-Hyp-Gly) hydrogels was evaluated by the appearance of calcium deposition as a late marker for osteogenic differentiation [13].

After 28 days of incubation in osteogenic medium, the hydrogels became opaque indicating calcium deposition in the hydrogels (**Figure 2-11**). Phase contrast microscope images of the rBMSCs in the hydrogels showed the formation of mineralized bone matrix, known as bone nodule (**Figure 2-12**). These results suggest that the encapsulated cells in the hydrogels had differentiated into osteogenic lineage and deposited calcium in the hydrogels.

Further confirmation of calcium deposition in the hydrogels was observed by SEM analysis, and Alizarin Red S and von Kossa stainings. SEM images of 6 μm hydrogel slices showed areas that were brighter compared to the surrounding areas (**Figure 2-13**). The contrast in the SEM images appeared because of higher electron reflection by calcium atoms, which indicates calcium deposition in those areas. The elements in the hydrogels themselves have low electron reflection ratio because the hydrogels contain only of low atomic number elements, such as carbon, hydrogen, nitrogen, and oxygen, which results in darker areas than the calcium containing areas. The SEM images revealed that 30 mg/mL of methacrylated poly(Pro-Hyp-Gly) hydrogel (5 min irradiation) showed the brightest area than that of other hydrogels, indicating higher calcium deposition in the hydrogel.

Positive calcium deposition using Alizarin Red S and von Kossa staining was observed by the appearance of areas that stained red and or dark brown, respectively (**Figures 2-14 and 2-15**). The results revealed that 50 mg/mL of methacrylated poly(Pro-Hyp-Gly) (3 min irradiation) hydrogel showed less staining both for Alizarin Red

S and von Kossa. Intense staining was observed in the hydrogel formed with 30 mg/mL of methacrylated poly(Pro-Hyp-Gly) (5 min irradiation). Quantification of the area stained by Alizarin Red S using ImageJ software showed that the 30 mg/mL methacrylated poly(Pro-Hyp-Gly) (5 min) hydrogel has a significantly larger stained area ($p < 0.001$) and the 50 mg/mL methacrylated poly(Pro-Hyp-Gly) (3 min) hydrogel exhibited the smallest stained area (**Figure 2-16(A)**). Quantification of the areas stained by von Kossa showed a comparable result with Alizarin red S staining (**Figure 2-16(B)**) ($p < 0.01$).

These results indicate that osteogenic differentiation of the rBMSCs in the photocrosslinked hydrogels may be influenced by polymer network density of the hydrogels. Hydrogels formed with 30 mg/mL of methacrylated poly(Pro-Hyp-Gly) with 5 min irradiation provided a suitable polymer network density for osteogenic differentiation of the rBMSCs. An increase in osteogenic differentiation of the rBMSCs in the 30 mg/mL methacrylated poly(Pro-Hyp-Gly) hydrogel may be caused by an increase in cell migration and aggregation (**Figure 2-12**). In cell aggregates, cells are allowing to interact with each other and with their environment. These interactions are closely similar to cell behavior in *in vivo* microenvironment [24]. It has been reported that cell aggregates can promote cell differentiation and expression of differentiation markers [34-36].

Hydrogels formed with high concentration of methacrylated poly(Pro-Hyp-Gly) (40–50 mg/mL) resulted in higher polymer network density, which may inhibit cell

migration and the formation of cell aggregates, leading to decrease in cell differentiation.

Hydrogels formed with 3 min irradiation also inhibited rBMSC differentiation due to their

low swelling ratio, which may reduce the ability of the hydrogels to facilitate transportation

of nutrients, waste, and oxygen during cell culture period [28,29]. Park *et al.* (2009) reported

that chondrogenic differentiation of encapsulated rabbit marrow mesenchymal stem cells in

oligo(poly(ethylene glycol) fumarate) hydrogels were accelerated in the hydrogel with

higher swelling ratio [29]. In addition, Sahai *et al.*, (2013) confirmed that capacity of

adipose-derived mesenchymal stem cells to differentiate into osteoblasts decreased in a

low-oxygen environment [37].

It is well known that the encapsulated cells can sense the difference of their

microenvironment and then, convert that information into morphological changes and

lineage commitment [32]. As already described previously, the morphology of rBMSC in

the 20 mg/mL methacrylated poly(Pro-Hyp-Gly) hydrogel was different from that in 30

mg/mL methacrylated poly(Pro-Hyp-Gly) hydrogel as a response to polymer network

density. These differences may directly affect the osteogenic differentiation of the

encapsulated rBMSCs. The rBMSCs in 30 mg/mL methacrylated poly(Pro-Hyp-Gly)

hydrogel exhibited a round shape morphology that is similar to that of osteoblastic cells in

in vivo microenvironment. As a result, the cells produced more calcium as an osteogenic

marker than that rBMSCs did in 20 mg/mL of methacrylated poly(Pro-Hyp-Gly) hydrogel.

Similarly, Tan *et al.*, (2014) reported that pre-myoblast C2C12 cells encapsulated in rigid TG-gel exhibited a round shape morphology, and higher osteogenic marker expression compared with cells in soft TG-gel [33].

These results clearly showed that osteogenic differentiation of the rBMSCs encapsulated in photocrosslinked poly(Pro-Hyp-Gly) hydrogels was significantly affected by the hydrogel properties.

2-4.   Conclusion

In summary, this chapter showed simultaneous encapsulation of rBMSCs into chemically-crosslinked poly(Pro-Hyp-Gly) hydrogels. The hydrogels were successfully fabricated by visible light photocrosslinking of methacrylated poly(Pro-Hyp-Gly) in the presence of eosin Y, triethanolamine, and NVP. It was found that hydrogel properties, such as polymer network density and swelling ratio, can be easily tuned by controlling the concentrations of eosin Y and methacrylated poly(Pro-Hyp-Gly), and the irradiation time. An appropriate photocrosslinking condition for stem cell encapsulation is required to maintain high viability of the encapsulated cells and to support their functions during culturing periods. The importance of hydrogel properties in controlling cell proliferation and morphology was suggested by comparing rBMSC behavior in the hydrogels formed with 20–50 mg/mL of methacrylated poly(Pro-Hyp-Gly) and 5 min irradiation. In the 20 mg/mL of methacrylated poly(Pro-Hyp-Gly) hydrogel, cells proliferated. While cell number did not change in the 30–50 mg/mL of methacrylated poly(Pro-Hyp-Gly) hydrogels. From morphology observations, elongated and branched morphology was only observed in the 20 mg/mL hydrogels. These suggest that hydrogel properties play an important role in controlling cell proliferation and morphology. It was also found that the hydrogel properties affect osteogenic differentiation of the rBMSCs encapsulated in the photocrosslinked

poly(Pro-Hyp-Gly) hydrogels. Hydrogel formed with 30 mg/mL of methacrylated poly(Pro-Hyp-Gly) (5 min irradiation) showed the highest calcium deposition as revealed by bone nodule formation, SEM analysis, and Alizarin Red S and von Kossa staining. On the contrary, hydrogel formed with 50 mg/mL of methacrylated poly(Pro-Hyp-Gly) (3 min irradiation) showed the lowest calcium deposition. These results show that by carefully controlling the photocrosslinking condition for photocrosslinked poly(Pro-Hyp-Gly) hydrogel fabrication, a cytocompatible 3D scaffold for simultaneous rBMSC encapsulation can be successfully fabricated. These results also confirm that hydrogel properties are important factors for cell encapsulation and can control cellular functions and cell ability to differentiate into specific cell lineages. Taken together, these results indicate that a photocrosslinked poly(Pro-Hyp-Gly) hydrogel is a promising 3D scaffold for simultaneous rBMSC encapsulation supporting cell viability, proliferation, and differentiation.

References

1. Nguyen KT, West JL. Photopolymerizable hydrogels for tissue engineering applications. Biomaterials 2002;23:4307–4314.

2. Fairbank BD, Schwartz MP, Bowman CN, Anseth KS. Photoinitiated polymerization of PEG-diacrylate with lithium phenyl-2,4,6-trimethylbenzoylphosphinate: polymerization rate and cytocompatibility. Biomaterials 2009;30:6702–6707.

3. Bryant SJ, Anseth KS. Photopolymerization of hydrogel scaffolds. In: Ma PX, Elisseeff J, editors. Scaffolding in tissue engineering. USA: CRC Press;2003. p.71–90.

4. Nicodemus GD, Bryant SJ. Cell encapsulation in biodegradable hydrogels for tissue engineering applications. Tissue Eng Part B Rev 2008;14:149–165.

5. Bahney CS, Lujan TJ, Hsu CW, Bottlang M, West JL, Johnstone B. Visible light photoionitiation of mesenchymal stem cell-laden bioresponsive hydrogels. Eur Cells Matter 2011;22:43–55.

6. Bryant SJ, Nuttelman CR, Anseth KS. Cytocompatibility of UV and visible light photoinitiating systems on cultured NIH/3T3 fibroblasts in vitro. J Biomater Sci Polym Ed 2000;11:439–457.

7. Cruise GM, Hegre OD, Scharp DS, Hubbell JA. A sensitivity study of the key parameters in the interfacial photopolymerization of poly(ethylene glycol) diacrylate

upon porcine islets. Biotechnol Bioeng 1998;57:655–665.

8. Hari DP, König B. Synthetic applications of eosin Y in photoredox catalysis. Chem Commun 2014;50:6688–6699.

9. Burdick JA, Prestwich GD. Hyaluronic acid hydrogels for biomedical applications. Adv Mater 2011;23:H41–H56.

10. Yoshii E. Cytotoxic effects of acrylates and methacrylates: Relationships of monomer structures and cytotoxicity. Biomed Mater Res 1997;37:517–524.

11. Kishimoto T, Morihara Y, Osanai M, Ogata S, Kamitakahara M, Ohtsuki C, Tanihara M. Synthesis of poly(Pro-Hyp-Gly)$_n$ by direct polycondensation of (Pro-Hyp-Gly)$_n$, where n = 1, 5, and 10, and stability of the triple-helical structure. Biopolymers 2005;79:163–172.

12. Shibasaki Y, Hirohara S, Terada K, Ando T, Tanihara M. Collagen-like polypeptide poly(Pro-Hyp-Gly) conjugated with Gly-Arg-Gly-Asp-Ser and Pro-His-Ser-Arg-Asn peptides enhances cell adhesion, migration, and stratification. Biopolymers Pep Sci 2011;96:302–312.

13. Bianco P, Kuznetsov SA, Riminucci M, Robey PG. Postnatal skeletal stem cells. Methods Enzymol 2006;419:117–148.

14. Tiffany ML, Krimm S. Effect of temperature on the circular dichroism spectra of polypeptides in the extended state. Biopolymers 1972;11:2309–2316.

15. Toniolo C, Formaggio F, Woody RW. Electronic circular dichroism of peptides. In: Berova N, Polavarapu PL, Nakanishi K, Woody RW, editors. Comprehensive chiroptical spectroscopy, Volume 2: Applications in stereochemical analysis of synthetic compounds, natural products, and biomolecules. USA: John Wiley and Sons;2012. p.499−544.

16. Holmgren SK, Bretscher LE, Taylor KM, Raines RT. A hyperstable collagen mimic. Chem Biol 1999;6:63−70.

17. Stuart B. Infrared Spectroscopy: Fundamentals and applications. USA: John Wiley & Sons;2004. p.1−224.

18. Li MH, Fan P, Brodsky B, Baum J. Two-dimensional NMR assignments and conformation of (Pro-Hyp-Gly)$_{10}$ and a designed collagen triple-helical peptide. Biochemistry 1993;32:7377−7387

19. Moad G, Solomon DH. The chemistry of radical polymerization. UK: Elsevier Ltd.;2006. p.98−103.

20. Hu J, Wang J, Nguyen TH, Zheng N. The chemistry of amine radical cations produced by visible light photoredox catalysis. Beilstein J Org Chem 2013;9:1977−2001.

21. Ligon SC, Husár B, Wutzel H, Holman R, Liska R. Strategies to reduce inhibition in photoinduced polymerization. Chem Rev 2014;114:557−589.

22. Zustiak SP, Leach JB. Hydrolytically degradable poly(ethylene glycol) hydrogel

scaffolds with tunable degradation and mechanical properties. Biomacromolecules 2010;11:1348–1357

23. Depalle B, Qin Z, Shefelbine SJ, Buehler MJ. Influence of cross-link structure, density and mechanical properties in the mesoscale deformation mechanism of collagen fibrils. J Mech Behav Biomed Mater 2015;52:1–13.

24. Edmondson R, Broglie JJ, Adcock AF, Yang L. Three-dimensional cell culture systems and their applications in drug discovery and cell-based biosensors. Assay Drug Dev Technol 2014;12:207–218.

25. Griffith LG, Swartz MA. Capturing complex 3D tissue physiology in vitro. Nat Rev Mol Cell Biol 2006;7:211–224.

26. Singh A, Elisseeff J. Biomaterials for stem cell differentiation. J Mater Chem 2010;20:8832–8847.

27. Guo WH, Frey MT, Burnham NA, Wang YL. Substrate rigidity regulates the formation and maintenance of tissues. Biophys J 2006;90:2213–2220.

28. Gasperini L, Mano JF, Reis RL. Natural polymers for the microencapsulation of cells. J R Soc Interface 2014;11:20140817.

29. Park H, Guo X, Temenoff JS, Tabata Y, Caplan AI, Kasper FK, Mikos AG. Effect of swelling ratio of injectable hydrogel composites on chondrogenic differentiation of encapsulated rabbit marrow mesenchymal stem cells in vitro. Biomacromolecules

2009;10:541–546.

30. Bott K, Upton Z, Schrobback K, Ehrbar M, Hubbel JA, Lutolf MP, Rizzi SC. The effect of matrix stiffness on fibroblast proliferation in 3D gels. Biomaterials 2010;31: 8454–8464.

31. Maia FR, Lourenço AH, Granja PL, Gonçalves RM, Barrias CC. Effect of cell density on mesenchymal stem cells aggregation in RGD-alginate 3D matrices under osteoinductive conditions. Macromol Biosci 2014; 14:759–771.

32. Engler AJ, Sen S, Sweeney HL, Discher DE. Matrix elasticity directs stem cell lineage specification. Cell 2006;126:677–689.

33. Tan S, Fang JY, Yang Z, Nimni ME, Han B. The synergetic effect of hydrogel stiffness and growth factor on osteogenic differentiation. Biomaterials 2014;35: 5294–5306.

34. Tang J, Peng R, Ding J. The regulation of stem cell differentiation by cell-cell contact on micropatterned material surfaces. Biomaterials 2010;31:2470–2476.

35. Clause KC, Liu LJ, Tobita K. Directed stem cell differentiation: The role of physical forces. Cell Commun Adhes 2010;17:48–54.

36. Deegan AJ, Aydin HM, Hu B, Konduru S, Kuiper JH, Yang Y. A facile *in vitro* model to study rapid mineralization in bone tissues. Biomed Eng Online 2014;13:136.

37. Sahai S, Williams A, Skiles ML, Blanchette DO. Osteogenic differentiation of

adipose-derived stem cells is hypoxia-inducible factor-1 independent. Tissue Eng

Part A 2013;19:1583–1591.
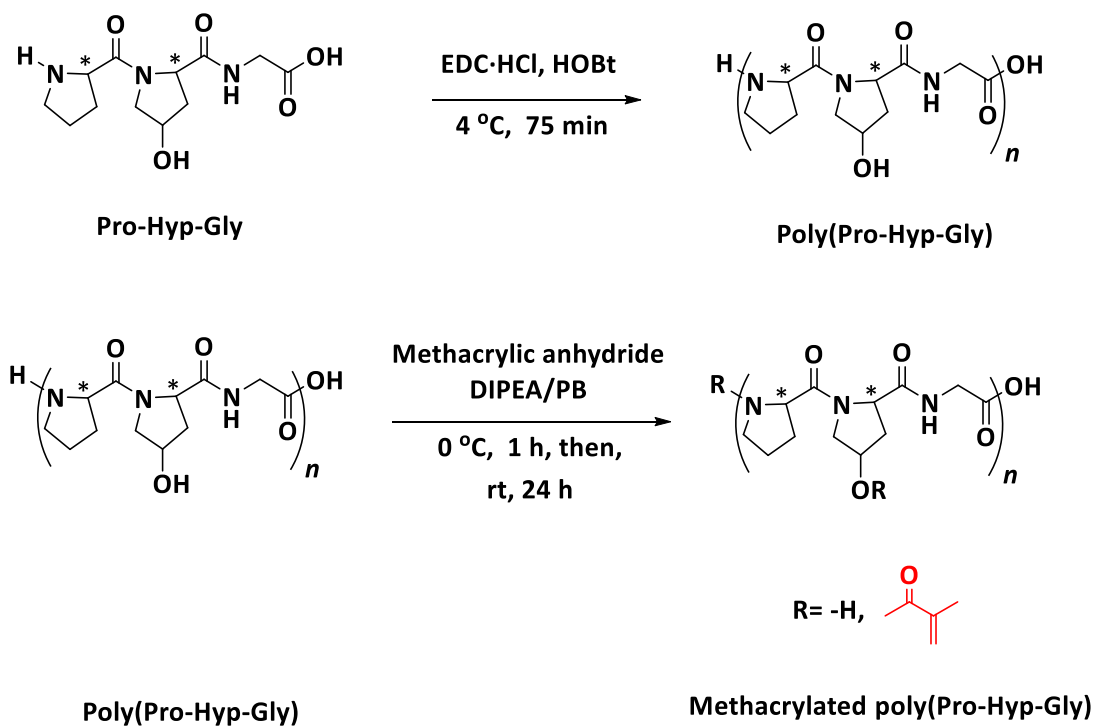
Scheme 2-1 The schematic diagram of synthesis of poly(Pro-Hyp-Gly) and methacrylated poly(Pro-Hyp-Gly). * indicate L-isomers.
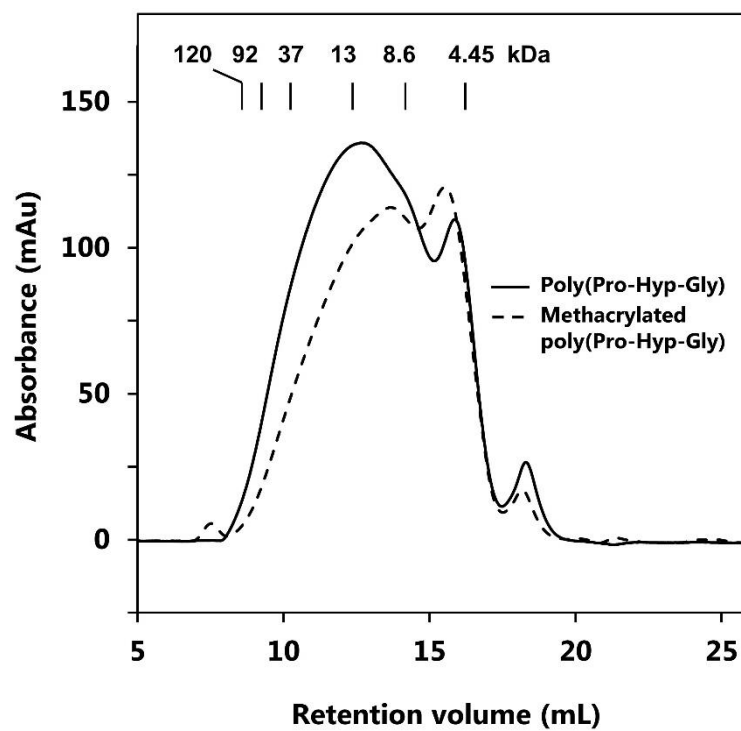
Figure 2-1 GPC profiles of poly(Pro-Hyp-Gly) and methacrylated poly(Pro-Hyp-Gly). The concentration of each sample was 0.5 mg/mL in PBS.
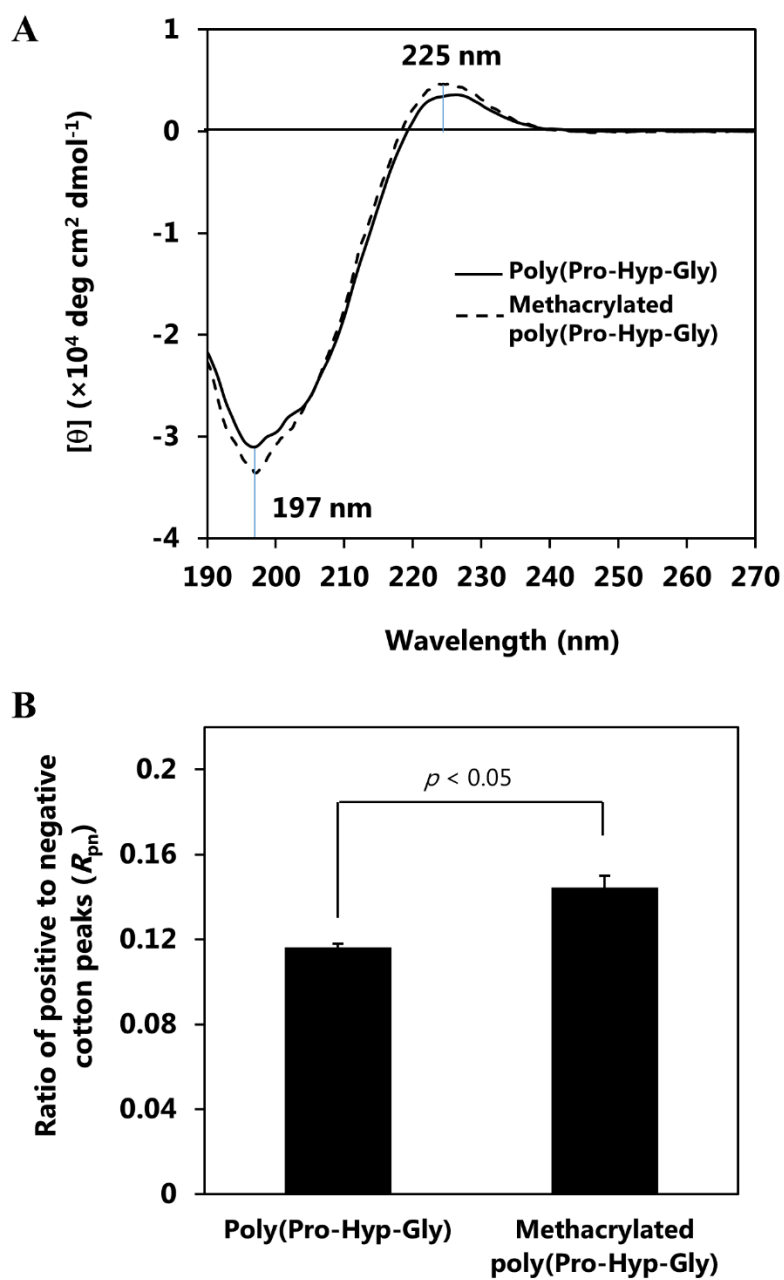
Figure 2-2 CD spectra (A) and R_{pn} value (B) of poly(Pro-Hyp-Gly), and methacrylated poly(Pro-Hyp-Gly). The concentration of each sample was 0.25 mg/mL in Milli-Q water. Milli-Q water was used as a blank.
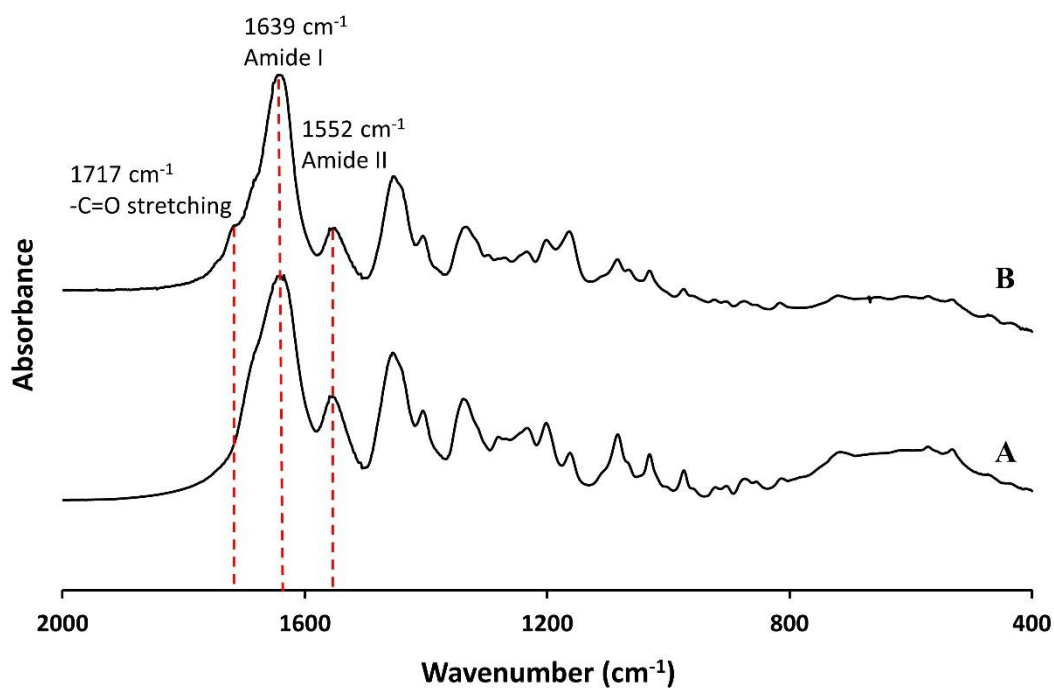
Figure 2-3 FTIR spectra of poly(Pro-Hyp-Gly) (A) and methacrylated poly(Pro-Hyp-Gly) (B). FTIR measurement was conducted using KBr method with resolution 1 cm^{-1} and 16 scans at room temperature.
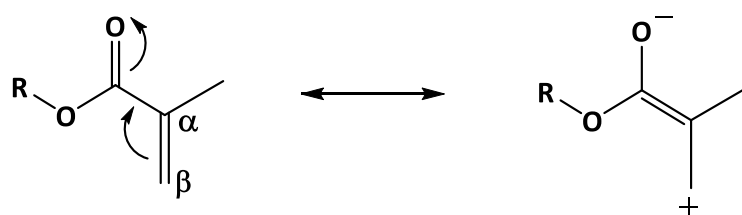
Scheme 2-2 Conjugation of the vinyl to the carbonyl group in methacrylated poly(Pro-Hyp-Gly).
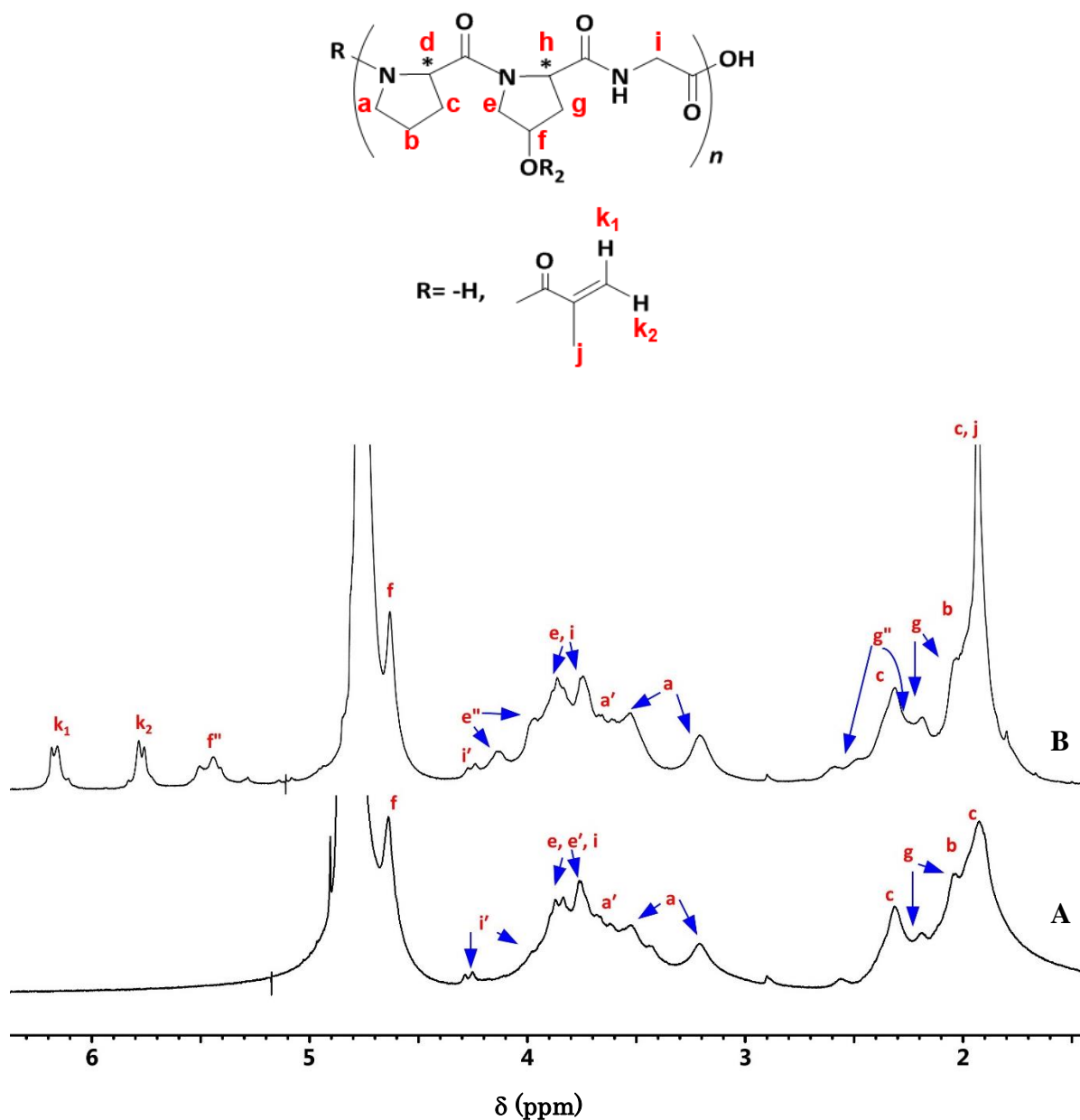
Figure 2-4 ^{1}H NMR spectra of poly(Pro-Hyp-Gly) (A) and methacrylated poly(Pro-Hyp-Gly) (B). a′, e′ and i′ are Pro-C$_\delta$H, Hyp-C$_\delta$H, and Gly-C$_\alpha$H, respectively, in non triple-helical structure of poly(Pro-Hyp-Gly). e″ and f ″ are Hyp-C$_\delta$H and Hyp-C$_\gamma$H, respectively, which appeared because of electron withdrawing effect of oxygen of the ester group of methacrylated poly(Pro-Hyp-Gly). The concentration of each sample was 4 mg/mL in D$_2$O with TMS as an internal standard. * indicate L-isomers.
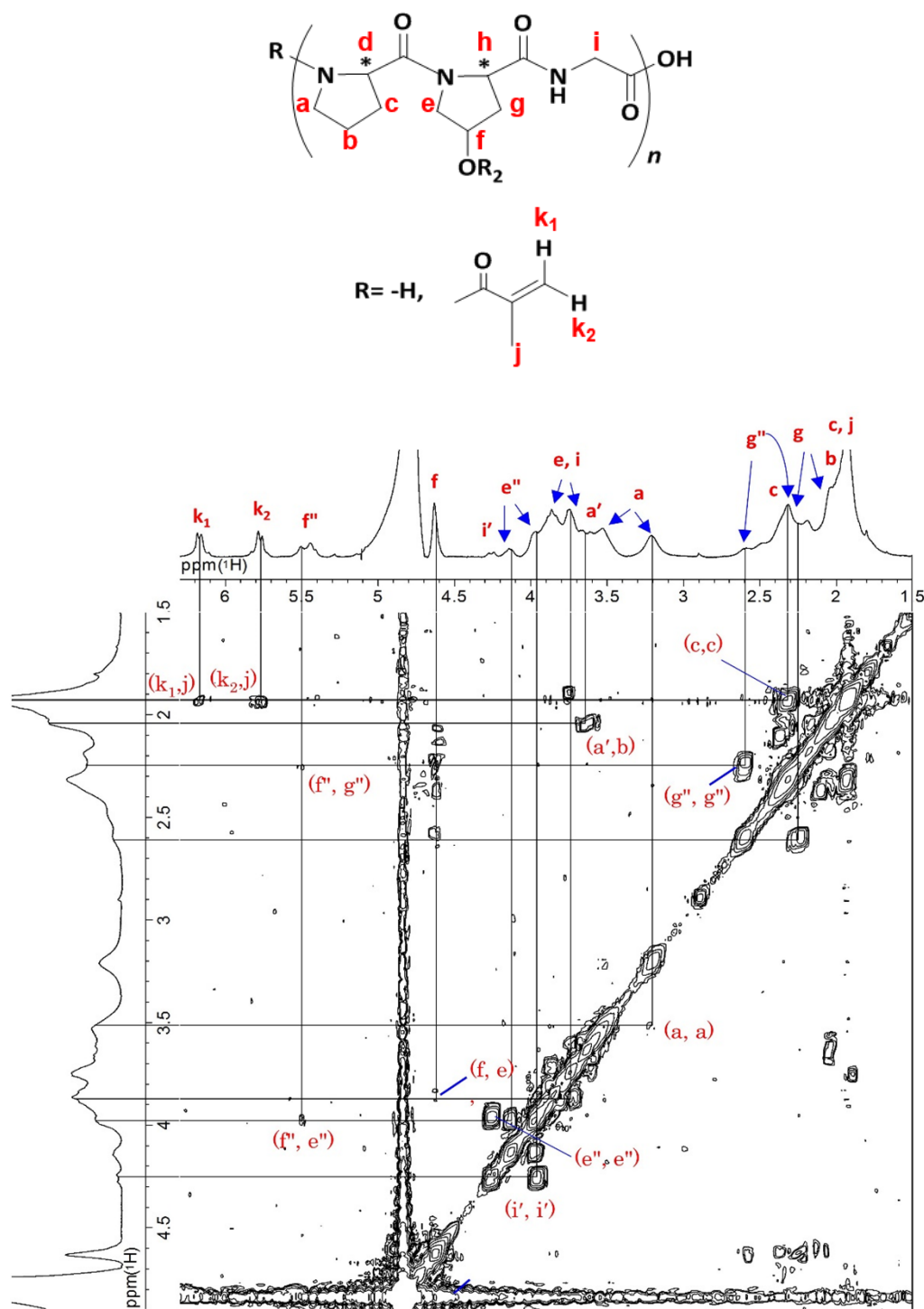
Figure 2-5 COSY spectrum of methacrylated poly(Pro-Hyp-Gly). The concentration was 4 mg/mL in D_2O with TMS as an internal standard. * indicate L-isomers.
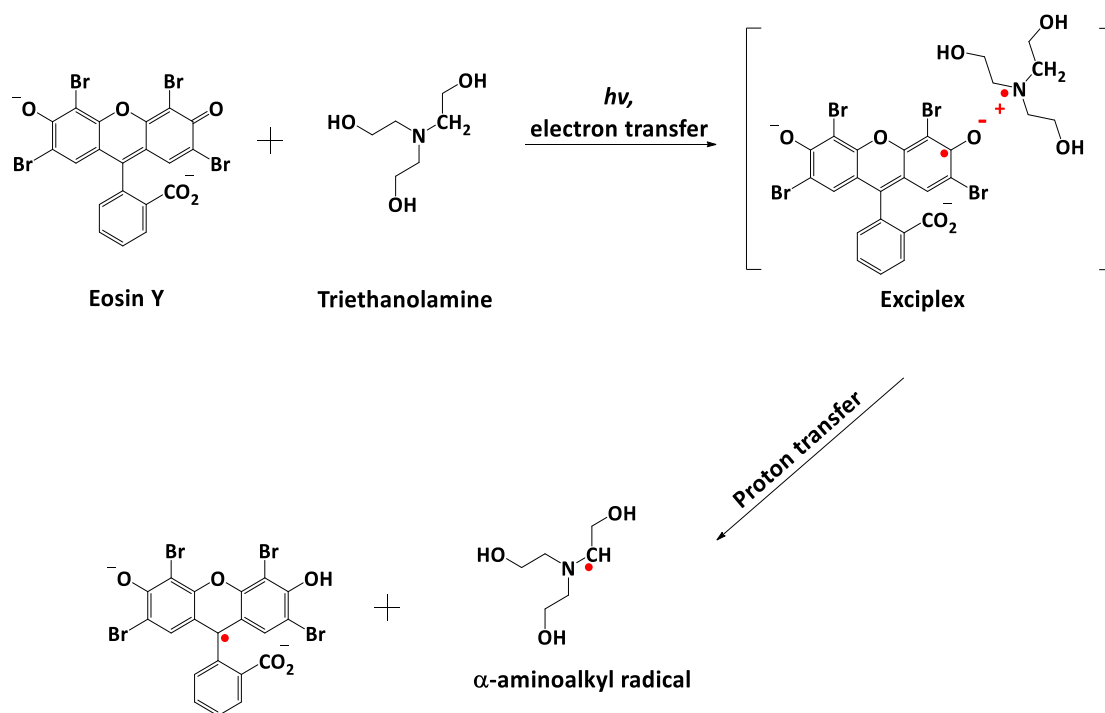
Scheme 2-3 Mechanism of radical formation during visible light irradiation of eosin Y as a photoinitoator in the presence of triethanolamine as a co-initiator [20,21].

(1) Route 1
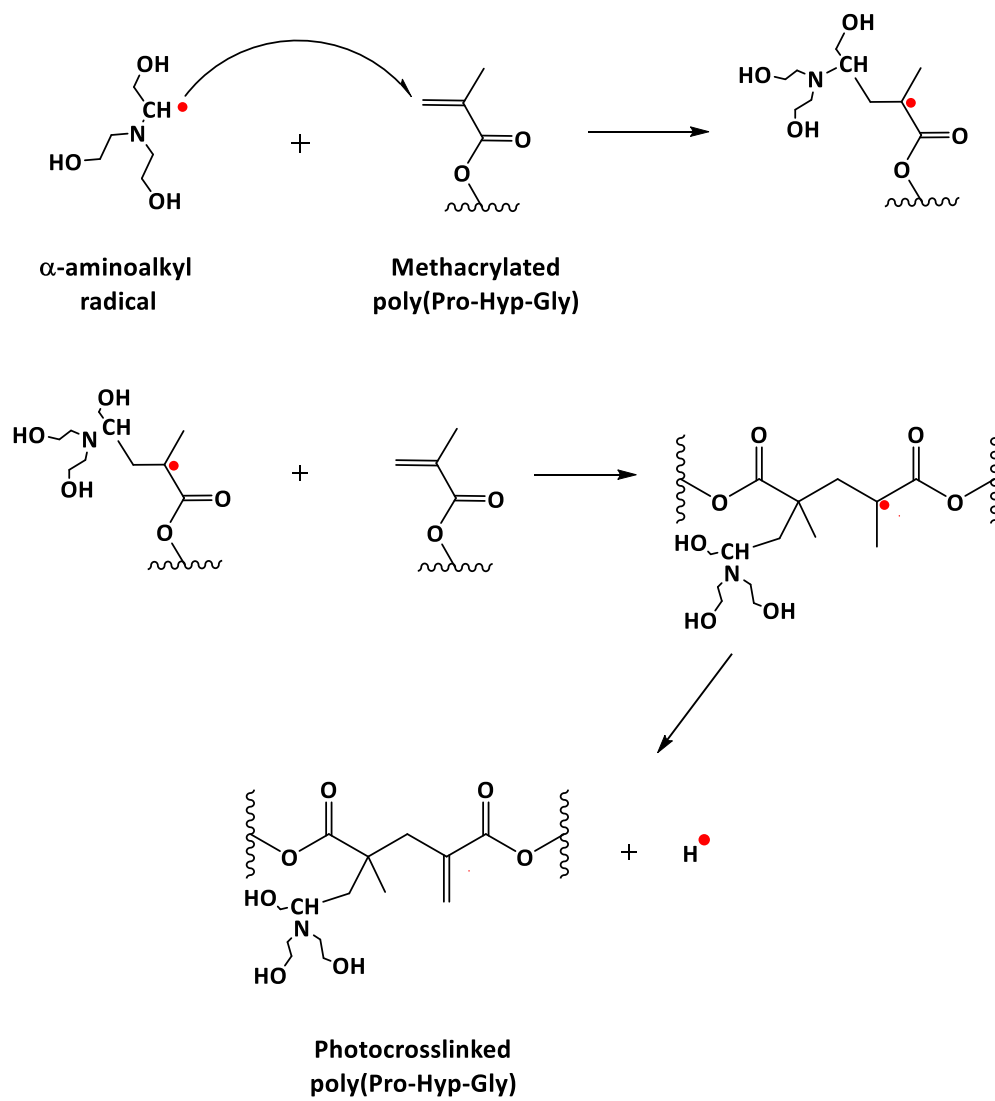
Scheme 2-4 Mechanism of photocrosslinked poly(Pro-Hyp-Gly) hydrogel formation.

(2) Route 2

**Photocrosslinked
poly(Pro-Hyp-Gly)**

(3) Route 3

(4) Route 4
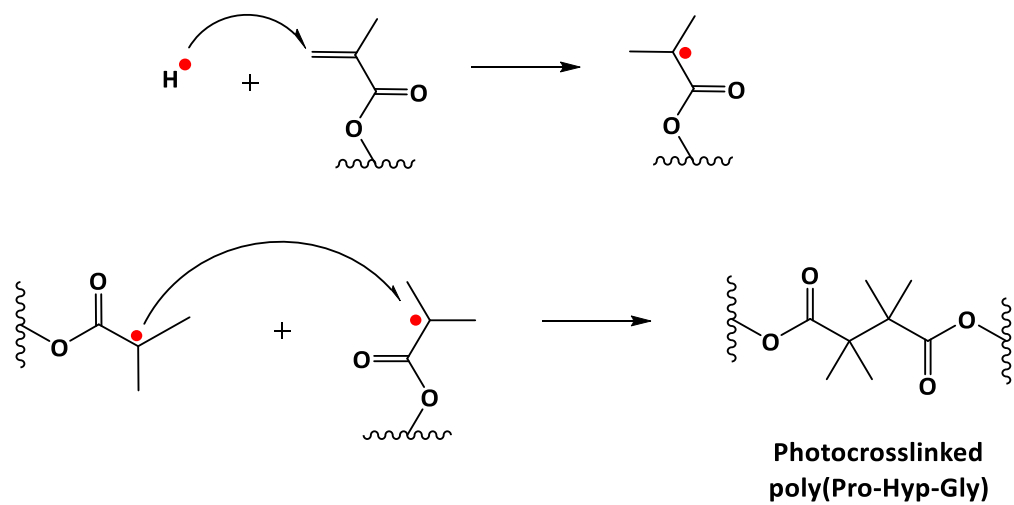
**Photocrosslinked
poly(Pro-Hyp-Gly)**
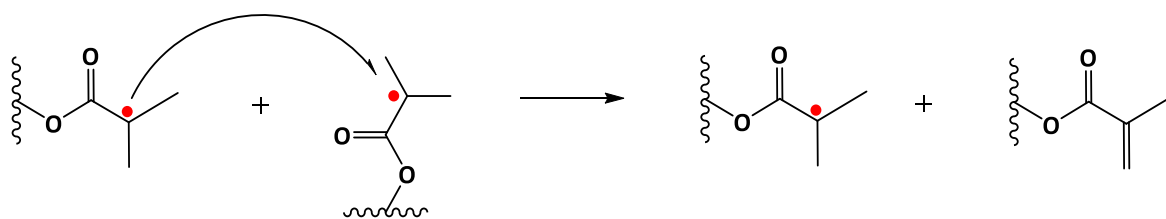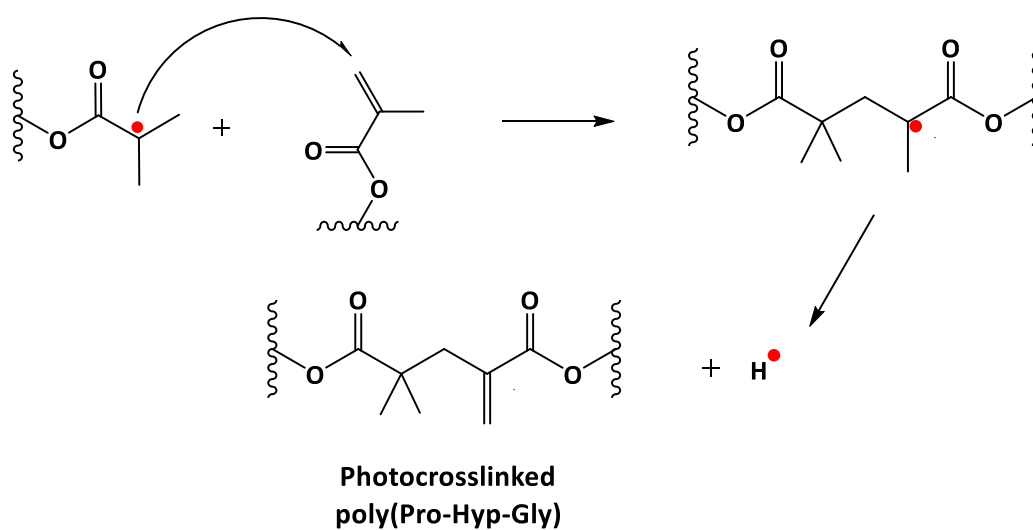
Scheme 2-4 (continue) Mechanism of photocrosslinked poly(Pro-Hyp-Gly) hydrogel
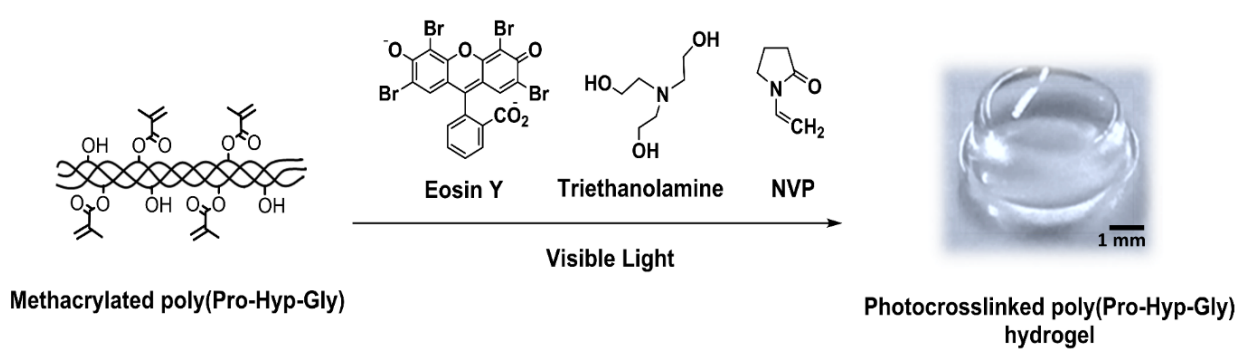
formation.

Scheme 2-5 The schematic diagram of the formation of photocrosslinked poly(Pro-Hyp-Gly) hydrogel.
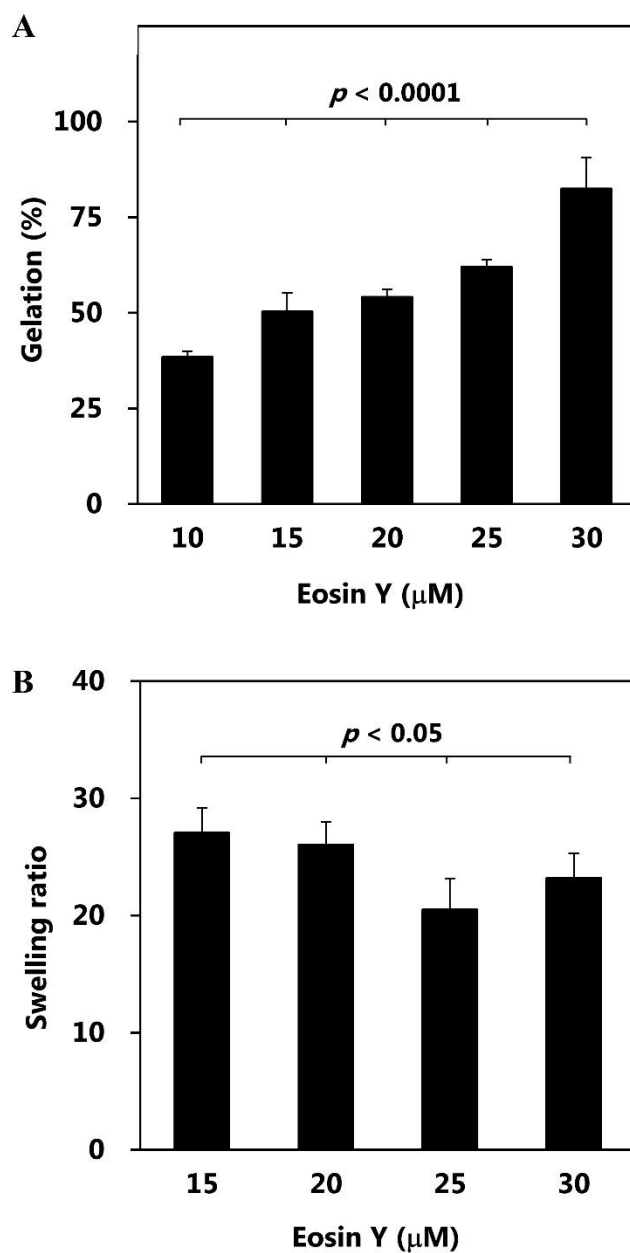
Figure 2-6 Gelation (A) and swelling ratio (B) of photocrosslinked poly(Pro-Hyp-Gly) hydrogels at different concentrations of eosin Y; the photocrosslinking system contained 30 mg/mL of methacrylated poly(Pro-Hyp-Gly), 10 mM triethanolamine, and 1 mM NVP in PBS. The irradiation time was 5 min.
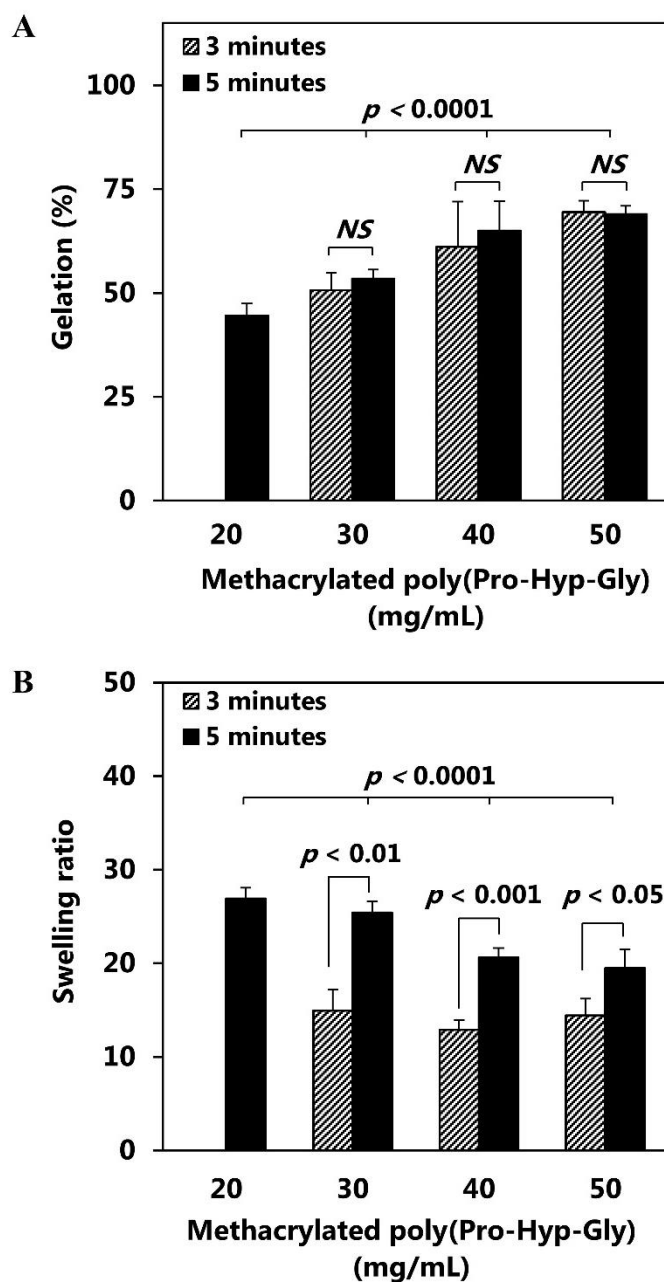
Figure 2-7 Gelation (A) and swelling ratio (B) of photocrosslinked poly(Pro-Hyp-Gly) hydrogels at different concentrations of methacrylated poly(Pro-Hyp-Gly) and irradiation times; the photocrosslinking system contained 20 μM eosin Y, 10 mM triethanolamine, and 1 mM NVP in PBS. The irradiation time was 3 or 5 min. NS = not significant.
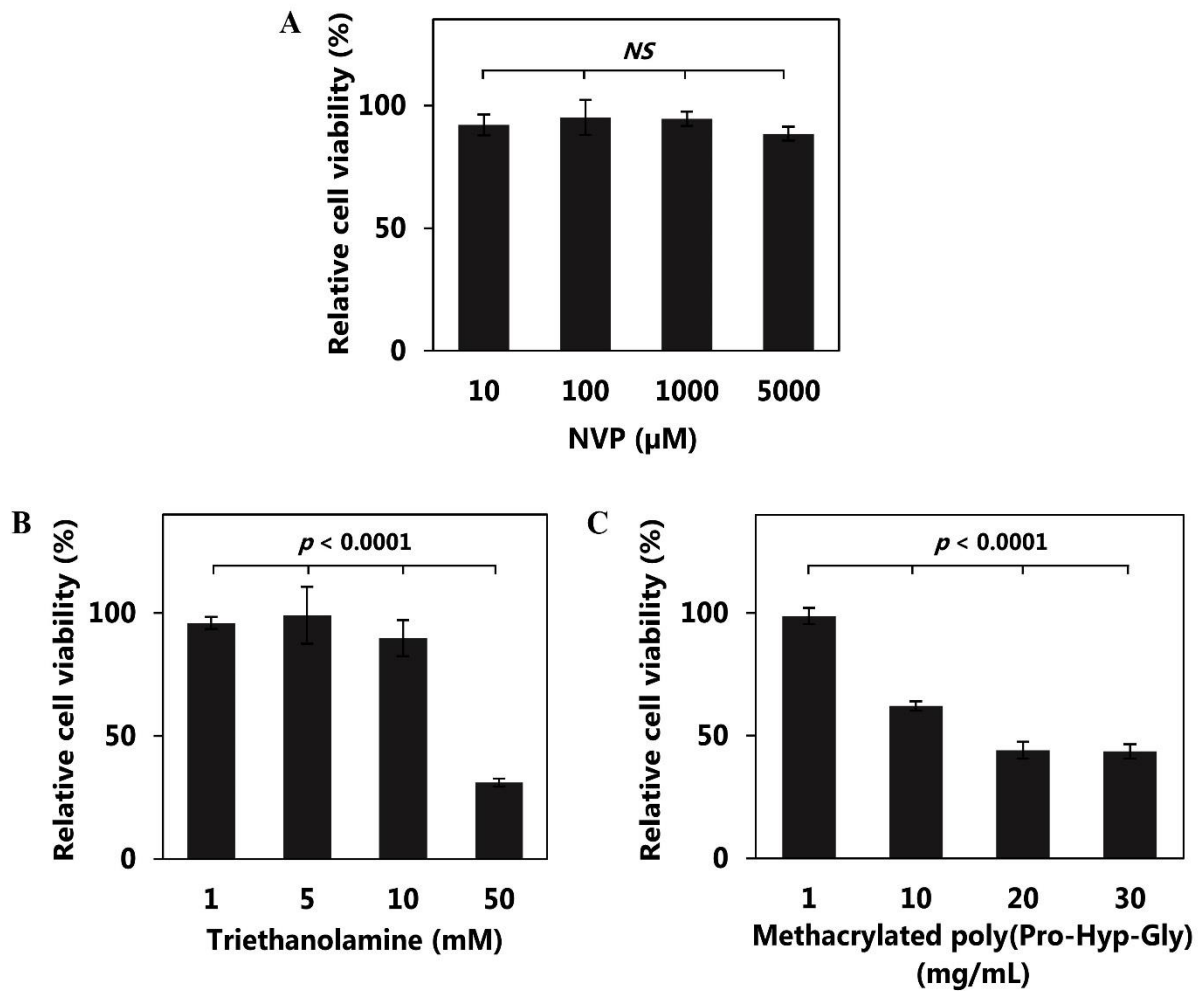
Figure 2-8 Relative cell viability of rBMSCs cultured in 20% FCS/α-MEM containing NVP (A), triethanolamine (B), and methacrylated poly(Pro-Hyp-Gly) (C) for 24 h.
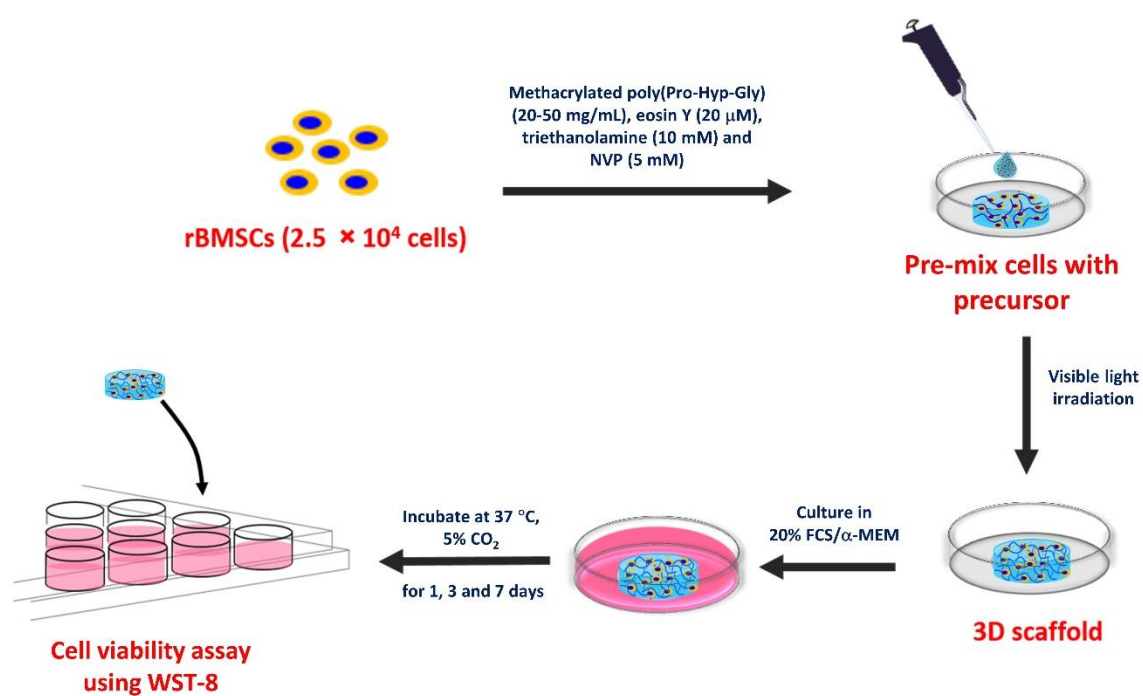
Scheme 2-6 The schematic diagram of rBMSCs cultured in photocrosslinked poly(Pro-Hyp-Gly) hydrogel as a 3D scaffold.
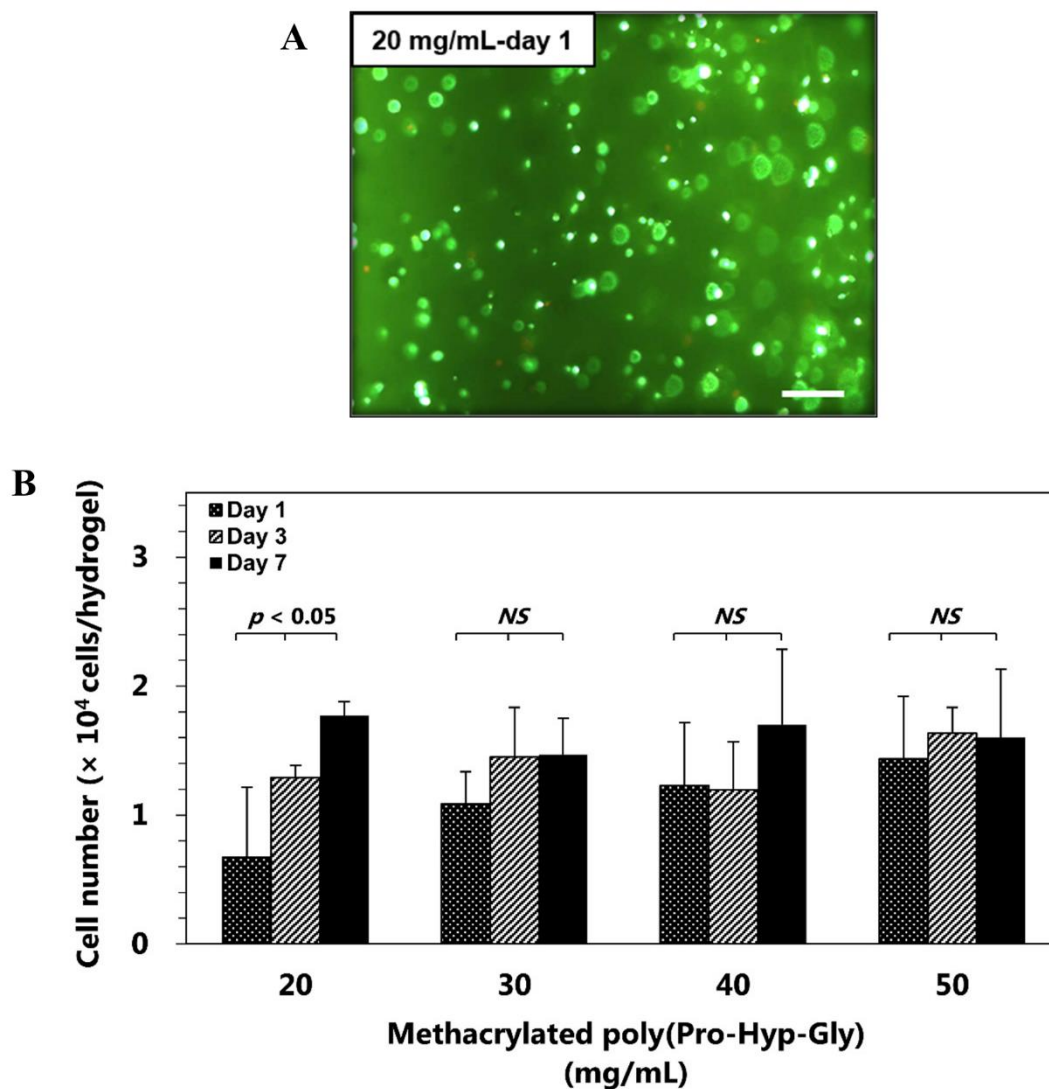
Figure 2-9 Live-Dead staining (A) and proliferation (B) of rBMSCs in photocrosslinked poly(Pro-Hyp-Gly) hydrogels formed with 20–50 mg/mL of methacrylated poly(Pro-Hyp-Gly); the photocrosslinking system contained 20 μM eosin Y, 10 mM triethanolamine, and 5 mM NVP in PBS. The irradiation time was 5 min. Scale bar represent 100 μm.
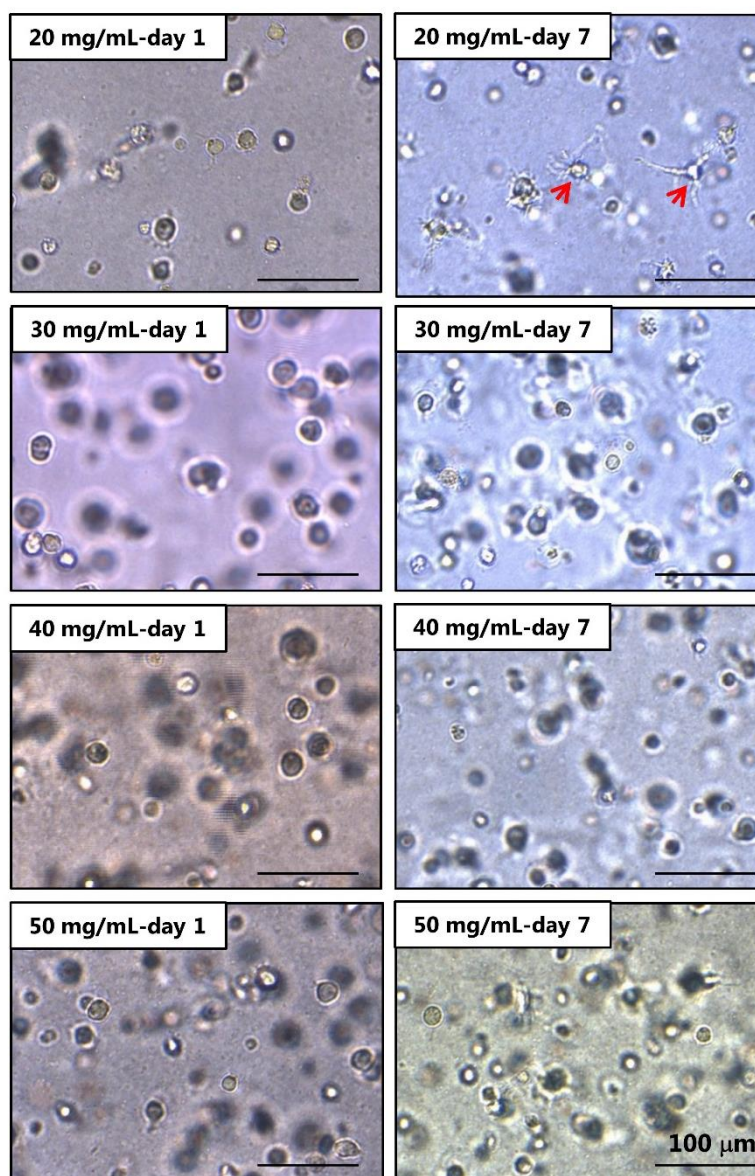
Figure 2-10 Phase contrast microscope images of rBMSCs in the photocrosslinked poly(Pro-Hyp-Gly) hydrogels formed at different concentration of methacrylated poly(Pro-Hyp-Gly) (20−50 mg/mL). The irradiation time was 5 min. Red arrows indicate rBMSCs with an elongated and branched morphology.
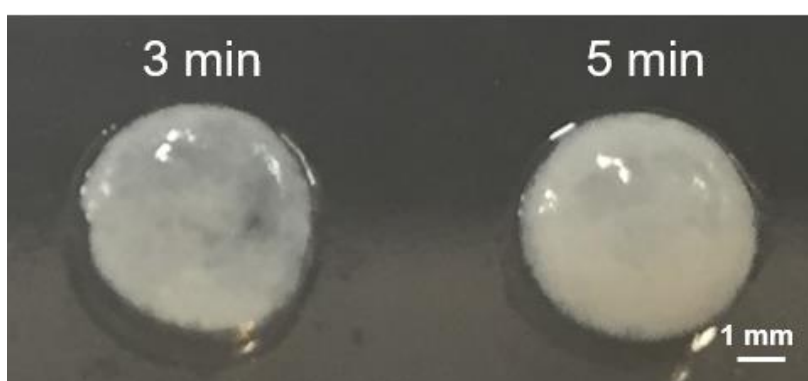
Figure 2-11 Macroscopic appearance of 30 mg/mL of methacrylated poly(Pro-Hyp-Gly) hydrogels incubated with an osteogenic medium at day 28.
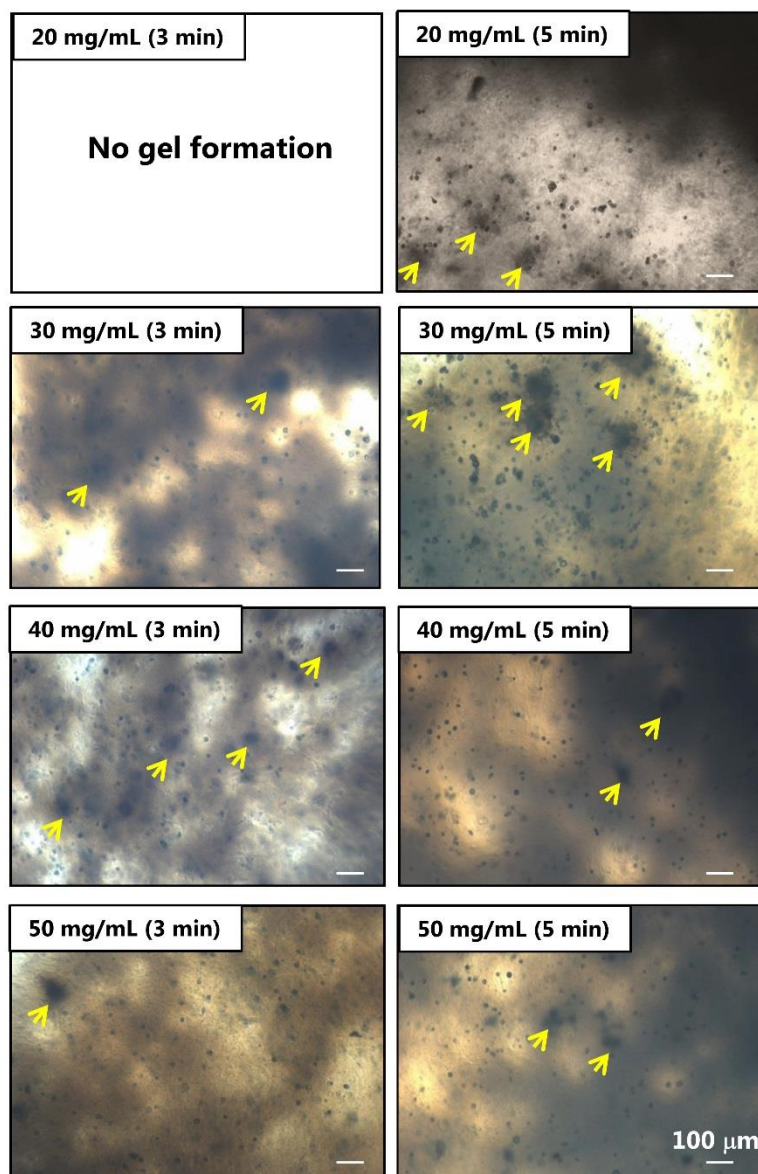
Figure 2-12 Phase contrast microscope images of rBMSCs in the photocrosslinked poly(Pro-Hyp-Gly) hydrogels incubated with an osteogenic medium at day 28. Yellow arrows indicate bone nodules.
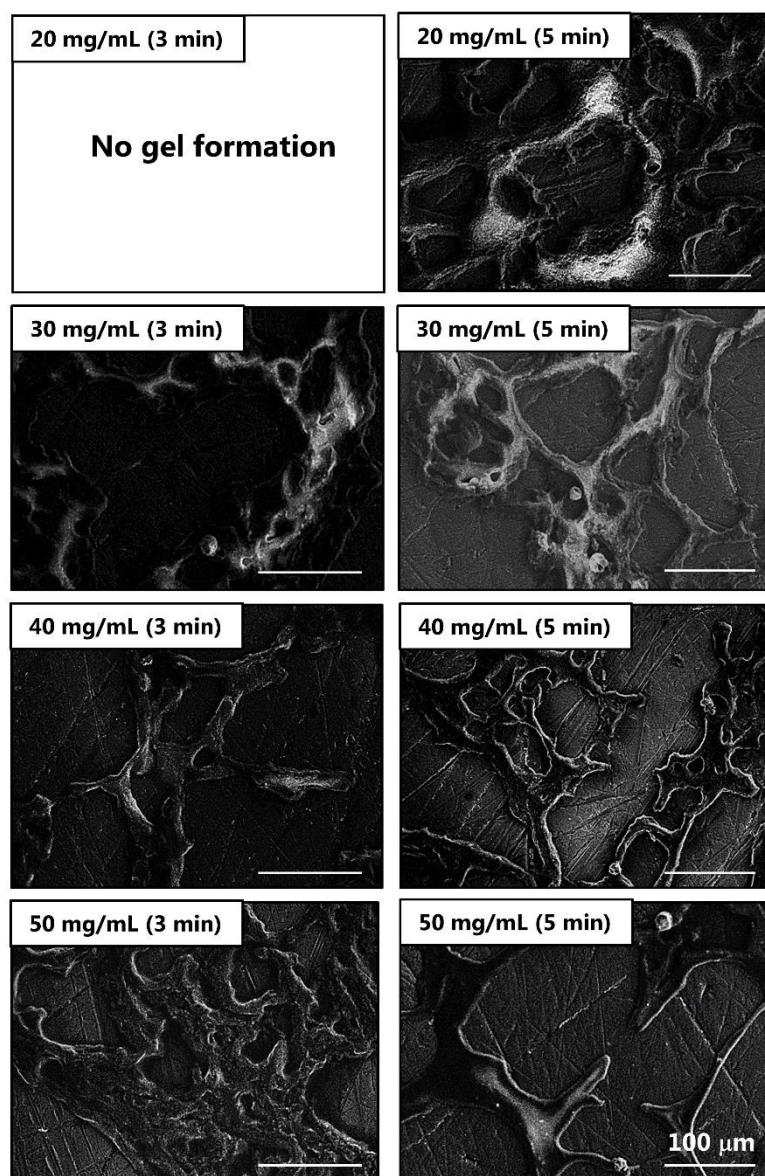
Figure 2-13 SEM images of 6 μm slices of photocrosslinked poly(Pro-Hyp-Gly) hydrogels containing rBMSCs.
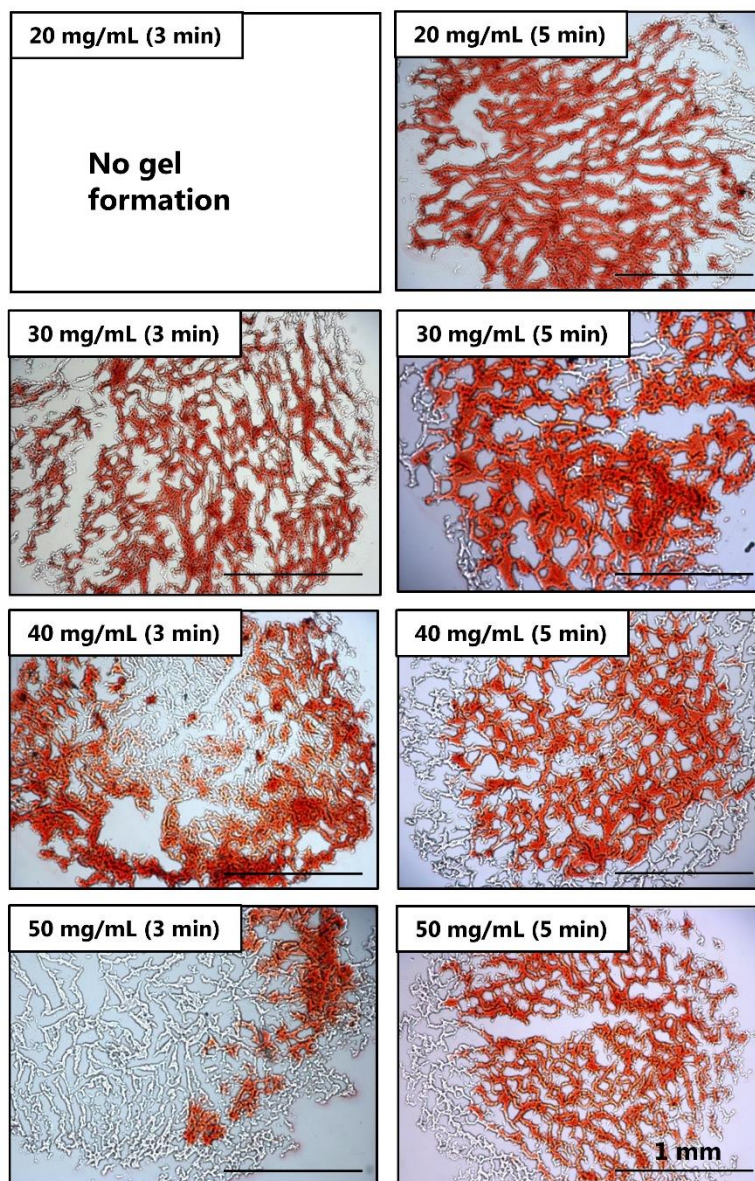
Figure 2-14 Alizarin Red S staining of 6 µm slices of photocrosslinked poly(Pro-Hyp-Gly) hydrogels containing rBMSCs.
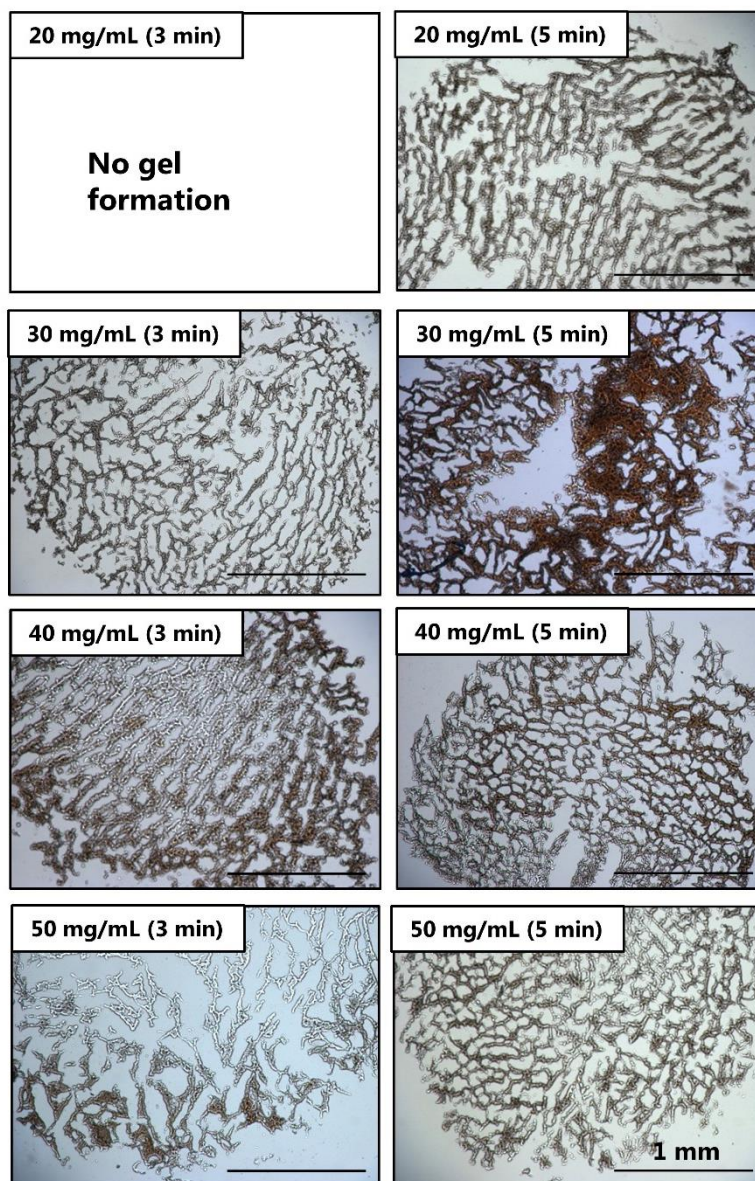
Figure 2-15 The von Kossa staining of 6 μm slices of photocrosslinked poly(Pro-Hyp-Gly) hydrogels containing rBMSCs.
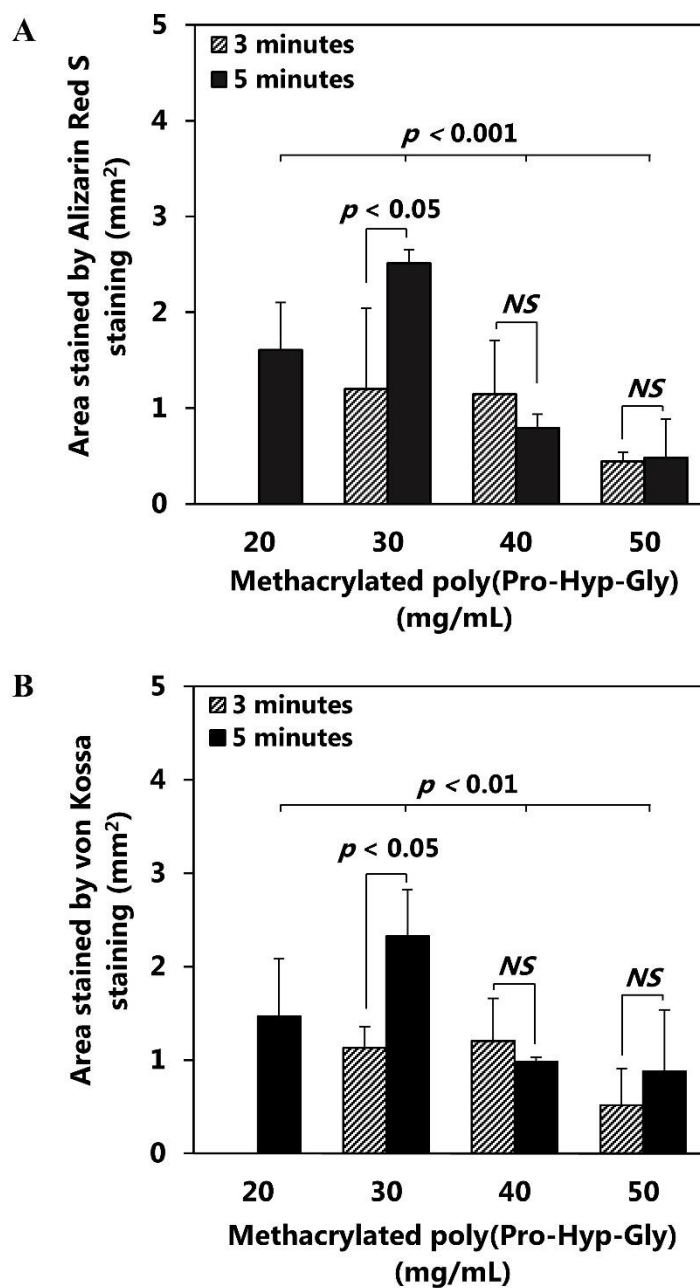
Figure 2-16 Quantification area of 6 μm slices of photocrosslinked poly(Pro-Hyp-Gly) hydrogels stained by Alizarin Red S (A) and von Kossa (B).

GENERAL CONCLUSION

The purpose of this study is to develop cytocompatible 3D scaffolds for stem cell encapsulation that can support cell survival and differentiation. Animal-derived collagens are commonly used as materials for fabricating 3D scaffolds because of their biocompatibility and biodegradability. However, there are limitations of using animal-derived collagens, such as low thermal stability and possible contamination with pathogenic substances. Poly(Pro-Hyp-Gly), a collagen-like polypeptide, is a promising material for fabricating 3D scaffolds because it can be synthesized with high reproducibility in its physical and chemical properties, has a high thermal stability, forms a collagen-like triple-helical structure, and shows excellent biocompatibility and biodegradability.

Hydrogels, 3D hydrated polymeric networks, have been widely investigated as 3D scaffolds for tissue regeneration because they can reproduce the features of ECM, allow diffusion of nutrients, oxygen, and cellular waste, and are able to encapsulate cells simultaneously during hydrogel formation. The hydrogel properties, such as degree of crosslinking, polymer network density, mechanical stiffness, and swelling ratio, can be controlled both by choosing the type of crosslinking, chemical or physical crosslinking, and

by controlling the crosslinking conditions, such as concentrations of polymers and crosslinkers. In this study, in order to provide cytocompatible hydrogels for stem cell encapsulation, physically-crosslinked and chemically-crosslinked poly(Pro-Hyp-Gly) hydrogels were fabricated and used for simultaneous rBMSC encapsulation. Viability and osteogenic differentiation of the encapsulated cells were then assessed.

Chapter 1 shows the fabrication of physically-crosslinked poly(Pro-Hyp-Gly) hydrogel by simply mixing polyanion and polycation of poly(Pro-Hyp-Gly). The polyanion, Suc-poly(Pro-Hyp-Gly), and the polycation, Arg-poly(Pro-Hyp-Gly), were successfully synthesized by conjugating succinyl group and arginine methyl ester, respectively, into the hydroxy group of poly(Pro-Hyp-Gly). The polyanion and the polycation contain a collagen-like triple-helical structure as revealed by CD and ^{1}H NMR analyses. Interaction between carboxy group of Suc-poly(Pro-Hyp-Gly) ($pK_a = 5.2$) and guanidinium group of Arg-poly(Pro-Hyp-Gly) ($pK_a = 12.4$) at physiological pH leads to PIC gel formation. The PIC gel formation was optimum at an equimolar ratio of carboxy to guanidinium groups, suggesting that ionic bonding is a key determinant for the hydrogel formation. The PIC gel was successfully used for simultaneous rBMSC encapsulation. The encapsulated cells survived and proliferated within the PIC gel. In addition, the rBMSCs exhibited different morphology in the PIC gel compared with the rBMSCs cultured on a tissue culture dish as a 2D control. A round shape morphology and homogeneous single cell distribution were

observed in the PIC gel. In contrast, the rBMSCs spread and formed a fibroblast-like morphology on 2D control. After 3 days, the rBMSCs in the PIC gel formed multicellular aggregates. In cell aggregates, cell-cell and cell-matrix interactions are similar to cell behavior in *in vivo* microenvironment. These results suggest that the PIC gel of poly(Pro-Hyp-Gly) is suitable for tissue regeneration because of its non-toxicity, ease of fabrication, and biocompatibility.

Chapter 2 shows fabrication of chemically-crosslinked poly(Pro-Hyp-Gly) hydrogels by visible light photocrosslinking of methacrylated poly(Pro-Hyp-Gly) in the presence of eosin Y as a photoinitiator, triethanolamine as a co-initiator, and NVP as a radical scavenger. The photocrosslinked poly(Pro-Hyp-Gly) hydrogel properties, such as gelation and swelling ratio, can be easily tuned by controlling concentrations of eosin Y (10–30 µM) and methacrylated poly(Pro-Hyp-Gly) (20–50 mg/mL), and the irradiation time (3 or 5 min). The increase in methacrylated poly(Pro-Hyp-Gly) concentration results in hydrogel with higher polymer network density and lower swelling ratio. The encapsulated rBMSCs were viable within the photocrosslinked poly(Pro-Hyp-Gly) hydrogels. However, they showed different proliferation at different concentrations of methacrylated poly(Pro-Hyp-Gly) hydrogels. The rBMSCs proliferated in 20 mg/mL of methacrylated poly(Pro-Hyp-Gly), while they did not proliferate in 30–50 mg/mL hydrogels. It suggests that the hydrogel properties influenced cell proliferation. Osteogenic differentiation of the rBMSCs in the

hydrogels was also affected by the hydrogel properties. Hydrogel formed with 30 mg/mL of methacrylated poly(Pro-Hyp-Gly) and 5 min irradiation showed a significantly higher calcium deposition as revealed by SEM observation, Alizarin Red S and von Kossa staining. In contrast, hydrogels formed with 50 mg/mL of methacrylated poly(Pro-Hyp-Gly) (3 min) exhibited the lowest calcium deposition. The low calcium deposition at high concentrations of methacrylated poly(Pro-Hyp-Gly) hydrogels (40–50 mg/mL) may be caused by their high polymer network density and low swelling ratio. These properties may limit cell migration and diffusion of nutrients, oxygen, and waste through the hydrogel network, and then influenced cell differentiation.

The results of this study indicate that physically-crosslinked and chemically-crosslinked poly(Pro-Hyp-Gly) hydrogels were successfully fabricated and used for simultaneous rBMSC encapsulation. The PIC gel is softer than photocrosslinked poly(Pro-Hyp-Gly) hydrogels because it is formed by non-covalent bonding between the polyanion and polycation of poly(Pro-Hyp-Gly). The photocrosslinked poly(Pro-Hyp-Gly) hydrogels showed high stiffness because the poly(Pro-Hyp-Gly) in the hydrogel network is connected by covalent bonding. The encapsulated rBMSCs in both hydrogels were homogeneously distributed and viable. From morphology observation, the rBMSCs in both hydrogels exhibited *in vivo*-like cell morphology, suggesting that the PIC gel and photocrosslinked poly(Pro-Hyp-Gly) hydrogels can reproduce 3D *in vivo* cellular

microenvironment. From bone nodule observation, osteogenic differentiation of the

rBMSCs in the photocrosslinked poly(Pro-Hyp-Gly) hydrogels was higher compared to that

of the rBMSCs in the PIC gel. These results revealed that the photocrosslinked

poly(Pro-Hyp-Gly) hydrogel provided a better environment for osteogenic differentiation of

the rBMSCs. It has been reported that stiff hydrogels display significantly higher expression

of osteogenic differentiation markers compared with soft hydrogels. The results from this

study clearly showed that type of crosslinking for hydrogel formation influences hydrogel

properties and then affects the behavior of the encapsulated cells. An appropriate

crosslinking type, process, and condition are required to support stem cell viability and direct

their differentiation into specific lineages. In conclusion, physically-crosslinked and

chemically-crosslinked poly(Pro-Hyp-Gly) hydrogels have a great potential to serve as 3D

scaffolding materials for tissue regeneration.

LIST OF PUBLICATIONS

Farah Nurlidar, Mime Kobayashi, Kayo Terada, Tsuyoshi Ando, Masao Tanihara. Cytocompatible polyion complex gel of poly(Pro-Hyp-Gly) for simultaneous rat bone marrow stromal cell encapsulation. Journal of Biomaterials Science: Polymer Edition, DOI: 10.1080/09205063.2017.1331872 (Accepted).

Farah Nurlidar, Keisuke Yamane, Mime Kobayashi, Kayo Terada, Tsuyoshi Ando, Masao Tanihara. Calcium deposition in photocrosslinked poly(Pro-Hyp-Gly) hydrogels encapsulated rat bone marrow stromal cells. Journal of Tissue Engineering and Regenerative Medicine (In revision).

CONFERENCES (ORAL PRESENTATION)

Farah Nurlidar, Keisuke Yamane, Mime Kobayashi, Kayo Terada, Tsuyoshi Ando, Masao Tanihara. Osteogenic differentiation of rat bone marrow stromal cells encapsulated into photocrosslinked collagen-like polypeptide hydrogels. Int J Artif Organs 2016;39(7):p. 326.

Farah Nurlidar, Keisuke Yamane, Mime Kobayashi, Kayo Terada, Tsuyoshi Ando, Masao Tanihara. Osteogenic differentiation of bone marrow stromal cells encapsulated in poly(Pro-Hyp-Gly) hydrogel. Proceeding of the 15th Congress of the Japanese Society for Regenerative Medicine 2016;15(suppl.):p.284.

Farah Nurlidar, Keisuke Yamane, Mime Kobayashi, Kayo Terada, Tsuyoshi Ando, Masao Tanihara. Stem cell encapsulation into photocrosslinked methacrylated collagen-like polypeptide hydrogel. Proceeding of the 14th Congress of the Japanese Society for Regenerative Medicine 2015;14(suppl.):p.191.

ACKNOWLEDGEMENTS

First and foremost, I would like to express my gratitude to the one and only, the al Mighty, Allah SWT, for blessing and giving me the valuable experiences to take a doctoral course in Nara Institute of Science and Technology (NAIST), Japan.

I would also like to express my wholehearted thanks to my supervisor, Professor Masao Tanihara, for his constructive suggestions, supports, and understanding during my doctoral course. I am very grateful for your patience and knowledge in helping me to improve my English skills, logical and rational thinking, and also for teaching me with many experiments in the laboratory.

I would also like to deliver many thanks to Professor Jun-ichi Kikuchi, Professor Michiya Fujiki, Associate Professor Tsuyoshi Ando, Assistant Professor Mime Kobayashi, and Assistant Professor Kayo Terada for their valuable comments, suggestions, and discussion throughout my time as a doctoral student in NAIST. I would like to thank Ms. Shinohara for her help in all administration stuffs and Dr. Masayasu Totani for his help during my study. My great thanks to all students in Biocompatible